NASA-CR-72275

WANL-PR-(ZZ)-001

JOINING REFRACTORY/AUSTENITIC BIMETAL TUBING

Final Technical Report

By

D. R. Stoner

Prepared for

National Aeronautics and Space Administration

Lewis Research Center

Space Power Systems Division

Under Contract NAS 3-7621

Astronuclear Laboratory

Westinghouse Electric Corporation

N67-36029 (ACCESSION NUMBER) 116 (PAGES) 1 (INASA CR OR TMX OR AD NUMBER) 1 (THRU) (CODE) 15 (CATEGORY)

Astronuclear Laboratory
WANL-PR-(ZZ)-001
NASA-CR-72275

JOINING REFRACTORY/AUSTENITIC BIMETAL TUBING

by

D. R. Stoner

Final Technical Report

Covering the Period

April 1965 to October 1966

Prepared for

NATIONAL AERONAUTICS AND SPACE ADMINISTRATION

Contract NAS 3-7621

Technical Management

P. L. Stone

NASA-Lewis Research Center
Space Power Systems Division

Westinghouse Astronuclear Laboratory
P.O. Box 10864
Pittsburgh, Pennsylvania 15236

PRECEDING PAGE BLANK NOT FILMED.

FOREWORD

This evaluation program was conducted in the performance of Contract NAS 3-7621, "Joining of Refractory/Austenitic Bimetal Tubing" for the NASA-Lewis Research Center. The evaluation is in support of the SNAP-8 turboelectric power system being developed for NASA by Aerojet General Corporation. The author wishes to acknowledge the realistic and practical position taken by the NASA technical project manager, P. Stone, in guiding the fabrication and evaluation program.

The author gratefully acknowledges those whose guidance and assistance greatly contributed to the successful conduct of this investigation. They include personnel of the Westinghouse Astronuclear Laboratory: for the initial program concept and process consulting throughout the program, G. G. Lessmann; for the precision electron beam and chamber gas tungsten arc welding, E. Urbas and R. Sprecace; for the construction and operation ofspecialized thermal cycling and pressure testing apparatus, E. Vandergrift and J. Lesczynski, and for metallographic work, K. Galbraith. Also included are personnel of Westinghouse Headquarters Manufacturing Laboratory: for gas tungsten arc butt joint development, F. V. Morely, Jr.; and for plasma arc welding, L. Manno and E. Pigan.

PRECEDING PAGE BLANK NOT FILMED.

Astronuclear Laboratory

ABSTRACT

Joining techniques were developed for bimetal tubing intended for applications involving high temperature liquid metal containment. Three basic configurations, the butt joint, tee joint, and tube-to-header joint were produced in quantity and evaluated in terms of performance and ease of fabrication.

The joints are designed to be leak tight at 1350° F and compatible with liquid metals, both at the inner refractory metal liner and at the exterior stainless steel joint. Welding most readily satisfies these requirements and, because it is more universally applicable than other methods, was selected as the process for this evaluation. Gas tungsten arc, including preplaced filler and wire feed modifications, plasma arc overlay, and electron beam welding processes were evaluated. Electron beam welds were made in a 10^{-5} torr vacuum using a high voltage, 150 KV, electron beam gun. Tungsten arc welding of the contamination-sensitive columbium was accomplished in a high purity inert gas chamber which was continually monitored for impurities. Total active impurity levels of 1 ppm were measured in the backfilled chamber. Tubing sizes of 0.800 inch OD and 0.510 inch OD were evaluated. In both sizes the 0.055 inch wall was composed of a 0.035 inch outer layer of 316 stainless steel and a 0.020 inch inner layer of unalloyed columbium.

Successful joint designs were developed for the three primary joint configurations. The durability of a bimetal joint under severe thermal cycling conditions was determined. Two samples of each joint design were rapidly cycled 20 times from 1350° F to 600° F in a non-contaminating environment. The structural integrity and bond interface condition was determined after thermal cycling. Data are also presented on the strength and efficiency of the butt joint at room temperature and 1350° F. Internal pressure-creep rupture data were obtained for welded and unwelded tubing at 1350° F, for test times up to 1000 hours. Complete metallographic studies of the weld metal and bimetal interface are presented, including microhardness and electron microprobe surveys of weld induced diffusion zones. Sufficient samples of each joint design were fabricated and evaluated to obtain a valid outline of the process capability.

Astronuclear Laboratory

TABLE OF CONTENTS

Astronuclear Laboratory

TABLE OF CONTENTS (CONTINUED)

Astronuclear Laboratory

LIST OF ILLUSTRATIONS

LIST OF ILLUSTRATIONS (Continued)

LIST OF ILLUSTRATIONS (Continued)

PRECEDING PAGE BLANK NOT FILMED.

LIST OF TABLES

PRECEDING PAGE BLANK NOT FILMED.

SECTION II
INTRODUCTION

There has been an increasing use of bimetallic construction, both to satisfy the demands of economy, where a protective clad is used over an inexpensive backing material, and for performance, where a particular combination of properties are required of a material. The tubing used in this fabrication evaluation is a 316 stainless steel-columbium combination designed for the SNAP-8 nuclear turbo-electric power system. The bimetal tubing is to serve as mercury boiler tubes, an application involving boiling mercury on the tube interior and 1350° F NaK on the tubing exterior. Initial data indicate the 316 stainless-clad columbium tubing provides a strong, corrosion resistant container with good heat transfer properties. A view of the SNAP-8 boiler is shown in Figure 1.

The application of bimetal tubing in operating systems requires adequate fabrication techniques including the basic plumbing configurations such as butt joints, tee joints, and tube-to-header joints. To satisfy this need a NASA-sponsored program, "Joining Refractory/Austenitic Bimetal Tubing", (Contract NAS 3-7621) was undertaken by the Westinghouse Astronuclear Laboratory.

Acceptable joints must be leak tight at 1350°F and compatible with liquid metals, both at the inner refractory metal liner, and in most applications, at the exterior stainless steel joint. Welding most readily satisfies these requirements and, because it is more universally applicable than other methods, was selected as the process for this evaluation. As a further practical concession, the basic philosophy used in evaluating the various welding techniques was to maintain a high degree of field welding capability in at least one joint configuration. In view of this criterion, gas tungsten arc welding of the tube-to-tube butt joint was favored since final assembly welds in large apparatus can most easily be made by clamp-on arc welders.

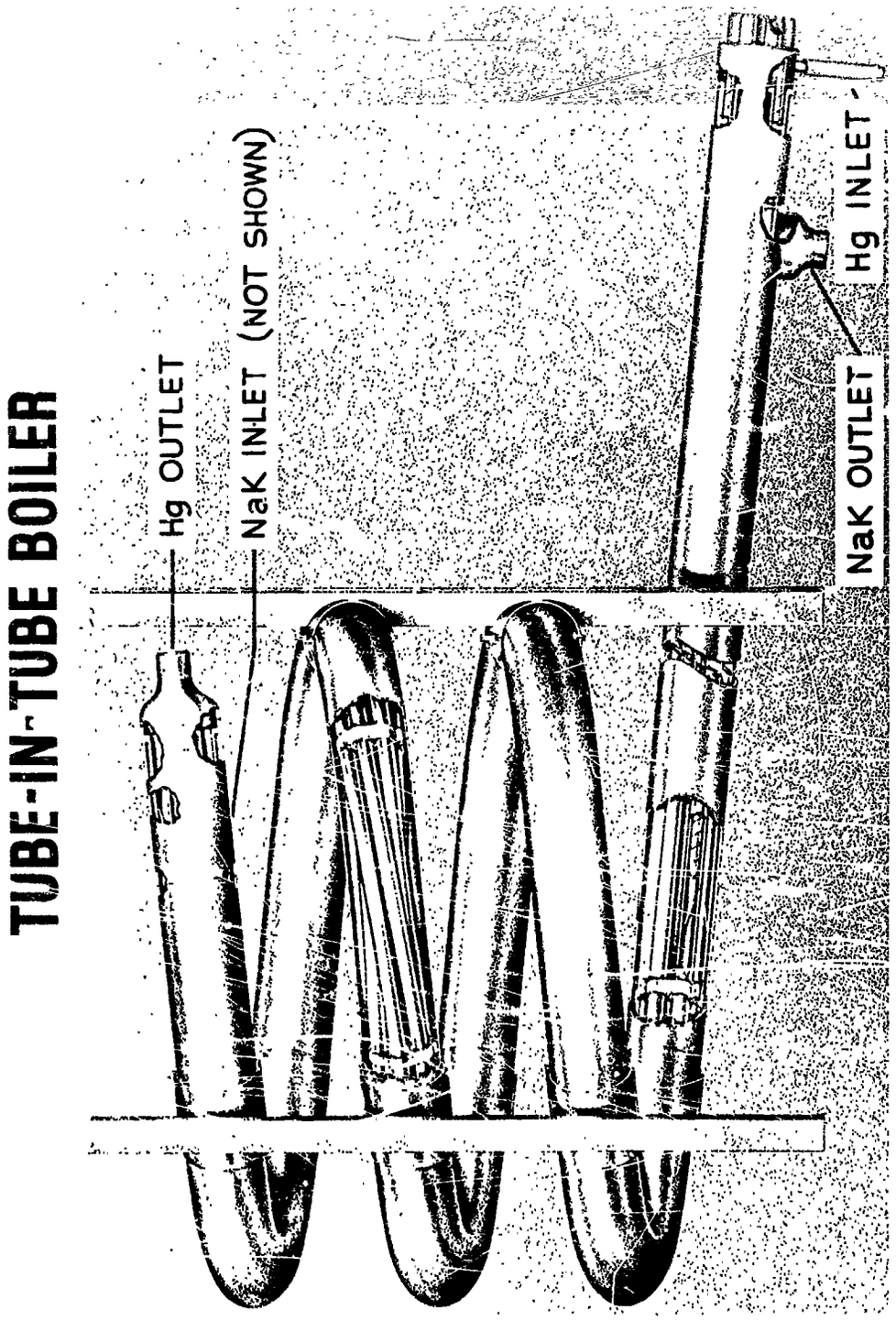

Figure 1. SNAP-8 Boiler

Because of the sensitivity of refractory metals to interstitial contamination resulting in degradation of mechanical properties, great care was taken during evaluation and welding to avoid contamination. Electron beam welding of the refractory metal components was done at pressures of 10^{-5} torr. Gas tungsten arc welding, including wire feed and preplaced filler was accomplished in a vacuum purged welding chamber in an ultra-high purity helium atmosphere. The backfilled chamber was continually monitored for oxygen and water vapor while welding the contamination-prone refractory metal. Total active impurity levels of 1 ppm were measured upon backfilling and welding was discontinued at concentrations above 5 ppm oxygen or water vapor.

The weld evaluation program included rapid thermal cycling from 1350° F to 600° F using vacuum induction heating and a high purity helium gas quench. Internal pressure creep testing for up to 1000 hours at 1350° F was done in a 10^{-6} torr vacuum using high pressure helium gas. Painstaking joint preparation procedures were used to prevent debonding of the bimetal tubing and weld induced alloying of the stainless steel and refractory metal. Special pickling techniques were developed to identify and remove traces of stainless steel from the refractory metal joint.

Tubing sizes of 0.800 inch OD and 0.510 OD were evaluated. In both sizes the 0.055 inch wall was composed of a 0.035 inch outer layer of 316 stainless steel and a 0.020 inch inner layer of unalloyed columbium. Three basic joint configurations, the butt joint, the tee joint, and the tube-to-header joint were evaluated. Generally, several acceptable designs of each joint configuration were made and a reference design and welding process was chosen considering both overall performance, ease of fabrication, and the type of welding process most adaptable to the particular joint assembly. Ten samples of each reference design weld joint were made and thoroughly evaluated.

SECTION II

EXPERIMENTAL PROGRAM

A. PROGRAM OUTLINE

The initial phase of the program was to evaluate the several possible variations of each joint design. Alternate designs were fabricated, sectioned, and after thorough consideration of several factors such as joint quality, ease of fabrication, and the complexity of the welding equipment required, a reference design was chosen for each basic weld joint. In all cases, several successful designs were developed, and the final choice was the welding process that could be best accommodated in the fabrication of a complete engineering system.

The second phase of the program involved the fabrication of 10 samples of each joint design using the selected reference process, and subsequently evaluating the samples. All specimens during and after fabrication were subjected to visual, helium leak check, dye penetrant, radiography, and ultrasonic inspections to guarantee 10 acceptable specimens. When necessary, spare samples were processed to provide the necessary number of specimens. The data obtained in processing a significant number of samples provided a fairly realistic appraisal of the process capability of the various joint designs.

Following the fabrication of 10 acceptable samples of each joint design, the evaluation program outlined in Figure 2 was followed.

The evaluation for all of the joint designs was based on an observation of the effect of thermal cycling on the weld joint mechanical strength and bimetal interface. The specimens were thermal cycled 20 times from 1350° F to 600° F, (a typical temperature trace is shown in Figure 3), destructively tested, and metallographically sectioned. The details of the destructive tests are shown in Figure 4 and consist of crush and tensile tests. The butt joints were subjected to additional tensile tests and internal pressure tests.

The data presentation is divided into three sections corresponding to the basic joint designs. Figure 4 shows examples of the three configurations; the butt joint, the tee joint, and the tube-to-header joint.

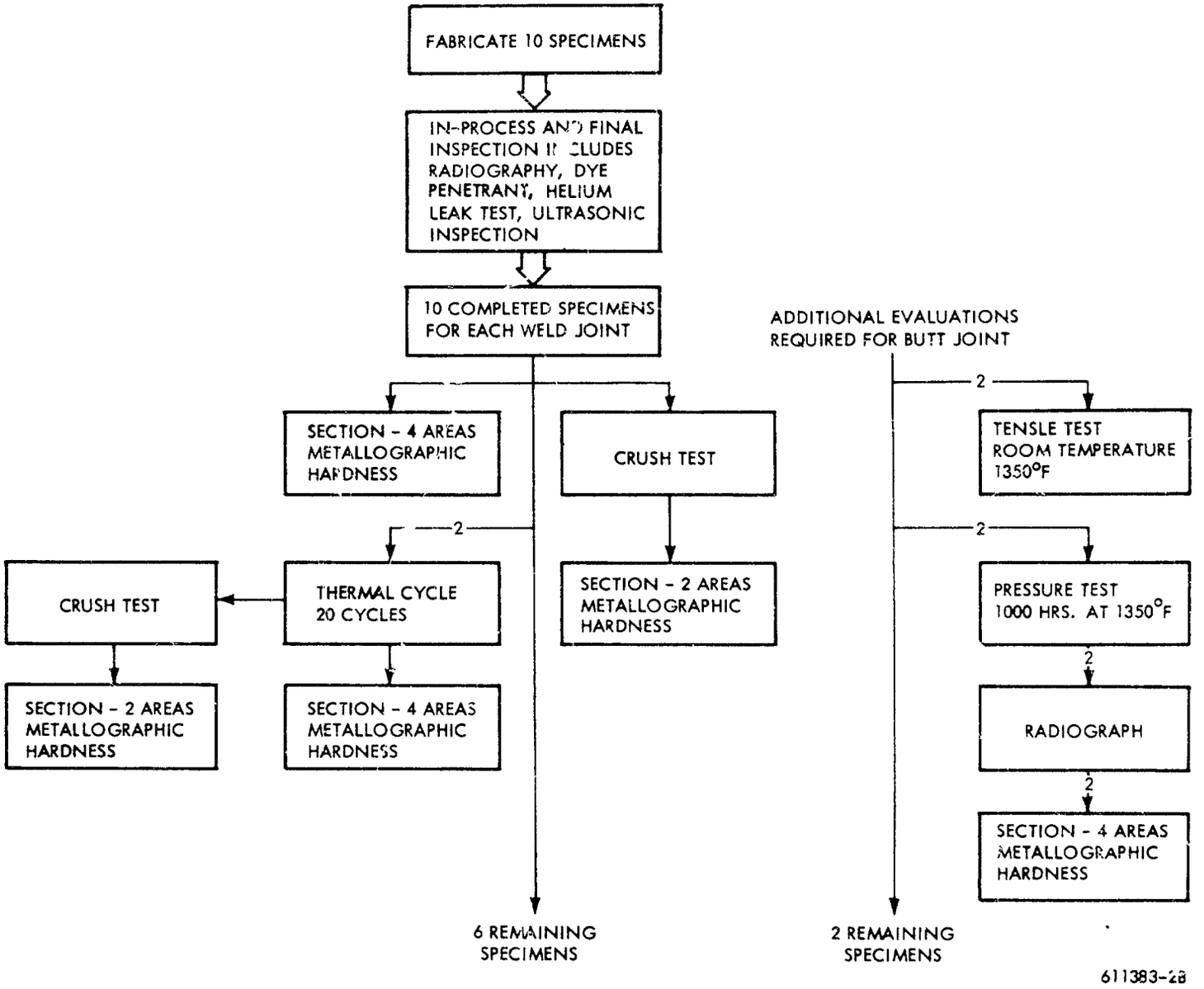

Figure 2. Evaluation Requirements for Bimetal Tubing

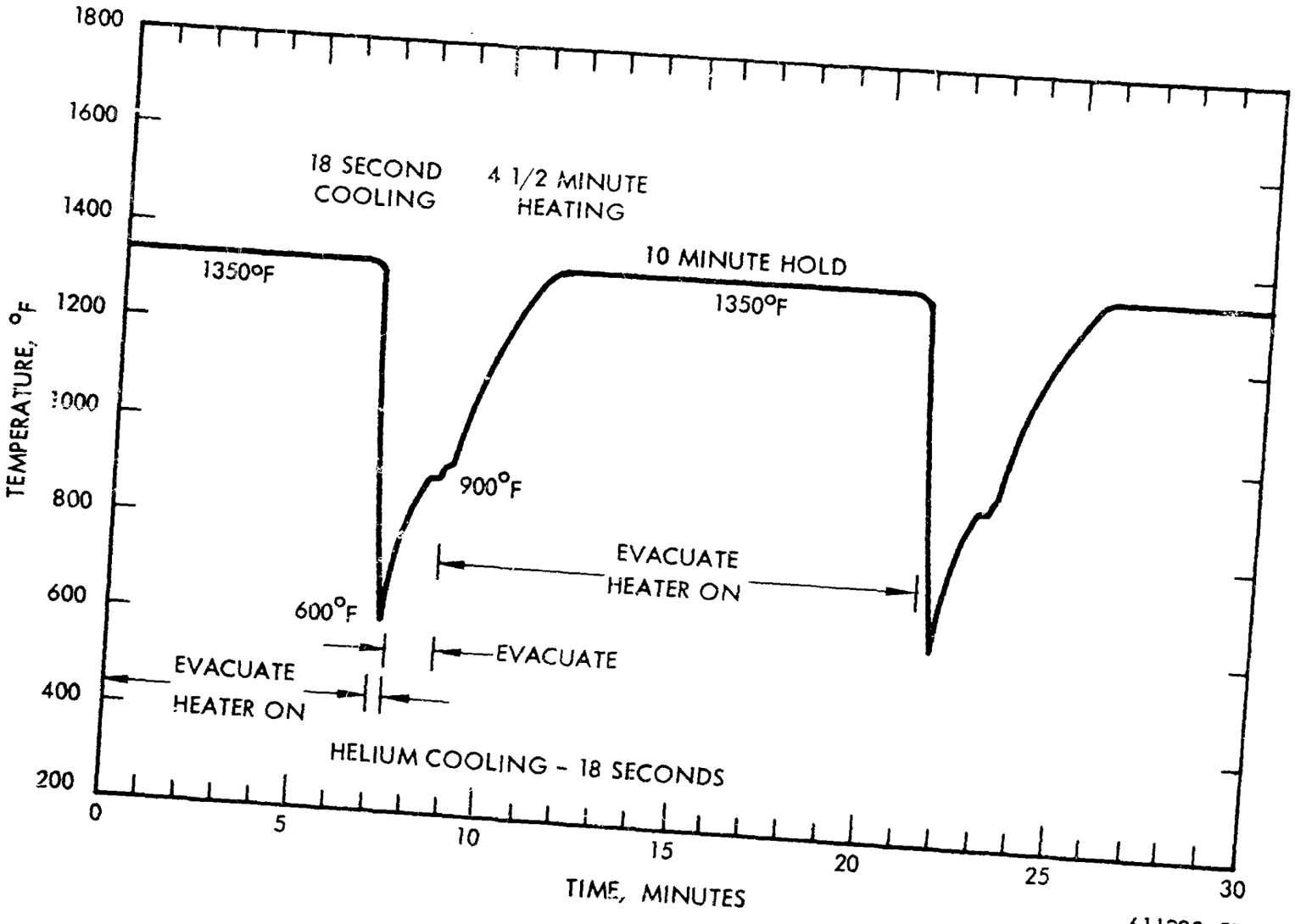

Figure 3. Thermal Cycle Temperature Trace for Butt Joint

Astronuclear Laboratory

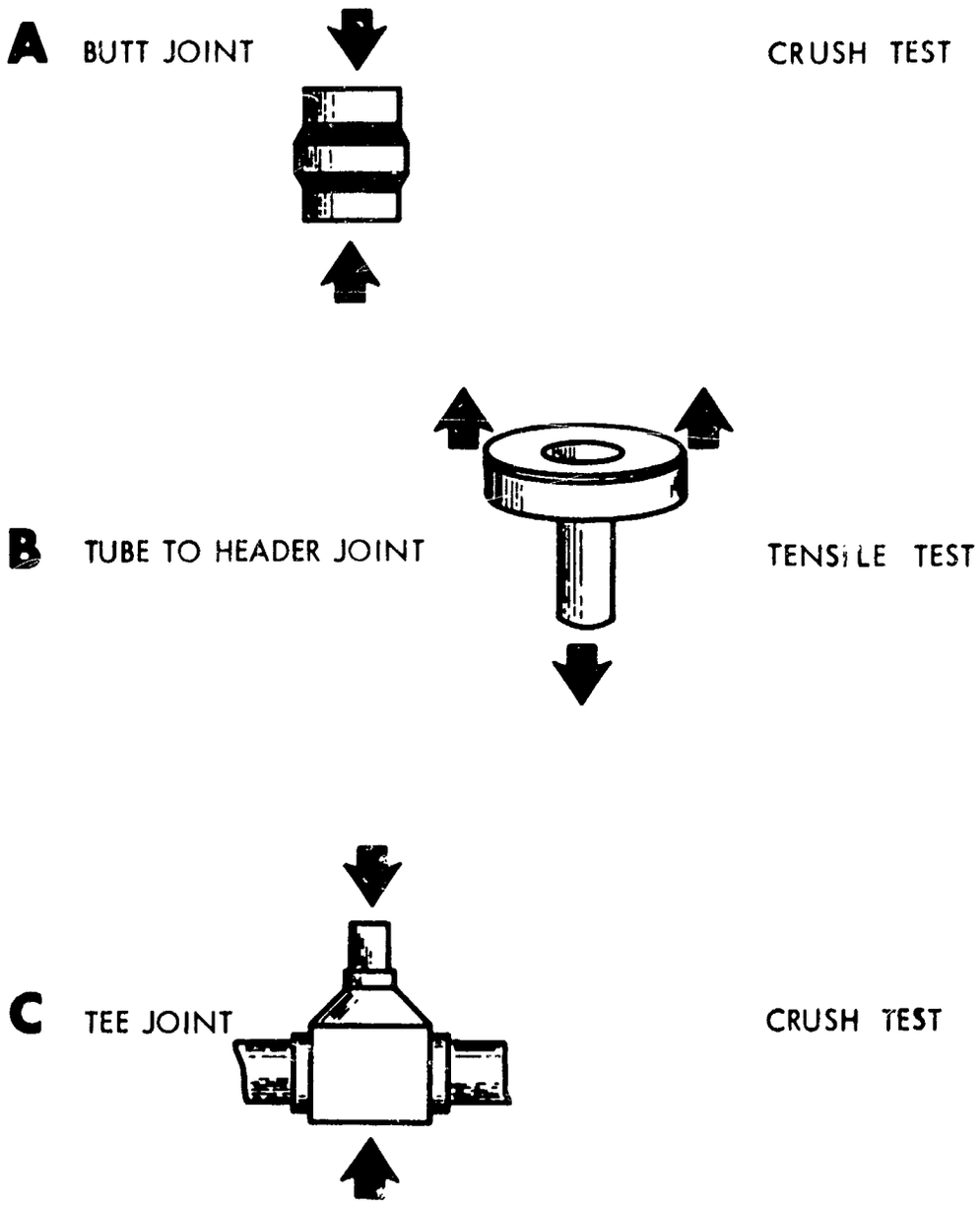

Figure 4. Destructive Tests Used for Weld Joints

B. BIMETAL TUBING

The co-extruded, co-drawn bimetal tubing used in this program was supplied by NASA. The material was fabricated in June 1964 by Nuclear Metals Inc. for the Aerojet General Corporation. Two basic sizes were fabricated, approximately 40 feet of 0.800 inch OD and 180 feet of 0.510 inch OD tubing. The tubing was produced by cold drawing a co-extruded tube blank to final size.

Typical photomicrographs of the two tubing sizes are shown in Figures 5 and 6. The higher magnification photographs in Figure 6 show the diffusion zone at the bimetal interface to be less than 0.0001 inch in width for the large diameter tubing, and less than 0.00005 inch in width for the small diameter tubing. The small diameter tubing interface is much more distorted, presumably as a result of the increased number of drawing operations. The complete fabrication history is not available, but the tubing was stress relieved at various steps in the drawing operation. The as-received hardness of the bimetal tubing is shown in Figure 7. For the evaluation program Astronuclear Laboratory received one 20-foot length of larger diameter tubing and two 20 foot lengths of small diameter tubing. The length of large diameter tubing was about 40-50 percent bonded as determined by ultrasonic pulse echo examination. The one 20-foot section of small diameter tubing used for this evaluation was rated at 55-65 percent bonded and the remaining section, which was preserved for fabrication applications, was rated at over 95 percent bonded. Thus, quite a few of the section views of weld joints will show obvious unbonding that is not a reflection upon the joining methods.

The two 20-foot lengths of tubing evaluated were sectioned into four 5-foot lengths. Five metallographic samples were prepared from each tube for bimetal dimensional analysis. The measured dimensions essentially agreed with those reported by the manufacturer, Nuclear Metals. The dimensional analyses are listed in Table 1. The 3σ variation predicted for the entire lot of tubing is also presented in the same table. The interaction between tube eccentricity and bimetal thickness variation is also presented in the same table as a calculated radius

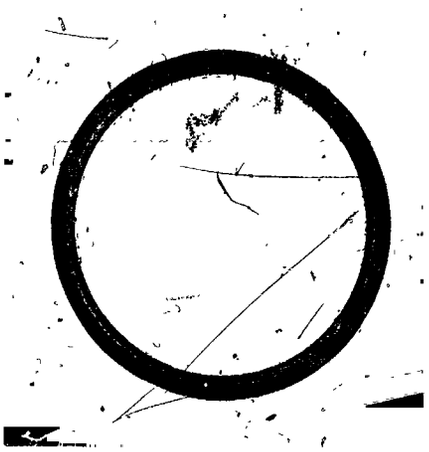

15.449 3X

0.800" OD
BIMETAL
TUBING

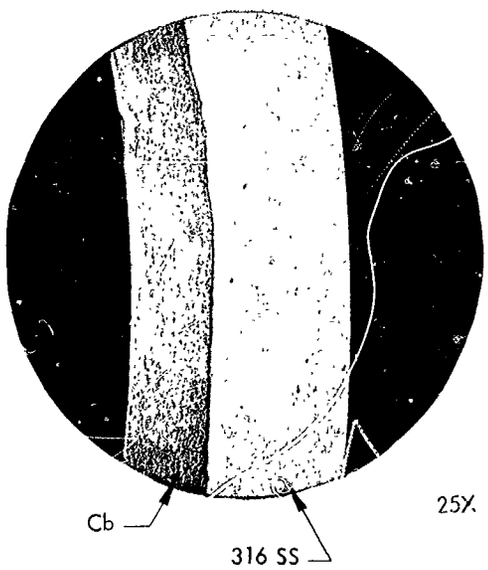

25X

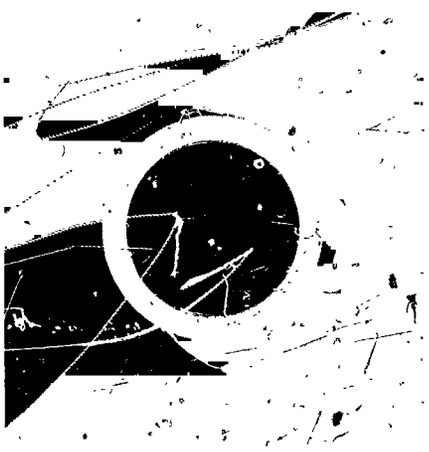

15.450

0.510" OD
BIMETAL
TUBING

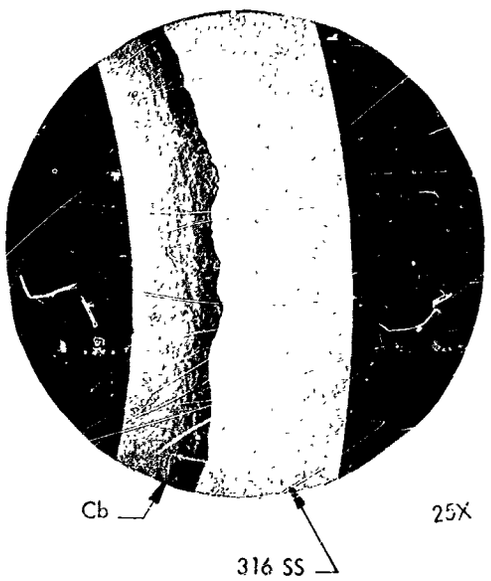

25X

611614-1B

Figure 5. Bimetal Tubing Macrophotographs

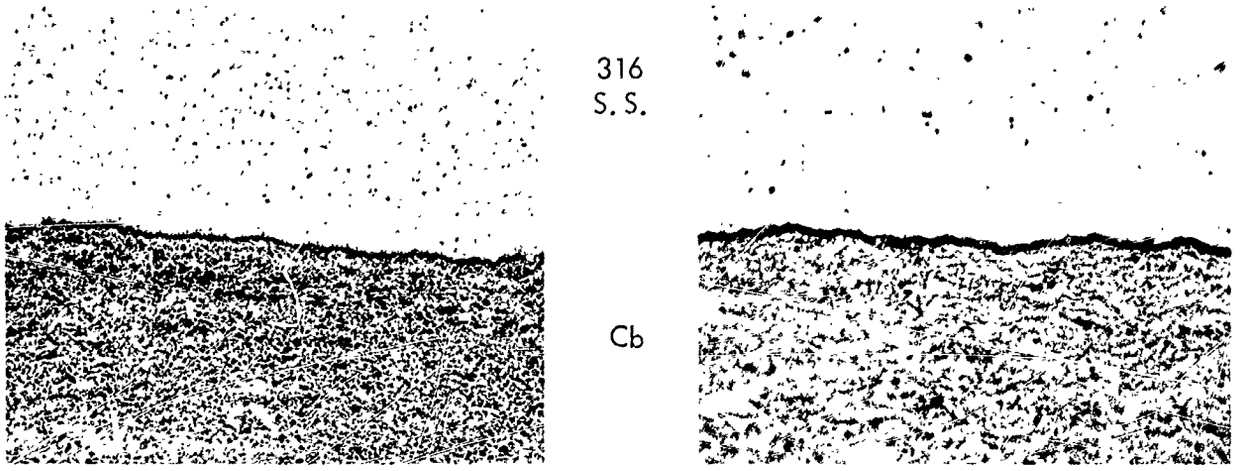

14,296 150X 14,296 400X

Large Diameter, . 800" O. D. Tubing
Transverse Section

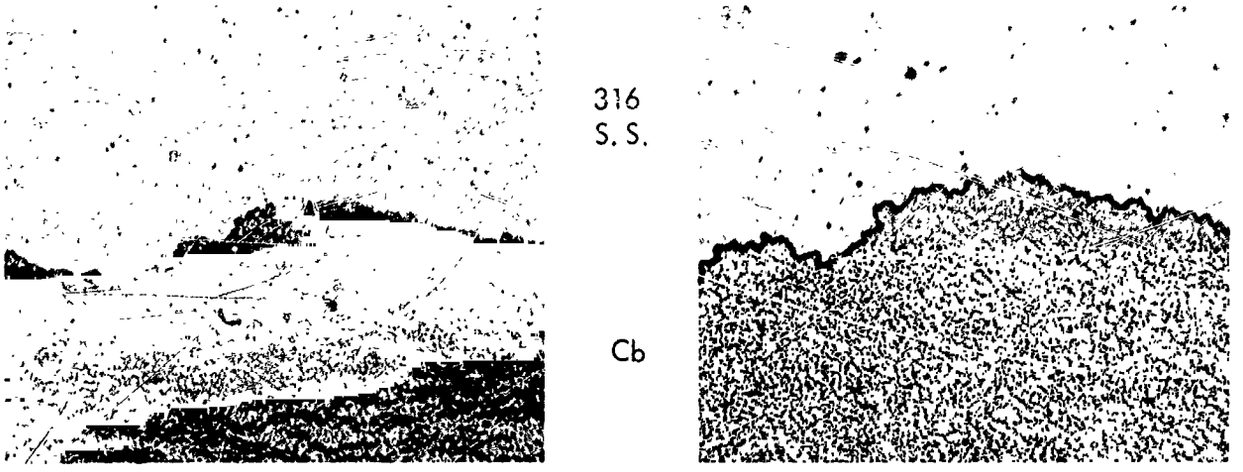

14,297 150X 14,297 400X

Small Diameter, . 510" O. D. Tubing
Transverse Section

Figure 6. Bimetal Tubing Microphotographs

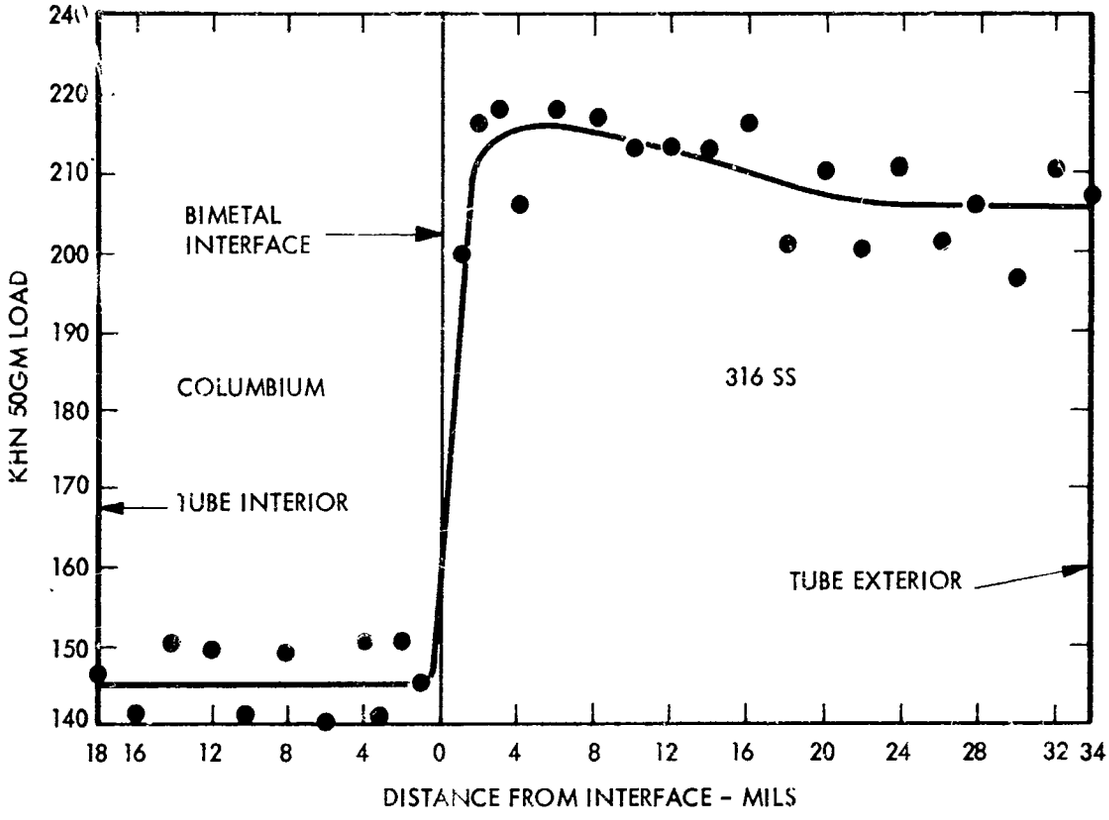

KNOOP HARDNESS TRAVERSE OF BIMETAL TUBE WALL

AVERAGE HARDNESS OF TUBE WALL

	VICKERS[6]	ROCKWELL B
0.800" OD TUBE		
316 SS	165	85
Cb	106	59
0.510" OD TUBE		
316 SS	178	88
Cb	117	66

6 10Kg LOAD FOR 316 SS
5Kg LOAD FOR Cb

611614-2B

Figure 7. Hardness Measurements of Bimetal Tubing

TABLE 1

DIMENSIONAL ANALYSIS OF BIMETAL TUBING

Tubing	Outside Diameter		Inside Diameter		Total Wall		316 S.S.		Columbium	
	Average	3σ	Average	3σ	Average	3σ	Average	3σ	Average	3σ
0.800" OD	0.7970	±0.0084	0.6838	±0.0132	0.0566	±0.0042	0.0352	±0.0035	0.0214	±0.0022
0.510" OD*	0.5116	±0.0024	0.4002	±0.0054	0.0557	±0.0025	0.0347	±0.0031	0.0210	±0.0033

*Small diameter tubing was centerless ground.

Variation In Clad Interface Location

	Ave.	3σ
Large Tube	.3633	± .0060
Small Tube	.2211	± .0036

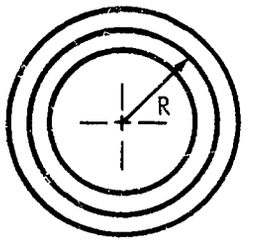

If the stainless steel cladding is removed in a lathe turning operation, the interface must be undercut by the 3σ variation to assure complete removal of stainless steel.

Astronuclear Laboratory

to the bimetal interface. The 3σ variation in this radius, 0.006 inch in the large tubing and 0.004 inch in the small tubing is significant because in weld joint preparation the columbium liner must be undercut by the above amount to assure complete removal of the stainless steel. In actual machining operations, the 0.021 inch columbium liner was generally machined to 0.015 inch thickness for successful weld joint preparation.

Columbium Liner Defects

Four defects consisting of 1/8 inch diameter holes in the columbium liner were found in the single 20-foot length of 0.800 inch OD tubing. The defects were observed after the tubing was sectioned and no record could be made of defect location along the tube length. Figure 8 shows typical longitudinal and transverse views of a defect, the total tube wall thickness remaining constant, but the stainless steel occupying the entire wall thickness. The defects are observable on tube radiographs. Hardness measurements showed no change in hardness in the defect area. The defects are true discontinuities falling outside the measured 3σ variation in the columbium clad thickness shown in Table 1.

C. BUTT JOINT DEVELOPMENT

Description and Fabrication

From a system fabrication standpoint, the butt joint is frequently required as a final assembly weld for large systems, often presenting weld shielding atmosphere problems since large apparatus may require local clamp-on atmosphere or vacuum enclosures.

Figure 9 shows previous solutions to the bimetal butt joint investigated by Aerojet General[1] in support of the SNAP-8 program. These joints were designed for high temperature liquid metal service, but were not entirely satisfactory because of materials compatibility or process control problems. Types A and B are acceptable if the bimetal interface and stainless steel surface is protected from mercury corrosion by a protective layer of refractory metal.

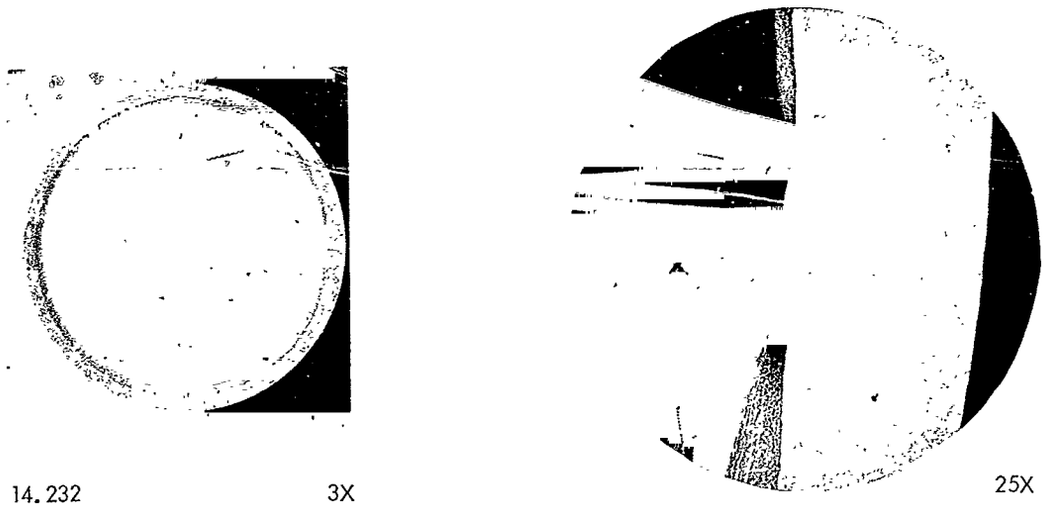

14.232 3X 25X

TRANSVERSE SECTION

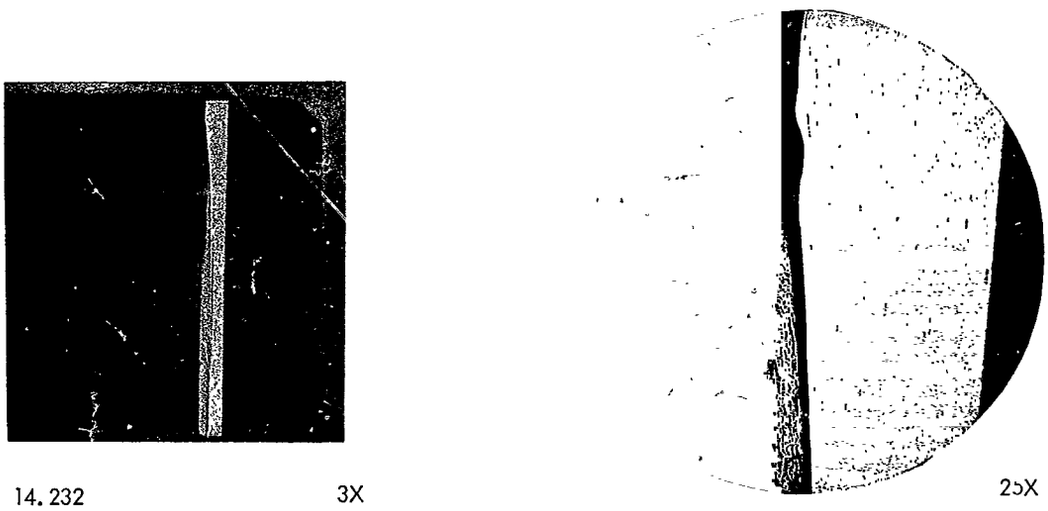

14.232 3X 25X

LONGITUDINAL SECTION

611614-3B

Figure 8. Local Defect in Large Diameter Bimetal Tubing

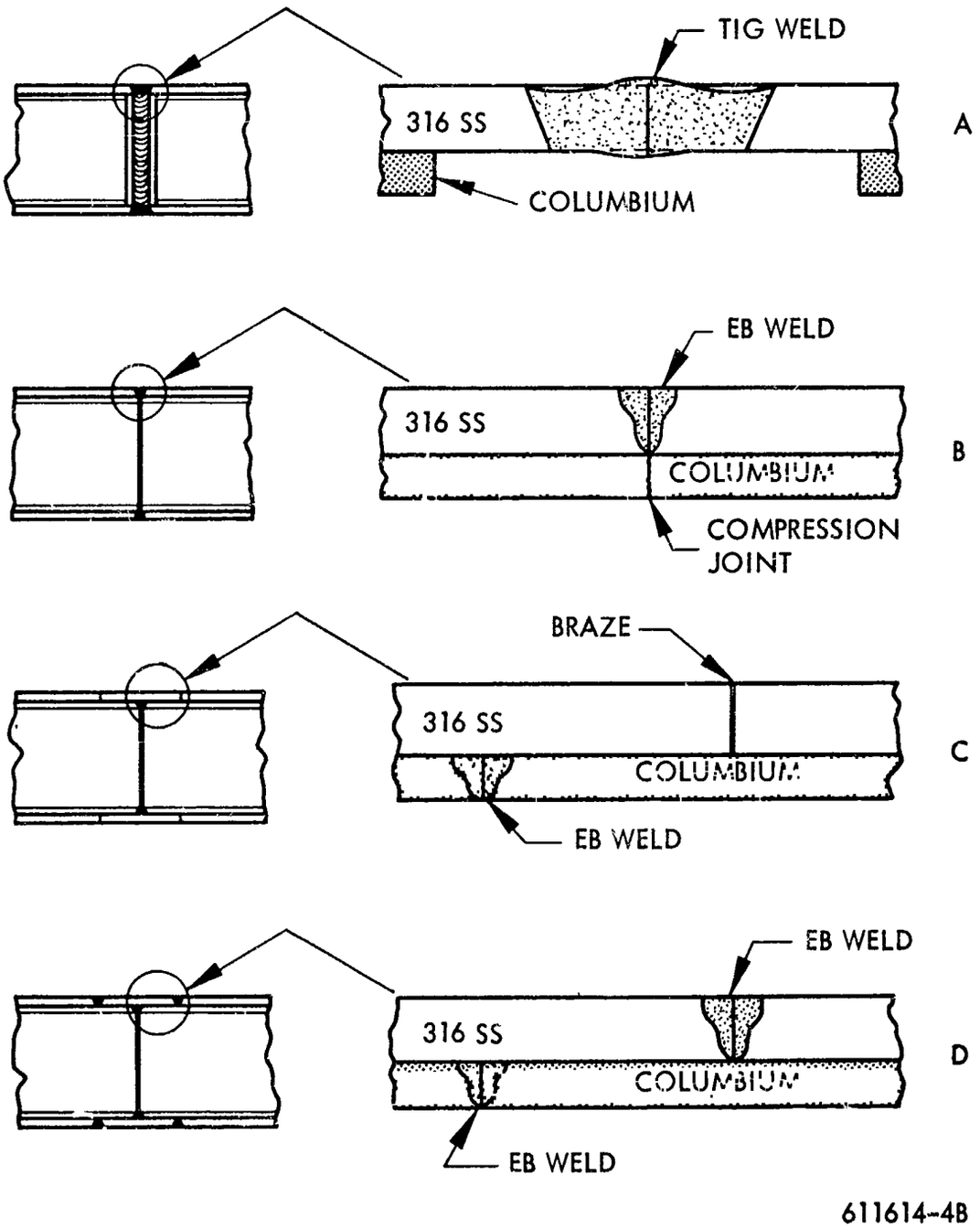

Figure 9. Previous Joining Processes for Bimetal Tube Butt Joints

Type C is a completely sealed joint, but required the development of braze systems compatible with high temperature alkali metals. Type D, in which a split stainless steel ring is placed over a previously electron beam welded columbium joint, requires the precise depth control of electron beam butt welds to prevent bimetal alloying. Normal tolerances in fabrication and fit-up generally do not permit this type of control for butt joints. The electron beam process produces complete weld puddle mixing whenever slight over-penetration is encountered. Thus, though an all welded joint was desired to meet the stringent requirements of high temperature liquid metal service, no design was available with the requisite process control.

Two basic approaches were used in developing a successful butt joint design. As shown in Figure 10 these were an electron beam lap weld process using a slip over, one piece sleeve, and a pre-placed filler process in which stainless steel is deposited over a columbium weld, using barrier layers if necessary to prevent alloying of the stainless steel and columbium. The same weld joint preparation is used for either joint design. The stainless steel outer cladding is first removed by machining to expose the columbium liner followed by pickling and handwork to remove all traces of the stainless steel. The inner columbium weld is made first using electron beam welding for the electron beam lap weld design and gas tungsten arc welding for the preplaced filler design. Examples of completed inner welds are shown in Figure 11. Approximately twice the length of exposed columbium is required for the tungsten arc weld to accommodate the larger weld bead and heat affected zone.

The electron beam process, for both the internal columbium weld and the external stainless steel lap weld, was immediately successful and produced the compact butt joint shown in Figure 12. The lap weld joint permitted precise depth control of the stainless steel weld in spite of the normal tolerances in part dimensions and in the welding process. Shown in Figure 12 is the split stainless steel ring used to reinforce the columbium liner. An external, one piece stainless steel ring is slipped over the columbium weld and split ring, and is lap welded in place to produce a completely sealed, all welded joint.

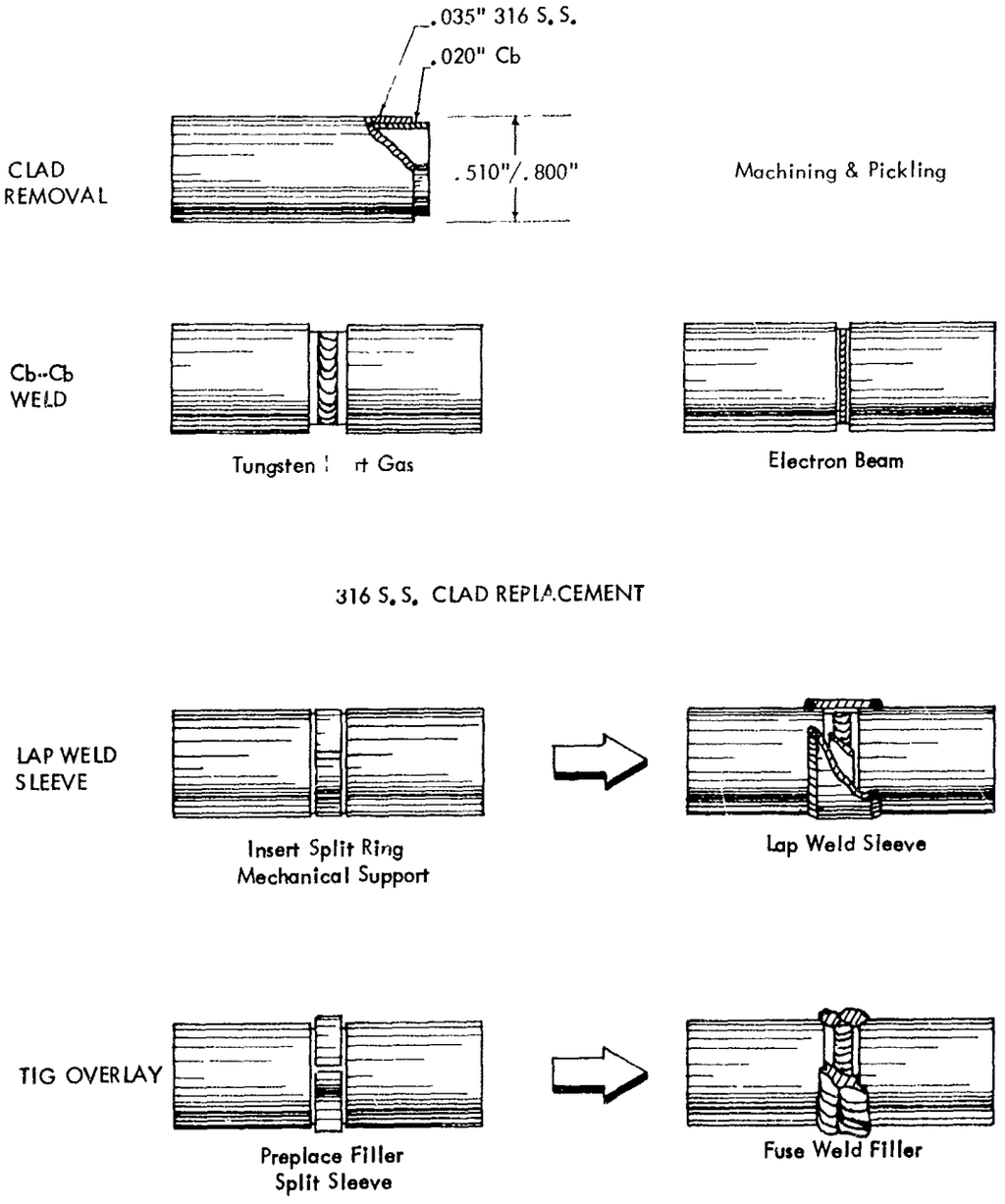

Figure 10. Butt Joint Fabrication Sequence

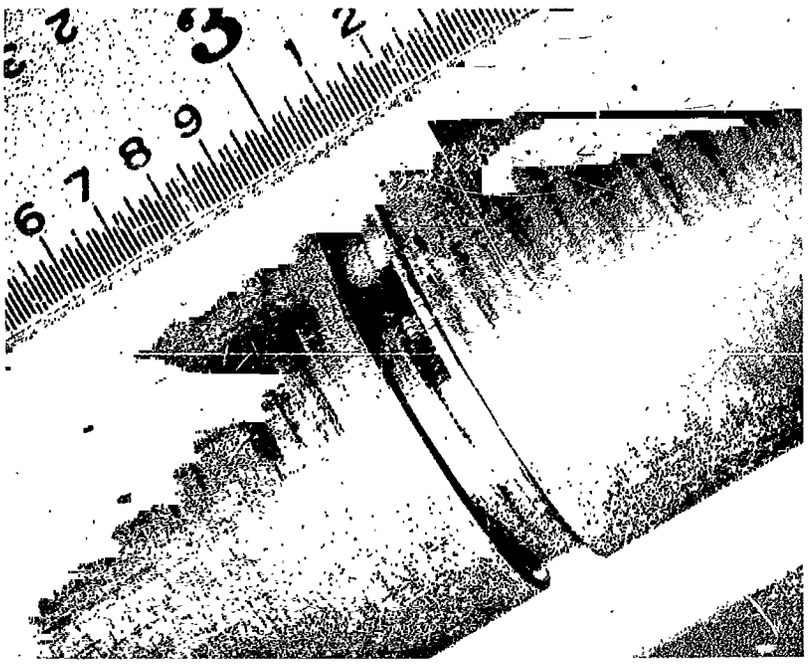

50 ipm
100 KV
.018 Trans. Def.
1st Pass - 2.5 MA
2nd Pass - 4.0 MA

EB WELD

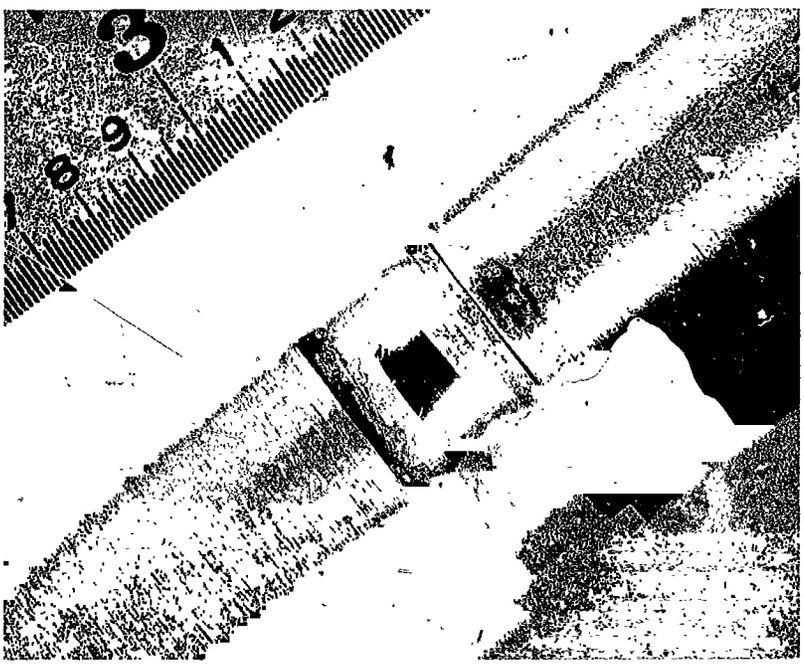

15 ipm
DCSP
20 amps

He Atmosphere
.040" electrode
.020" gap

TIG WELD

Figure 11. Columbium Butt Weld Joint

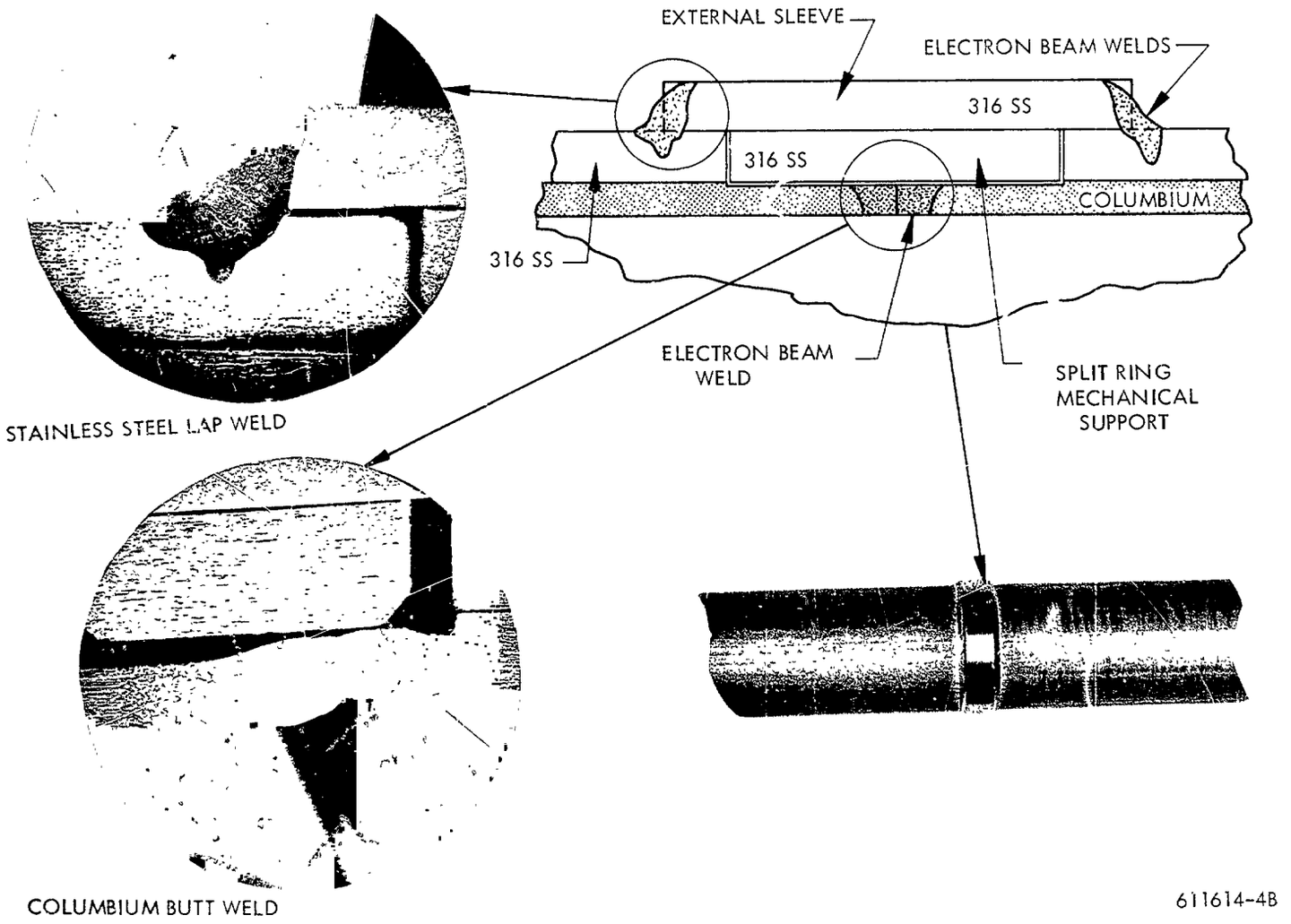

Figure 12. Butt Joint - Electron Beam Lap Weld

Since the electron beam process is not very adaptable to final assembly welds on large apparatus, work was continued to develop a welding process more amenable to "field welding" conditions, namely gas tungsten arc and associated processes. The plasma arc overlay process was evaluated using a powder feed nozzle with variable plasma and transferred arcs. The initial development effort was made with 316 stainless steel tubing using internal water cooling. Although the plasma arc equipment had produced acceptable metal overlays on flat work such as turbine blades, extreme difficulty was encountered in producing quality overlays on the relatively thin tubing. As the power level was increased to produce a smooth overlay, burn through usually occurred, indicating unacceptable process control. Figure 13 shows the best quality deposits obtained on stainless steel tubing. A section of the tubing is shown indicating the acceptable penetration obtained with water cooling. Difficulties were increased when the overlay was deposited in a shallow groove, simulating the initial columbium weld joint. The plasma arc wandered to the groove edges, straying from side to side and produced an unacceptable deposit. A complete description of the process and welding parameters used is included in the equipment section of this report.

Gas tungsten arc welding, using automatic wire feed, was also used to produce a stainless steel overlay. Trial welds were made on grooved stainless steel tubing, but problems of non-uniform deposit and burn through occurred. Barrier layers in the form of thin stainless steel split rings and flame sprayed layers of molybdenum and zirconia were evaluated. Burn through was reduced while problems with cold shuts and weld puddle blowouts developed, and an acceptable welding process was not developed. However, an observation of the thin stainless steel barrier layer performance led to a trial using full thickness split rings and gas tungsten arc welding. These trials, essentially preplaced filler welding, were very successful, having the form shown in Figure 14.

Figure 15 shows overall and cross-sectional views of the double girth butt weld joint. An alloyed diffusion zone is sometimes produced at the stainless steel weld-columbium interface, but hardness and electron beam microprobe traverse measurements indicate the alloying to be confined to within a few mils of the interface.

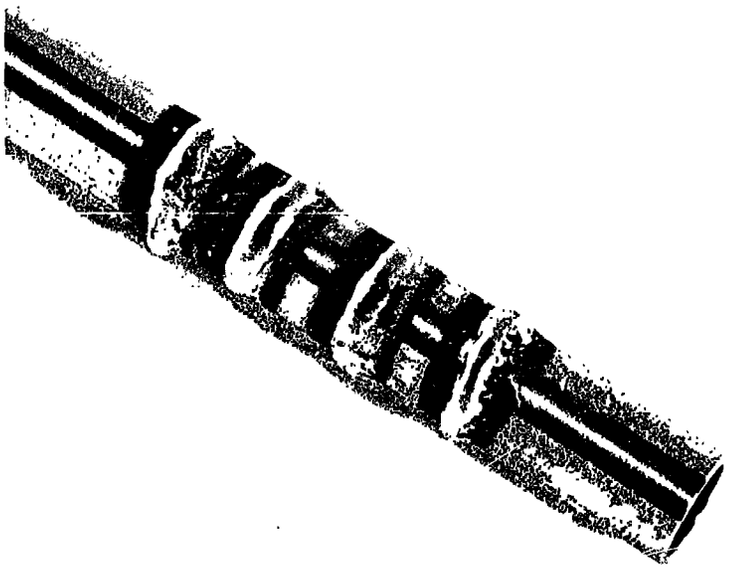

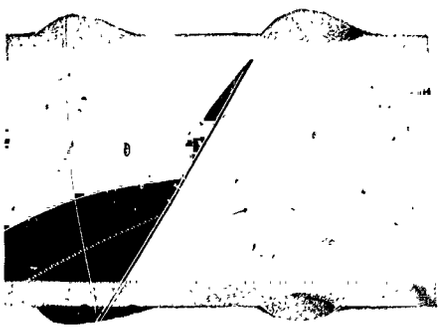

14, 563A

2X

SECTION VIEW OF PLASMA ARC OVERLAY

611614-6B

Figure 13. Plasma Arc Overlay Process

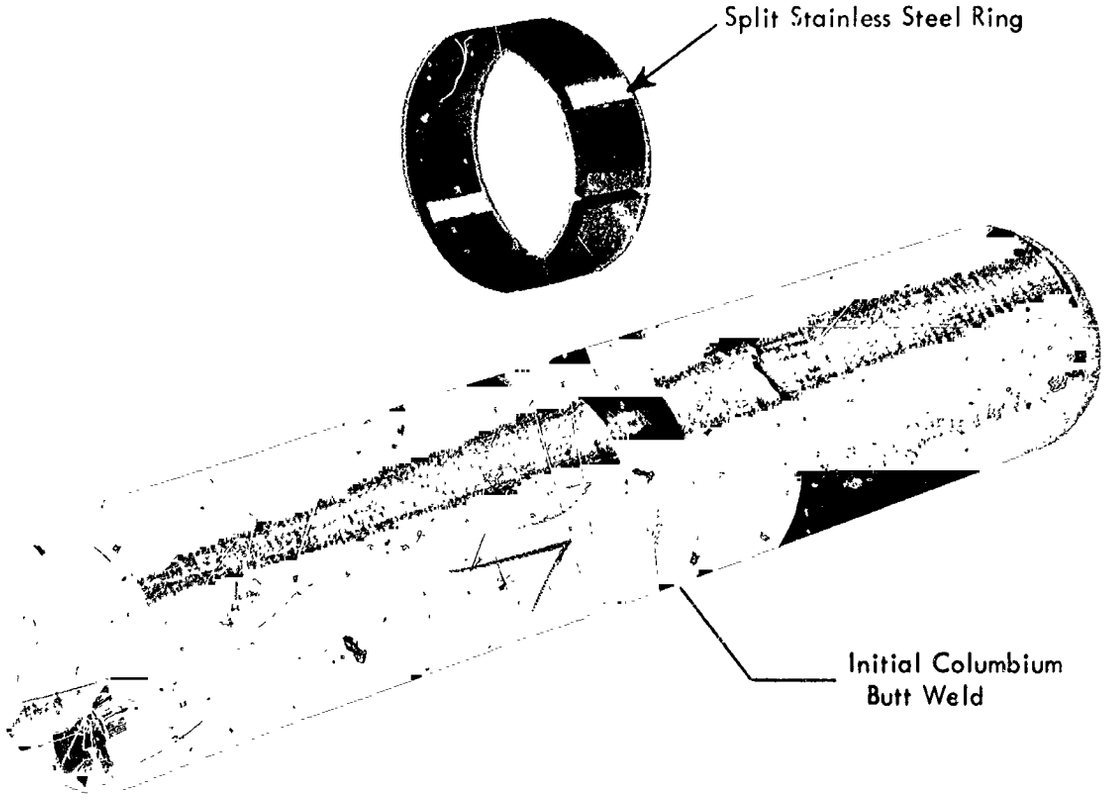

Figure 14. Reference Design Butt Joint - Assembly View

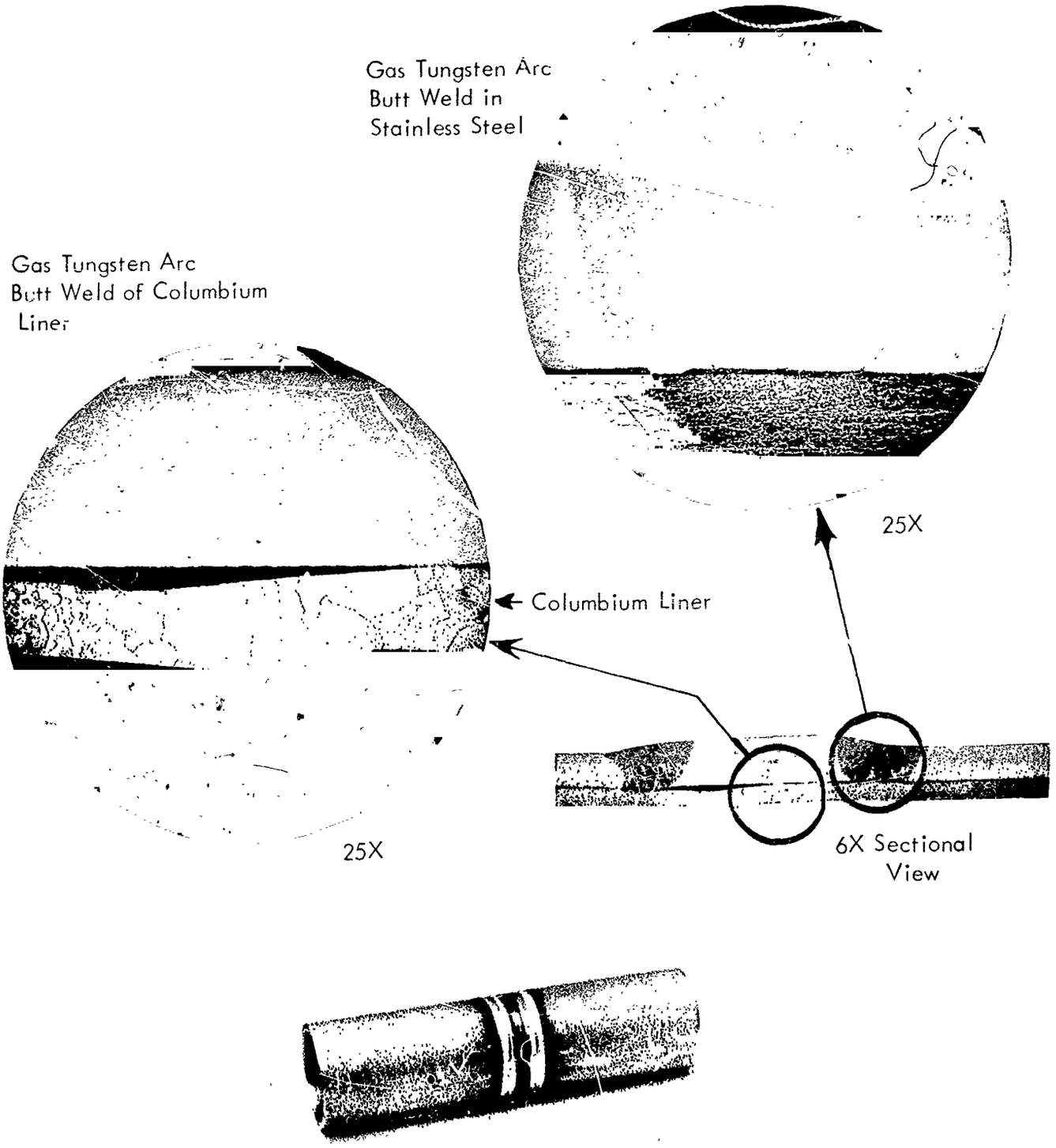

Figure 1.5. Double Girth Butt Weld - Section View

A gas tungsten arc lap welded joint was also evaluated, similar in design to the electron beam lap welded joint, but of greater length to accommodate a columbium-tungsten arc weld. The stainless steel lap weld required very fine control of power input. Too little power produced "peel back" and lack of fusion. Slightly higher power input produced a successful lap joint, but with excessive penetration into the columbium. The threshold power level was difficult to control and for this reason the process was abandoned.

In summary, two successful processes were developed. The electron beam lap weld provided acceptable process control, but in view of the "field welding" capability desired, the second process, the "double girth butt weld" was selected as the reference process for the butt joint. If a small, 1 KW electron beam gun were available, similar to the clamp on, rotating, tungsten arc torches, the electron beam process could be considered for assembly welding. Table 2 lists the welding parameters used for the two successful designs. The welding equipment is fully described in the equipment section of this report. Fourteen pair of butt joint specimens were initially machined and utilized for the fabrication and in-process evaluation sequence outlined below:

Fabrication and Evaluation Sequence

1) Gas tungsten arc weld columbium
2) Visual inspection, internal and external
3) Dye penetrant inspection
4) Radiography
5) Helium leak test
6) Gas tungsten arc weld stainless steel overlay
7) Visual inspection, internal and external
8) Dye penetrant inspection
9) Radiography

On Selected Specimens

10) Metallographic sectioning
11) Ultrasonic inspection of bimetal bond

TABLE 2

WELDING PARAMETERS FOR BUTT JOINTS

Electron Beam Lap Weld		
	Columbium Butt Weld	Stainless Lap Weld
Amps	3.6 MA	2.0 MA
Volts	80 KV	100 KV
Speed	50 ipm	25 ipm
Deflection	.018" transverse	.018" transverse
Double Girth Butt Weld (Gas Tungsten Arc Process in Helium Atmosphere Welding Chamber)		
	Columbium Butt Weld	Stainless Butt Weld
Amps	25 DCSP	25 DCSP
Volts	15	15
Speed	15 ipm	15 ipm
Gap	.032"	.045"

The in-process inspection sequence is require since most of the observations of the initial weld cannot be made after the stainless steel cladding is replaced. This is particularly true of the helium leak test and external dye penetrant inspection. Conversely, the helium leak test could not be used on the final evaluation because the first weld seals the specimen. The documentary process sequence shown in Table 3 can be used as an approximation of the process capability. The various repair operations and rejections are shown. The overall process yield was 78 percent, but most of the difficulty was caused by the longitudinal weld of the split stainless steel ring. This weld, which was subject to over-penetration was made manually and consequently suffered from variability in process control. Automatic welding, which could be used for this critical weld, should improve the overall yield. It is significant that no problems were encountered with stainless steel-columbium alloying due to residual smears of stainless steel on the columbium. This was a problem during the first phase of the program, but the improved joint preparation procedure used, including pickling, appears to have solved the problem. The tungsten arc changes to a green color whenever alloying occurs, providing an indication of a defective joint.

Following the fabrication of 10 acceptable specimens, the evaluation program outlined in Figure 2 was followed.

Sectioning Data-Weld Penetration Control

Seven butt weld specimens were each sectioned into four quadrants providing 56 individual sections of the stainless steel lap weld and half as many sections of the columbium weld. These data are summarized in Table 4. A statistical distribution of the penetration is shown in Figure 16a and indicates both marginal process control and two different weld penetration populations; one centered around 50 percent penetration and another group near 100 percent penetration. Full penetration, near 100 percent, is desired for this type of weld joint.

TABLE 3

PROCESS SEQUENCE OF REFERENCE BUTT JOINT DESIGN

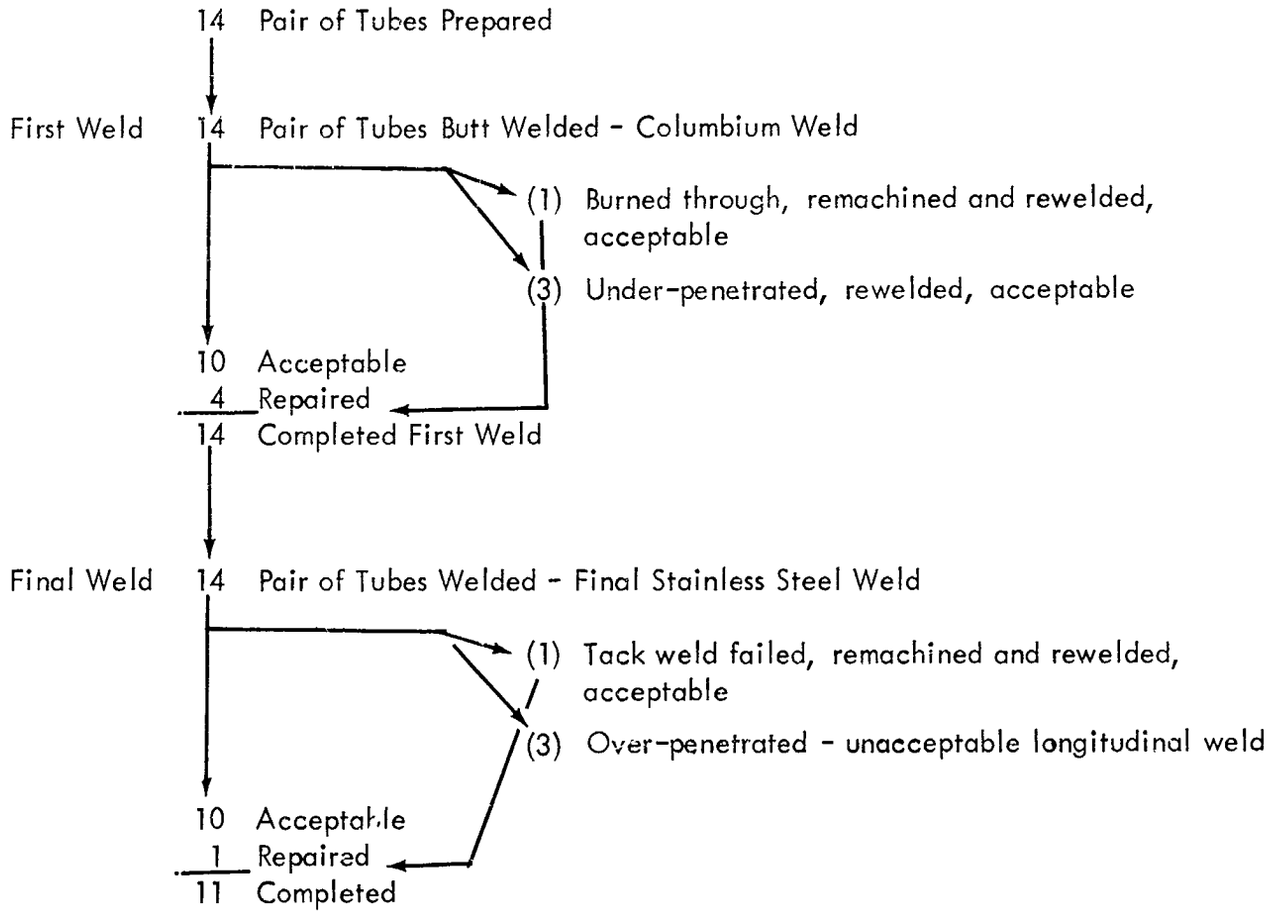

Process Yield 11/14 = 78 Percent

TABLE 4

BUTT JOINT - WELD PENETRATION SUMMARY

Tube No.	Section	Weld No. 1		Weld No. 2		Columbium Weld	Tube Average	
		% Pen.	Misalign. Mils	% Pen.	Misalign. Mils	% Pen.	% Pen.	Misalign. Mils
2	A	100	10	100	-20	100		
	B	100	0	100	0	100		
	C	100	10	100	0	100		
	D	100	10	100	0	100	100	2
4	A	100	0	67	0	100		
	B	77	0	100	10	100		
	C	100	0	100	0	100		
	D	100	20	100	20	100	92	6
5	A	78	30	56	30	100		
	B	50	40	50	60	100		
	C	100	40	33	40	100		
	D	61	40	56	40	100	60	40
6	A	56	40	30	89	100		
	B	6	50	50	72	100		
	C	22	50	50	44	100		
	D	33	45	40	44	100	46	46
7	A	100	20	30	52	100		
	B	100	20	30	43	100		
	C	61	30	20	100	100		
	D	95	30	30	44	100	76	26
9	A	100	30	100	50	100		
	B	39	40	22	40	100		
	C	78	40	44	50	100		
	D	56	40	95	30	100	66	40
12	A	100	30	100	-10	100		
	B	83	15	100	15	100		
	C	100	0	100	20	100		
	D	100	16	100	16	100	98	12

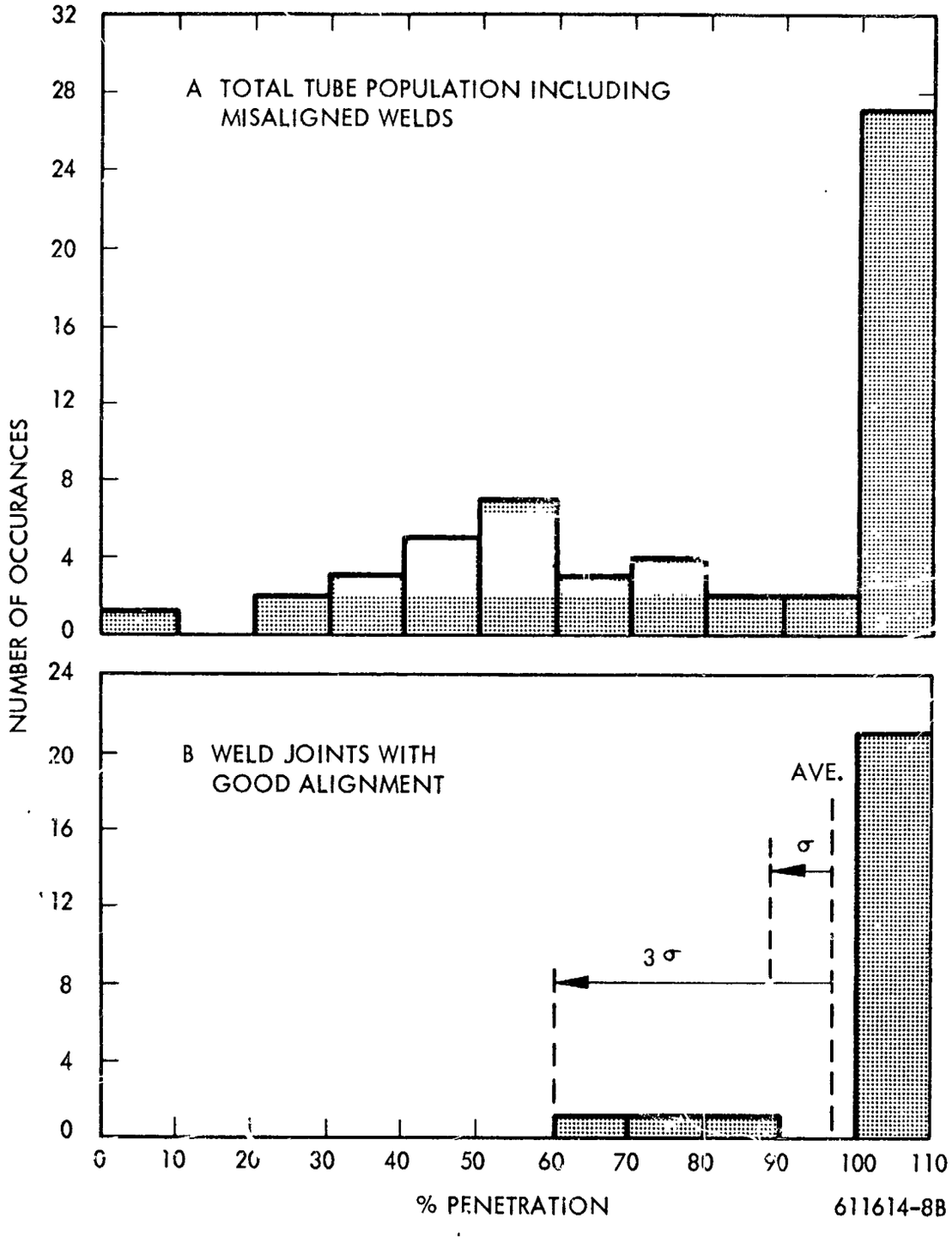

Figure 16. Statistical Distribution of Butt Weld Penetration Data

An examination of the sectioned weld indicated that under-penetration was caused by the weld bead missing the seam or misalignment of the weld. The proper sized weld puddle was always present, but it was often displaced too far towards the split ring. The split ring used was slightly thicker than the original tube wall, and the sharp corner of the ring insert strongly attracted the weld arc. Table 4 also lists the joint alignment which indicates that three out of the seven sectioned tubes had good alignment and a segregation of these tubes from the total population results in the distribution shown in Figure 16b. This distribution is close to that required for adequate process control, indicating that over 99 percent of all the welds made would have at least 60 percent penetration.

All welds were made by the same technician using identical alignment techniques, and the variation in weld puddle location indicates need for improved joint design or better weld tooling. Since an electrode movement of 0.030 inch or 1/3 the diameter of the welding electrode is the tolerance involved, precision welding tooling incorporating dial gages or micrometer adjustments may solve the problem. Figure 17 shows the method of measuring weld penetration and examples of sectioned welds.

Excess Penetration

One anticipated problem of the reference butt joint design is alloying between the columbium liner and the cast-in-place stainless steel butt weld. The process is made feasible by the 1800° F difference in melting points, (2550°F for the 316 stainless steel and 4380°F for columbium.) The weld is made quickly enough to limit the diffusion formation of low melting point eutectics. Figure 18 shows a hardness traverse through the stainless steel-columbium weld interface. The weld interface displays one of the larger alloy zones of all the welds' sections and should represent the limit of stainless steel weld alloying. The hardness traverse does not indicate extensive diffusion alloying of either the columbium liner or the stainless steel.

Electron Microprobe Analysis. As a further check on the extent of alloying at the stainless steel weld-columbium interface, an electron microprobe analysis was made by the Advanced Metals Research Corporation. Selected point analyses, line scans, and complete

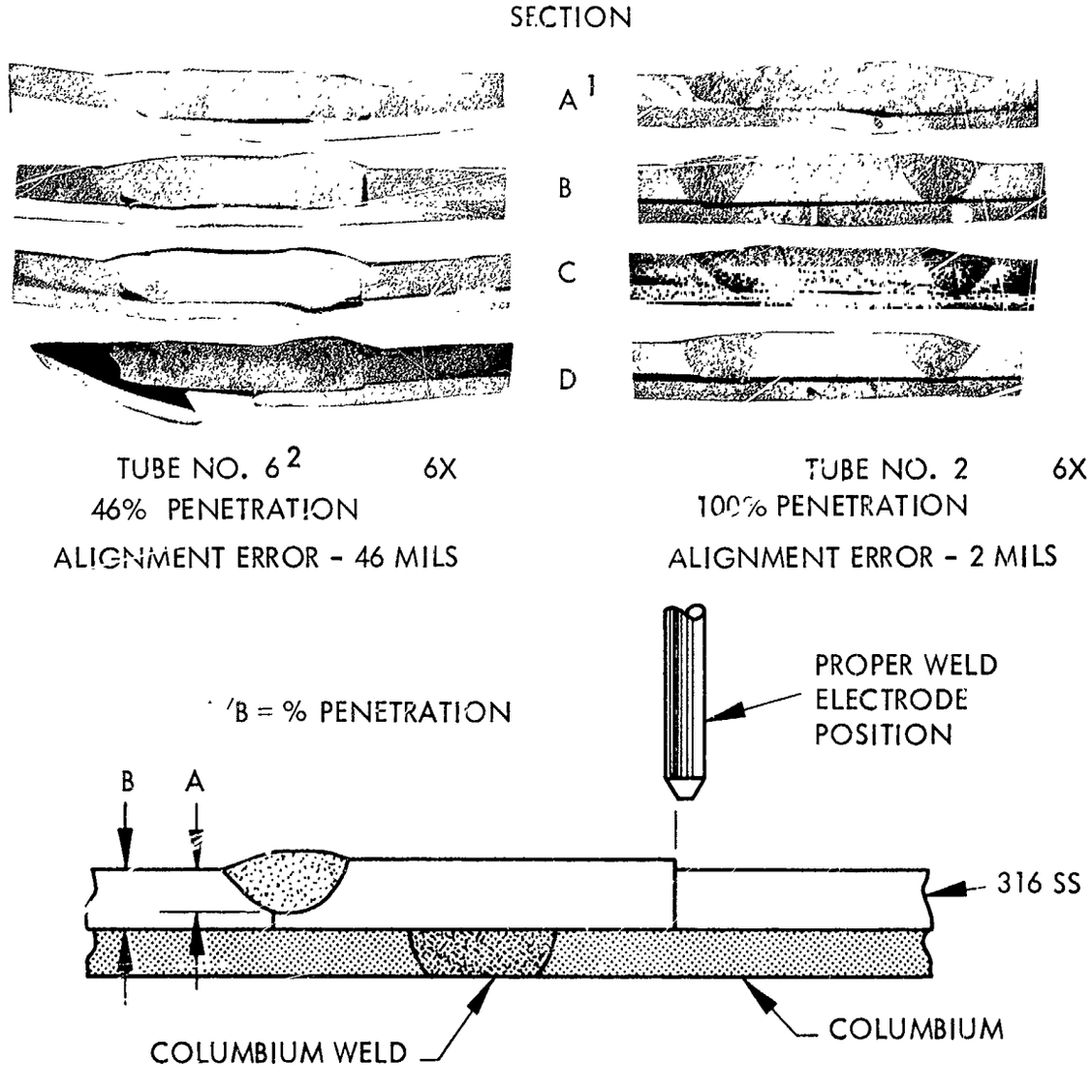

1 SECTION OF LONGITUDINAL TACK WELD

2 TUBE DISTORTION DUE TO INTERNAL PRESSURE TESTING

611614-7B

Figure 17. Weld Penetration Measurement of Butt Joint

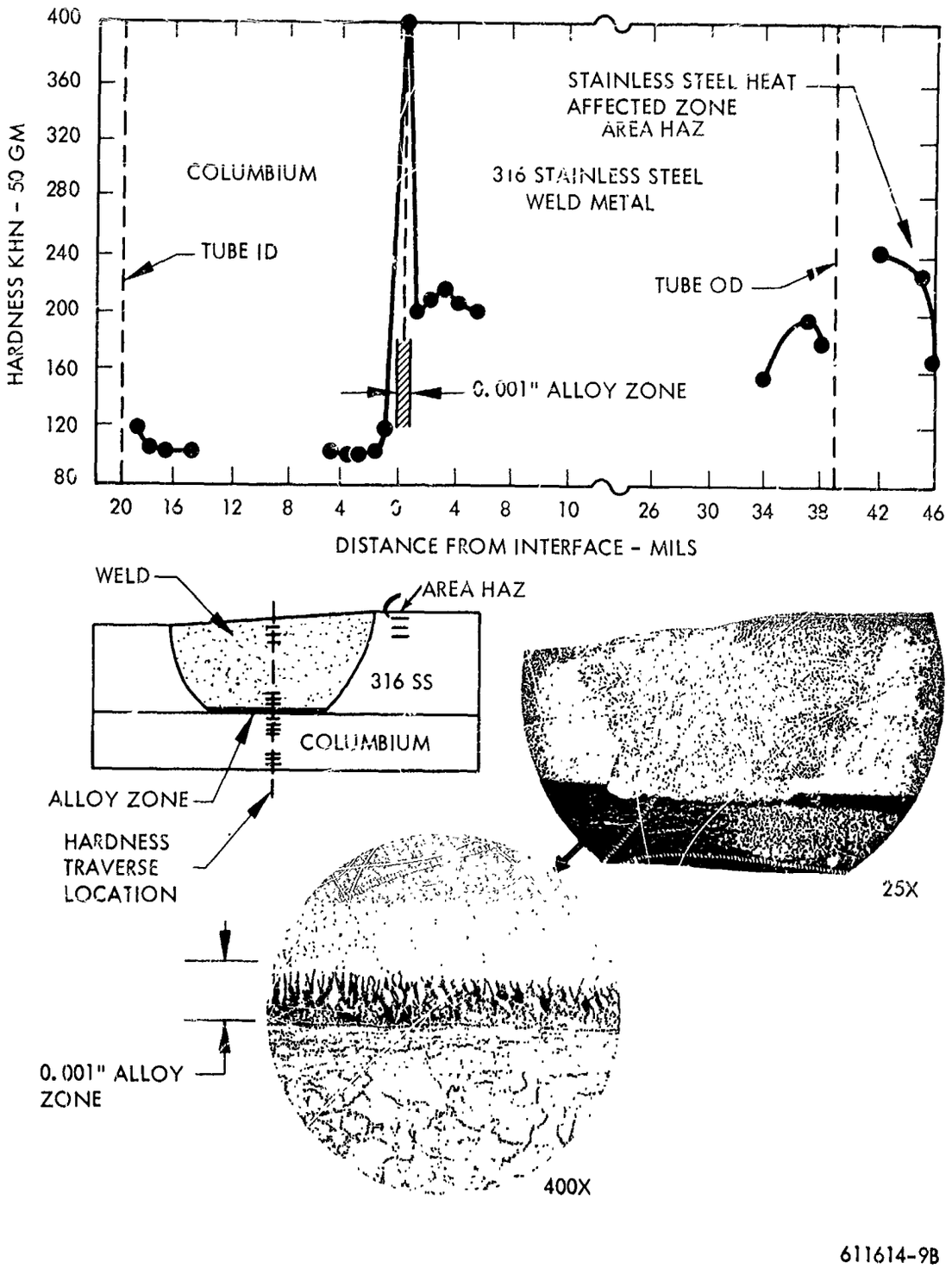

Figure 18. Hardness Traverse Through Weld Interface

area scanning techniques were employed. Figure 19 shows a trace of columbium concentration obtained by traversing along a path inclined 45° to the columbium-stainless steel interface. The "banded" areas intersected are evidently formed by the swirling motion of the stainless steel weld puddle. The line traverse indicates the columbium concentration quickly drops to negligible values except in the banded areas. Similar line scans were obtained for Fe, N, and Cr, but the results were not significant. A line scan for Cb made perpendicular to the surface through band "K" on Figure 19 yielded similar results. The width of the electron beam line scan is 1 micron. Point chemical analyses were made using a 1 micron spot size and the results are shown in Figure 20. The point analyses describe the composition of the cell structure produced at the bimetal interface and in the banded areas shown in Figure 19. Because of the concentration of Cb at the cell boundaries, the structure is thought to represent incompletely mixed liquids which were formed and solidified in a very short time. Columbium has not diffused to any extent into the bulk of the stainless steel weld and significant diffusion of Fe and Cr into the columbium appears to be limited to within 35 microns (1.4 mils). An area was scanned to produce a "raster" image for the various alloy elements. Figure 21 shows the results obtained in scanning for columbium concentration. The top view shows a photomicrograph of the area as compared to the electron beam scan shown below. The light areas, which show areas of high columbium concentration, are the cell boundaries and correspond to the point analyses shown in Figure 20.

In summary, bulk diffusion of alloying elements is limited to within a few mils of the interface. In the stainless steel weld, however, local areas of columbium contamination extend for a considerable distance through the weld. Since columbium and tantalum are used as carbide stabilizers in stainless steels, a minor amount of columbium alloying should not be detrimental.

Longitudinal Weld Excess-Penetration. The split ring is first welded into place by manually tacking and then seal welding the longitudinal split ring. Excess penetration was observed on three out of fourteen welds. The most massive sample is shown in Figure 22 as penetration of the entire tube wall. The excessive penetration was visually observed on the tube inside diameter and on tube radiographs. None of the seven tubes sectioned for weld penetration showed evidences of massive alloying. One section on each tube is cut directly through the longitudinal weld.

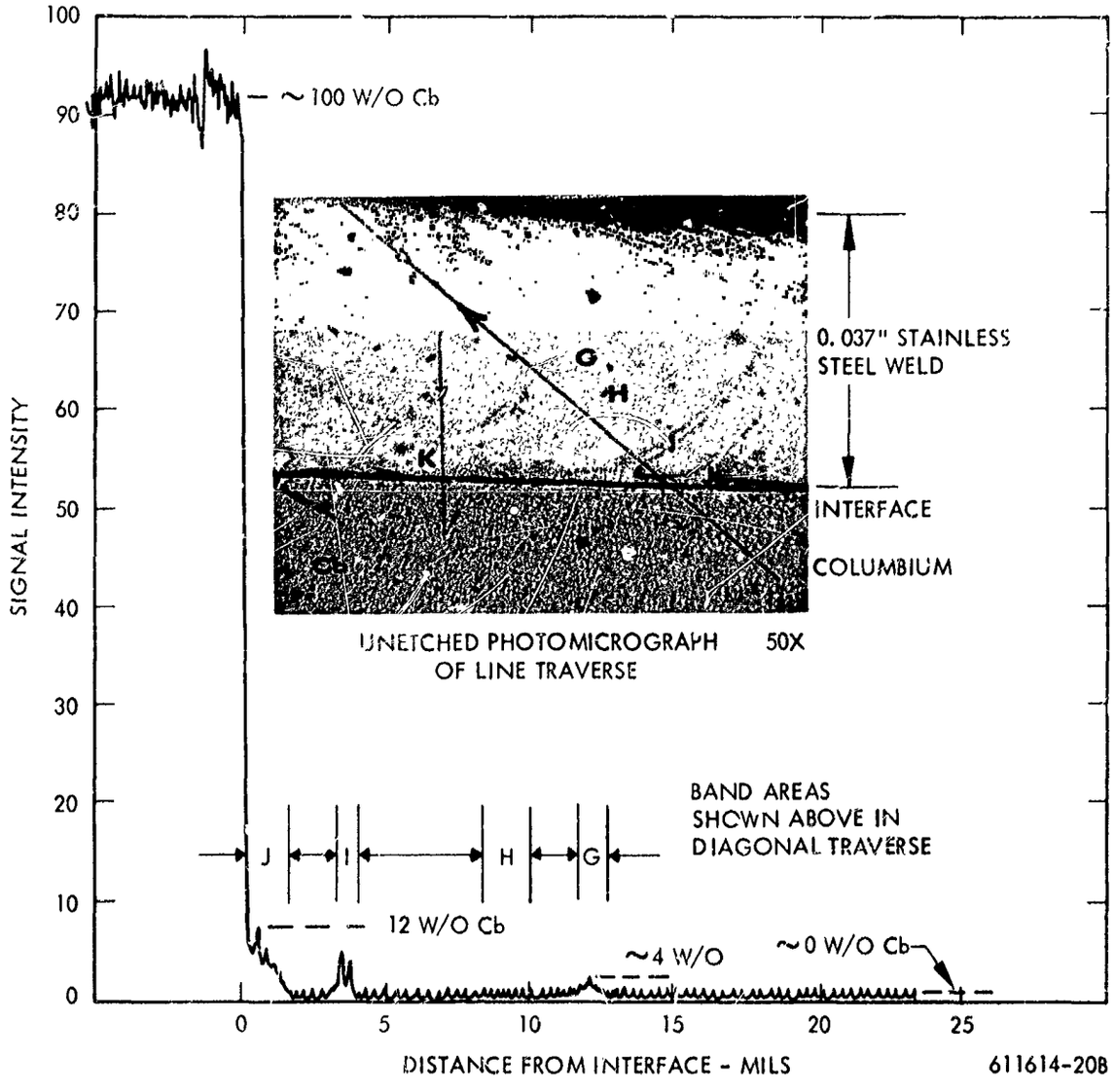

Figure 19. Electron Microprobe/Line Traverse of Weld Interface

POINT ANALYSIS CHEMISTRIES

AREA		Cb	Fe	Ni	Cr	Mo (w/o)
A	(~ 60μ into 316SS)	0.8	64.7	12.8	16.0	2.2
B	(open end of cell)	0.7	66.4	12.5	15.4	1.7
C	(center of cell)	1.7	65.3	12.4	14.9	1.7
C'	(cell boundary)	8.0	60.3	12.6	13.5	2.2
D	(~ 5-8μ from int.*)	11.8	57.2	12.4	12.0	2.3
E	(interface Cb side)	Bal.	2.9	0.3	0.4	0.3
F	(~ 10μ from int.*)	Bal.	0.1	0.03	0.03	0.03
G	(~ 25μ from int.*)	Bal.	0.04	~0	0.01	~ 0
H	(~ 35μ from int.*)	Bal.	0.01	~0	0.01	~ 0

POINT ANALYSES MADE IN BAND "H"
SHOWN IN FIGURE 19

	Cb	Fe	Ni	Cr	Mo (w/o)
Center of Cell	1.2	66.2	12.7	15.2	1.7
Cell Boundary	6.5	61.0	13.2	14.6	2.2

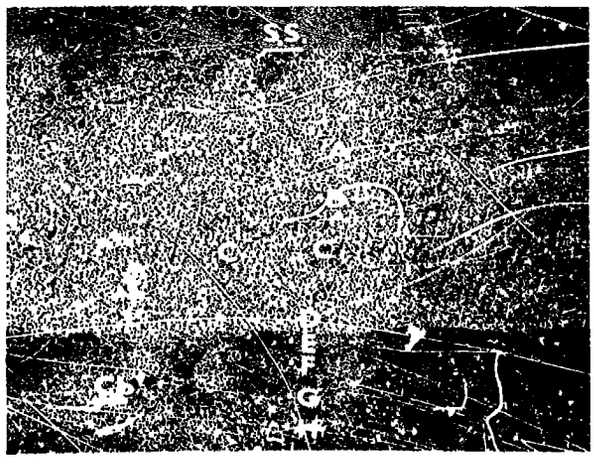

*int. = Cb/316 SS Interface Region

Unetched Photomicrograph 540X

611614-26B

Figure 20. Electron Microprobe Point Analyses of Weld Interface

STAINLESS STEEL WELD

0.001"

COLUMBIUM

600X

PHOTOMICROGRAPH - "RASTER" AREA

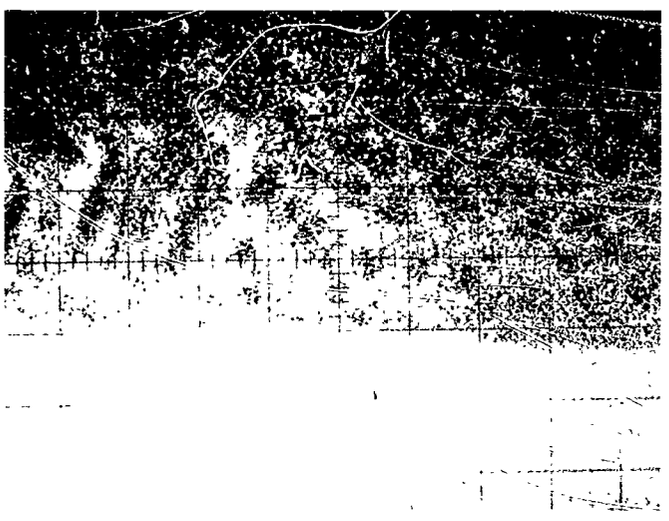

STAINLESS STEEL WELD

INTERFACE

COLUMBIUM

600X

COLUMBIUM X-RAY IMAGE

611614-27

Figure 21. Electron Microprobe Area Scan of Weld Interface

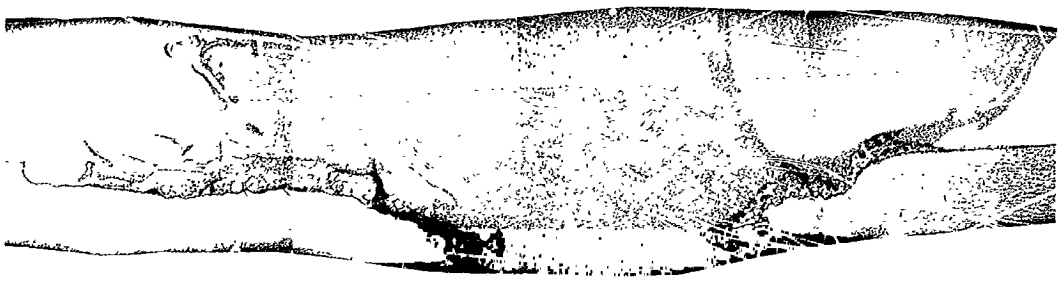

316 SS

COLUMBIUM

EXCESSIVE PENETRATION OF STAINLESS STEEL LONGITUDINAL WELD SHOWING ALLOYING OF BIMETAL COMPONENTS

12.5X
14.543

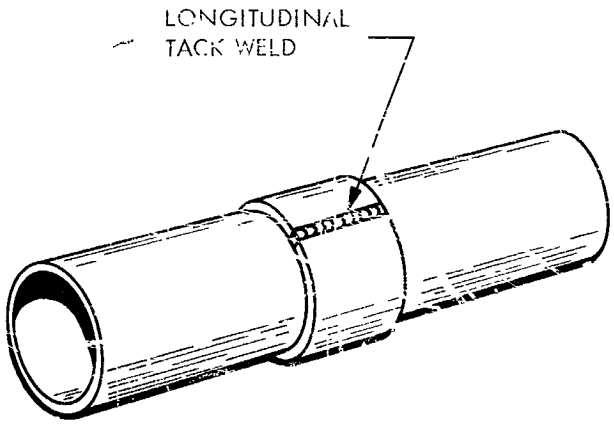

611614-15B

Figure 22. Excessive Penetration of Longitudinal Weld

X-Ray Fluorescence Analysis for Excessive Weld Penetration. An X-ray fluorescence analysis for Cb in the stainless steel weld was evaluated as a non-destructive inspection technique. Although chemical or spectrographic analysis would offer much greater sensitivity, the direct weld surface fluorescence could provide a fast in-process inspection technique. A preliminary trial demonstrated that surface fluorescence could detect Cb in one of the over-penetrated welds and a purposely defective weld was then prepared and examined. Figure 23 shows the method of defect preparation and the analysis results. Two types of defects were prepared; a single spot of excessive-penetration made by dwelling an arc over a previously welded sample and a diluted weld made by passing a normal penetration girth weld through a spot defect. The diluted version is very similar to what would be expected from subsequent girth welding of an excessively penetrated longitudinal weld. A surface analysis was first made using a 1/4 inch x 1/8 inch mask which detected Cb in both defects. Successive scans of the diluted weld showed a surprisingly rapid decrease in the Cb level indicating the higher melting point Cb is not transported with the molten weld puddle.

Machine chip samples were also removed from the welds and analyzed by X-ray fluorescence. Such an analysis technique would be amenable to weld conditioning practice and would eliminate the need for special tooling to adapt long lengths of tubing to X-ray fluorescence apparatus. The results support the surface analysis and indicate that chip samples could also be analyzed by conventional chemical or spectrographic techniques with much greater sensitivity.

Thermal Cycling and Mechanical Property Testing

Thermal Cycle. Two butt joint specimens were thermal cycled from 1350°F to 600°F as shown in the temperature curve of Figure 3. Two holes were drilled from the tube exterior to the bimetal interface at which point Pt / Pt-13Rh thermocouples were pinned in place. High purity helium gas was used to cool the induction heated specimens, (the apparatus is described in detail in the equipment section) and the cooling cycle was completed in 18 seconds.

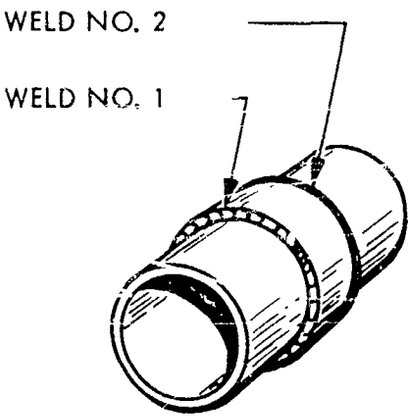

DEFECT PREPARATION

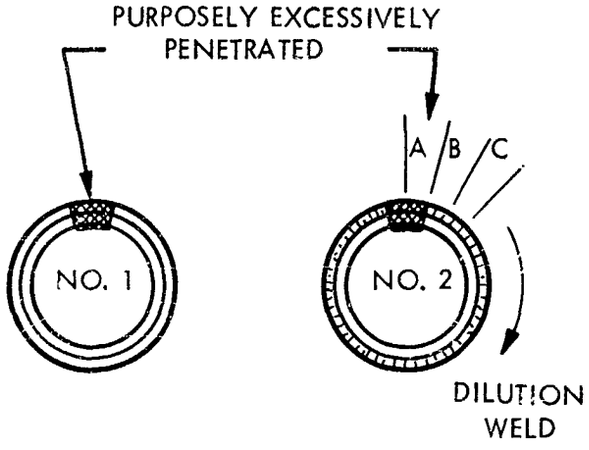

SURFACE SCAN (1/4" x 1/8" AREA MASK)

	W/O
WELD NO. 1 - DIRECTLY OVER WELD PUDDLE -----	0.39
WELD NO. 2 -	
AREA A - DIRECTLY OVER WELD----	3.5
AREA B - 1/4 " FROM WELD--------	"TRACE" ≈ 0.1 W/O
AREA C - 1/2 " FROM WELD--------	NOT DETECTABLE < 0.1 W/O

MACHINE CHIP SCAN

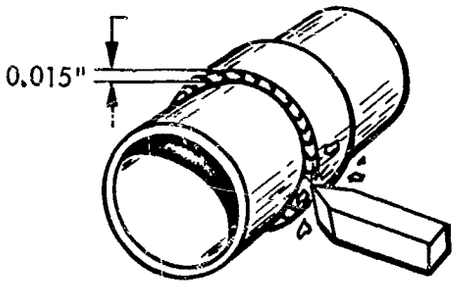

0.005" THICK LAYERS WERE REMOVED AND ANALYZED BY X-RAY FLUORESENCE

LAYER	WELD NO. 1 W/O	WELD NO. 2 W/O
1	0.17	0.12
2	0.12	0.12
3	0.22	0.27
4	0.37	

Figure 23. X-Ray Fluorescence Analysis for Excessive Weld Penetration

Bond Quality Determination. One of the purposes of the thermal cycling test was to determine the effect on bond quality adjacent to the butt joint. Observations of these effects were complicated because the large diameter tubing was initially 50 percent unbonded.

Ultrasonic inspection techniques were used to examine the bond quality before and after thermal cycling. Figure 24 shows traces obtained by an angled reflection technique. The trace following thermal cycling for tube No. 5 shows a greater degree of unbonding. An examination of bonding in the sectioned weld samples showed no difference between thermal cycled and non-thermal cycled specimens because of the clad removal operations prior to welding.

Crush Test. Two specimens of the butt joint were compression crush tested as shown in Figure 4. The total deformation was 1/4 inch, producing severe distortion in the bimetal components. Typical views of the sectioned tubes are shown in Figure 25. These photographs indicate no brittle failures in either the columbium or stainless steel weld. The thermally cycled specimen supported a higher load than the as-welded specimen indicating possible strengthening of the stainless steel weld and heat affected zone by the thermal cycling. An examination of the thermally cycled specimen shows very little deformation in the stainless steel weld and heat affected zone. The hardness measurements shown in Table 5, made in the welds before and after thermal cycling, show a corresponding increase in weld hardness. The crush test indicates that the joint design can tolerate considerable room temperature deformation without failure.

Internal Pressure Tests. The butt weld specimens were internal pressure tested for up to 1000 hours at a temperature of 1350°F. Two specimens were tested; one at a low stress level approximately twice the expected operating pressure (550 psi), and another at a higher stress level calculated to produce rupture in 1000 hours. A gas pressure apparatus was designed and built using a vacuum hot wall furnace.

The apparatus is described in detail in the equipment section of this report, but basically the specimens were pressurized with high purity helium gas and the test specimen external environment consisted of 10^{-6} torr vacuum. Automatic controls were included to

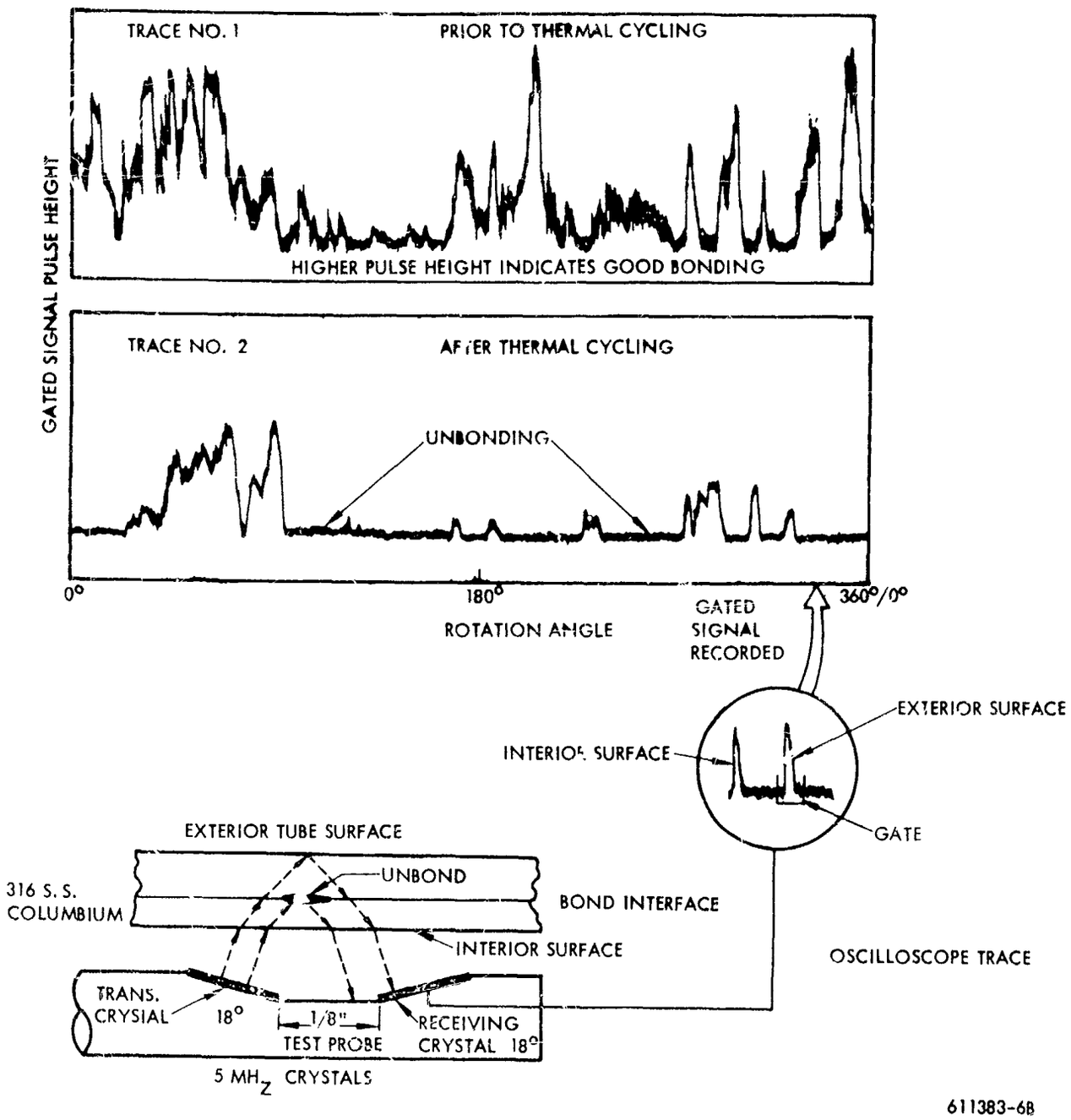

Figure 24. Ultrasonic Traces of Thermally Cycled Butt Welds

BUTT JOINT NO. 7

Tested As Welded

(1)Stress, Undeformed - 40,000 psi
Stress, Maximum - 59,000 psi

5 Section 7D

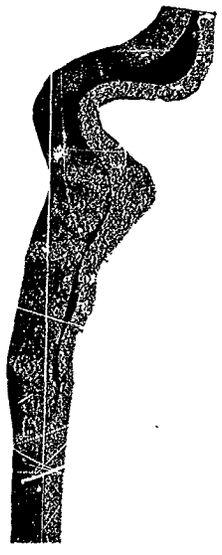

BUTT JOINT NO. 4

Tested As Thermal C ·led

(1)Stress, Undeformed - 56,000 psi
Stress, Maximum - 65,000 psi

5X Section 4D

(1) Stress calculated from transverse wall area of 0.126 in^2

611614-2GB

Figure 25. Crush Test of Butt Joint

TABLE 5

HARDNESS MEASUREMENTS OF BUTT WELD SPECIMEN

Tubing	316 S. S. Base	316 S. S. Weld	Cb Base	Cb Weld	316 S.S. Split Ring
As Received	165	---	106	---	---
As Welded	170	161	115	76	251
Welded and 172 hr 1350°F Pressure Test	196	176	104	90	145
Welded and Thermal Cycled	162	174	98	85	141
DPH Indenter Load	10 Kg	10 Kg	5 Kg	$2\frac{1}{2}$ Kg	10 Kg

3165.5 Split Ring

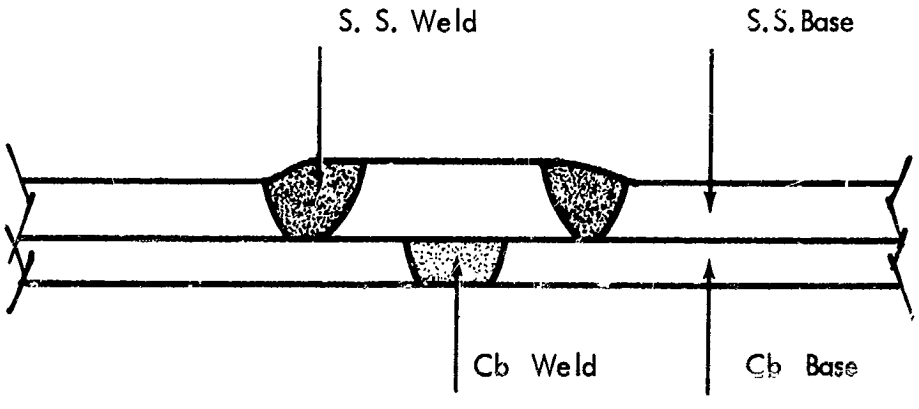

safely terminate the test in the event of specimen rupture. Selected test parameters were also recorded up to the time of failure.

A unique end fitting was developed for pressure testing the bimetal tubing. Cross-sectional views of the electron beam welded fitting are shown in Figure 26, the unique feature being that the tube was sealed at the columbium inner clad since helium leak tests had shown that the unbonded condition would permit the pressurizing medium to leak into the bimetal interface and essentially place only the outer cladding under stress if external seal welds were used. A reinforcing ring of stainless steel was lap welded to the stainless cladding of the tubing to provide the required hoop and longitudinal strength for the columbium end seals. A mechanical compression seal was used to connect the columbium end fitting to the stainless steel high pressure gas system. As might be expected, the 3:1 thermal expansion ratio of stainless steel to columbium produced an excellent seal except during cooling to room temperature after the test was completed. Leaks would develop below 1000°F during cooling from the test temperature at 1350°F. The joint would, however, reseal on reheating to test temperature.

The results of the tubular internal pressure test are presented both as a calculated effective stress[2] and also as the internal gas pressure to permit independent calculation of the stress-strain[3] relationships. Diametral strain is presented rather than an equivalent plain strain and as a further simplification, the partially bonded bimetal tube wall is treated as a homogeneous cross section.

For a thin walled tube, the effective stress σ, may be represented as $\sqrt{3/2}\ Pr/t$ where P = internal pressure, r = mean tube radius, and t = wall thickness. It is interesting to note that the effective stress for producing a given diametral strain is less than the uniaxial stress by $\sqrt{3/2}$ or 0.866. This would indicate that an internally pressurized tube with restrained ends (thus essentially producing uniaxial loading in the wall) would show a higher strain rate with a given internal pressure than the unrestrained tests in this program.

As a part of the equipment and specimen design evaluation, a preliminary specimen of unwelded tubing was fabricated and tested at varied stress levels. The resultant cumulative strain versus time curve is shown in Figure 27. Since continuous strain measurement instrumentation was not available, the tests were interrupted and the specimen was removed and measured following each change

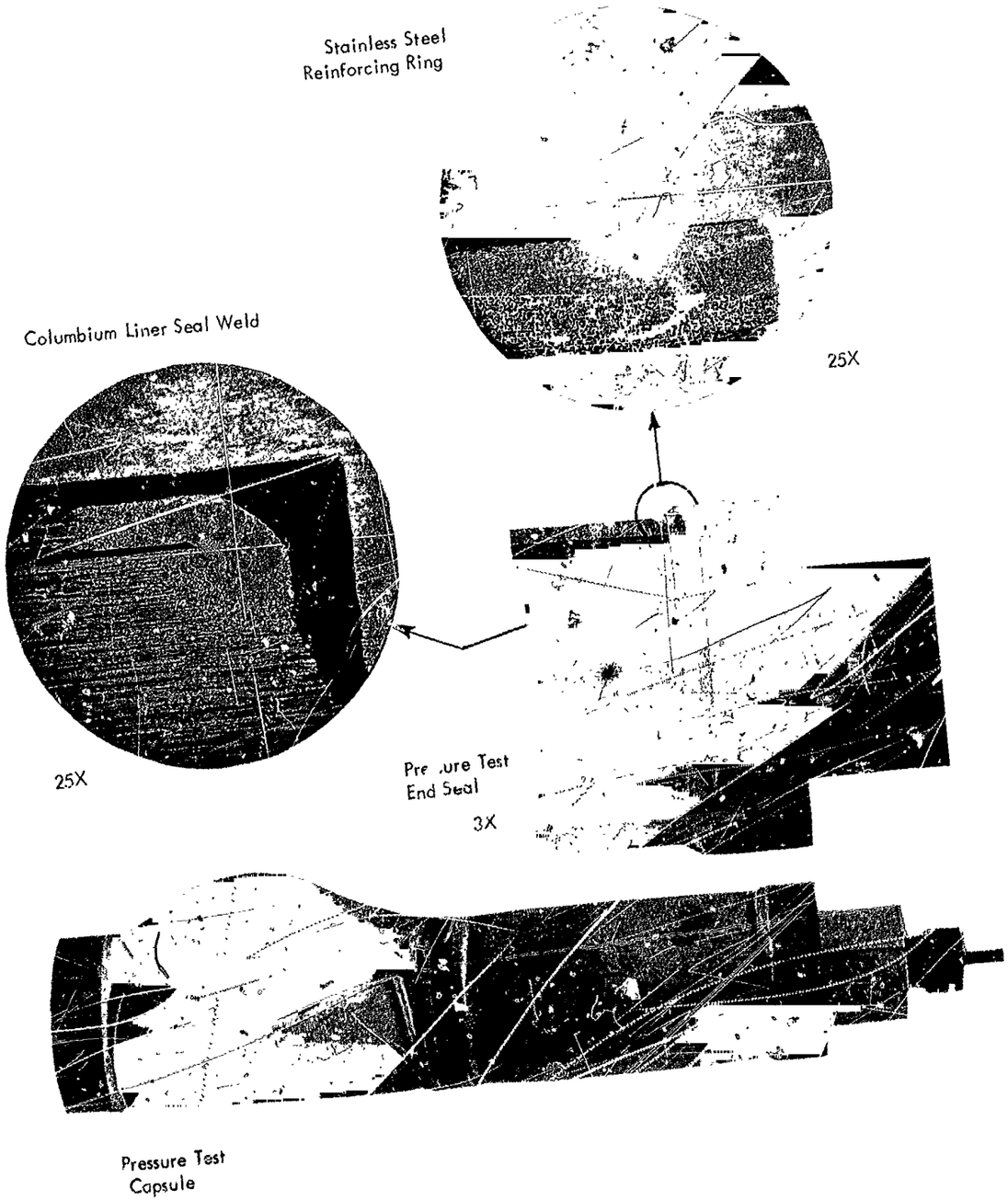

Figure 26. Pressure Test Capsule Design

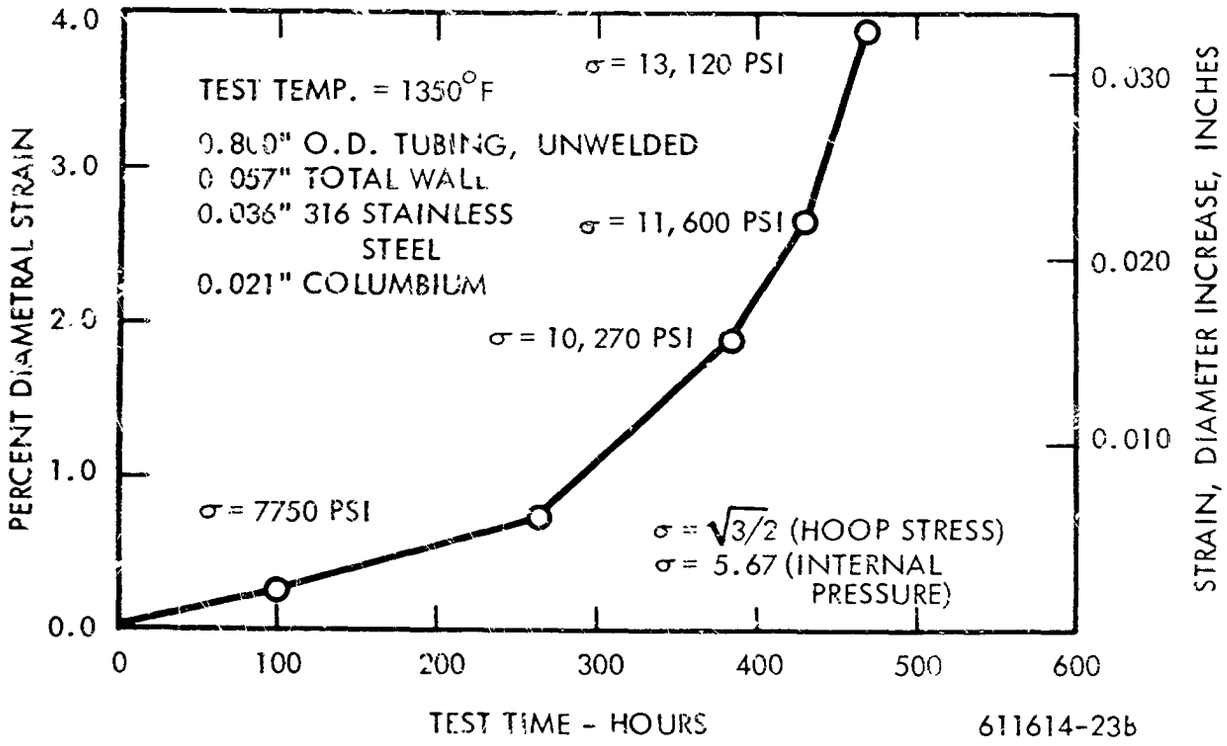

Figure 27. Cumulative Diametral Strain at Various Stress Levels

Astronuclear Laboratory

in stress level. The internal gas pressure and detailed test conditions are listed in Table 6. The five interrupted diametral strain points were plotted as the logarithm of the strain rate versus stress as shown in Figure 28 to provide an empirical stress-strain rate relationship. Rate of diametral change was assumed to be linear for a given stress level. Two welded specimens were tested at high and low stress levels respectively. One specimen was run at double the design stress of the liquid metal system, (2 x 275 psi or 550 psi) for 1000 hours and a second specimen was tested at a high stress level designed to produce rupture in 500 hours. Although no rupture data were available, a stress level of about 12,000 psi was predicted from the preliminary data to produce 10 percent diametral strain in 500 hours. Rupture would be expected to occur before 10 percent strain was achieved. As indicated in Figure 28, the high stress level specimen ruptured in 172 hours and the diametral strain of the unruptured half is plotted. Figure 26 shows the ruptured specimen. The low stress level specimen produced somewhat less strain than predicted from the initial data of the unwelded specimens. Although two curves are suggested in Figure 28 for welded and unwelded tubing, the data could be included in the usual variation in creep and stress rupture tests. Also, the stress level on the ruptured specimen, Figure 28, at the time of rupture was higher than indicated since the tube diameter had increased by 6 percent and the tube wall had thinned proportionately. Correcting the stress level to include the dimensional changes at the time of rupture would increase the stress by 12 percent or 1400 psi.

As is evident in the photograph of the ruptured specimen, Figure 26, the bimetal tubing was not well bonded and the bimetal layers essentially acted like a two layer tube. This may produce different creep strength results than completely bonded bimetal tubing. In summary, the internal pressure tests of butt welded tubing indicated no significant decrease in creep strength over the unwelded tubing.

Tensile Tests. Tensile tests were required for butt welded tubing specimens at room temperature and 1350°F. In addition, an unwelded section of tubing was tensile tested at 1350°F to provide a measure of the weld joint efficiency. Sheet tensile specimens were

TABLE 6

BIMETAL TUBING INTERNAL PRESSURE TEST RESULTS

Tube	Run	Time Hours	Total Time Hours	Total Strain ΔD	Incremen. Strain ΔD	Incremen. Strain % $\frac{\Delta D}{D}$	Creep Rate % $\frac{\Delta D}{D}$ /Hour	Internal Pressure P.S.I.	Effective[1] Stress P.S.I.	Total Strain % $\frac{\Delta D}{D}$
A	1	99	99	.0020	.0020	.251	2.54×10^{-5}	1375	7,750	.251
A	2	165	264	.0056	.0036	.451	2.73×10^{-5}	1375	7,750	.704
A	3	121	385	.0150	.0094	1.173	9.82×10^{-5}	1800	10,270	1.883
A	4	45	430	.0210	.0050	.616	1.37×10^{-4}	2000	11,600	2.640
A	5	38	468	.0310	.0100	1.225	3.22×10^{-4}	2250	13,120	3.89
1	1	1000	1000	.0014	.0014	.175	1.75×10^{-6}	550	3,130	.175
2	1	172	172	.0471	.0471	5.91	3.43×10^{-4}	2100	11,900	5.91

[1] Effective Stress

$\sigma = \sqrt{3/2}$ (hoop stress)

Astronuclear Laboratory

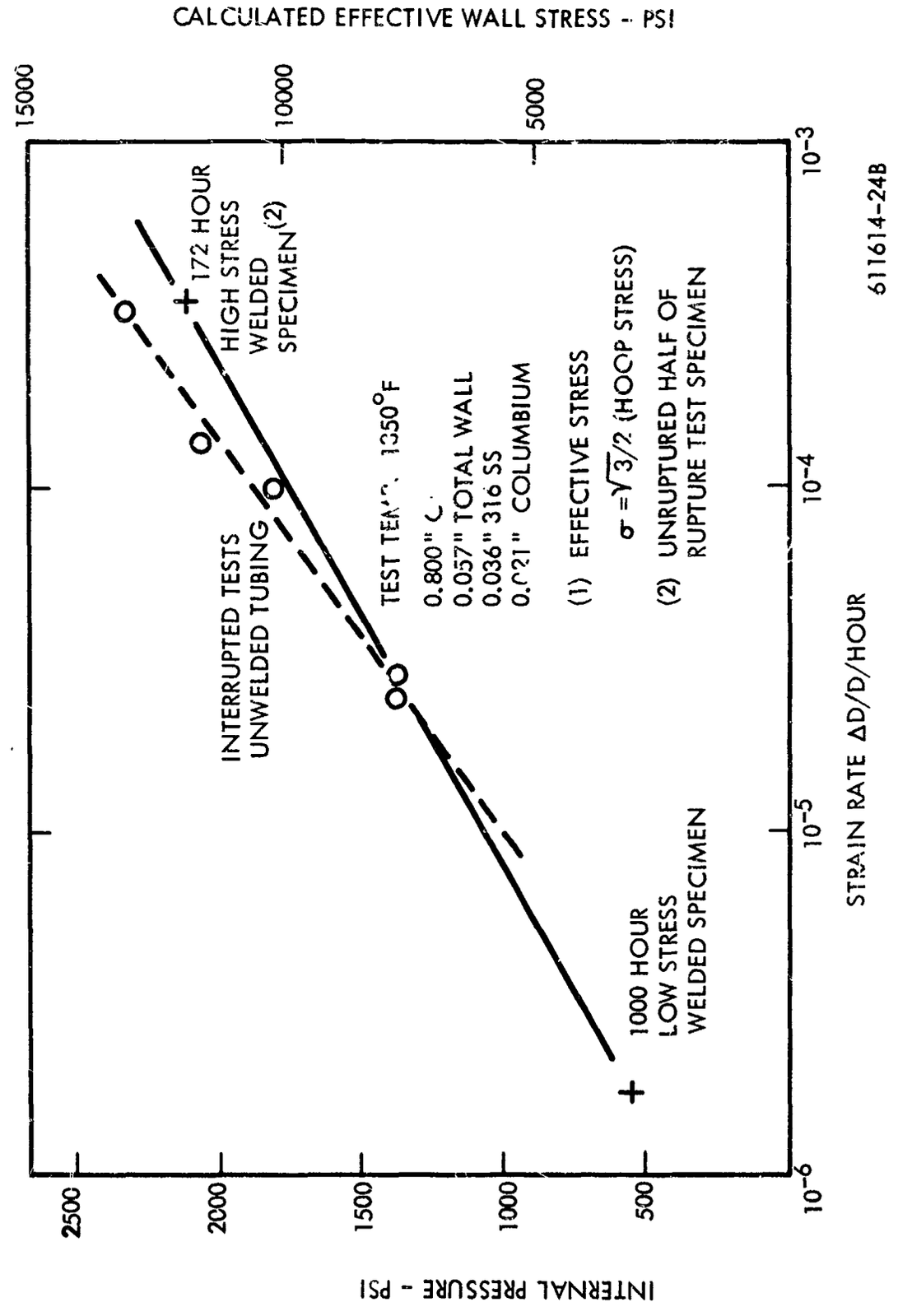

Figure 28. Diametral Strain Rate Versus Stress for Internally Pressurized Tubing

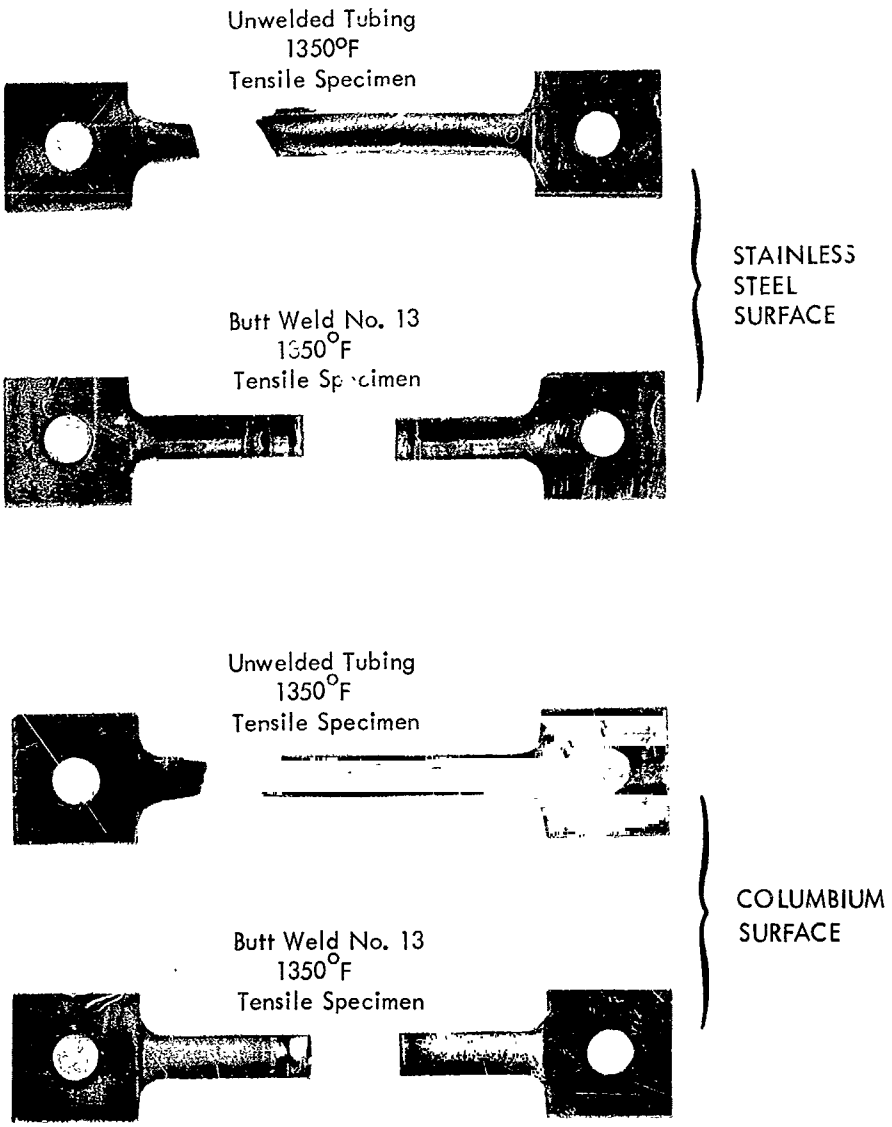

Figure 29. 1350°F Tensile Specimens of Welded and Unwelded Tubing

machined from the tubing and the elevated temperature specimens were tested in 10^{-5} torr vacuum. Figure 29 shows the elevated temperature tensile specimens and the problem of bimetal debonding both during and prior to the tests. The unbonded specimen test resulted in separate ultimate tensile strength and elongation values as; first the columbium, and then the stainless steel component failed. These results are presented in Figure 30 and in Table 7. The joint efficiency, considering ultimate strength, is 55 percent for the columbium joint and 82 percent for the stainless steel joint at 1350°F. The low joint efficiency and the very low elongation values obtained for the columbium part of the bimetal may be due to local weld and heat affected zone annealing of the cold worked columbium. A sharp hardness decrease was observed in the weld and heat affected zone, of the columbium liners, as shown in Table 5. The columbium fracture surface shows a ductile shear lip at the weld edge and the low overall elongation value (approximately 0.2 percent) is due to extreme local yielding and is not indicative of a brittle failure. The columbium weld displayed over 90 percent local reduction in area. The stainless steel portion of the bimetal tubing displayed a similar behavior of failure in the weld-annealed heat affected zone. Not expected, however, is the lower elongation values for both columbium and stainless steel at 1350°F as compared to room temperature.

Radiographic Inspection of Butt Weld

Radiographic inspection of the butt welds provides a non-destructive inspection technique for excessive penetration of both the stainless steel girth welds and longitudinal welds. Figure 31 shows positive prints of butt weld radiographs. Tube No. 12 shows an example of excess longitudinal weld penetration. Two views (direct and a 90° view) are shown, and the penetration depth may be estimated from the 90° view.

Adequate penetration of the girth weld may be measured as shown in tube No's 4 and 5. Tube No. 4 has 93 percent penetration as measured by sectioning and tube No. 5 has 60 percent penetration as measured in the same manner. A fine line is observable in tube No. 5 indicating lack of penetration. An example of an inner clad defect is shown in tube No. 8.

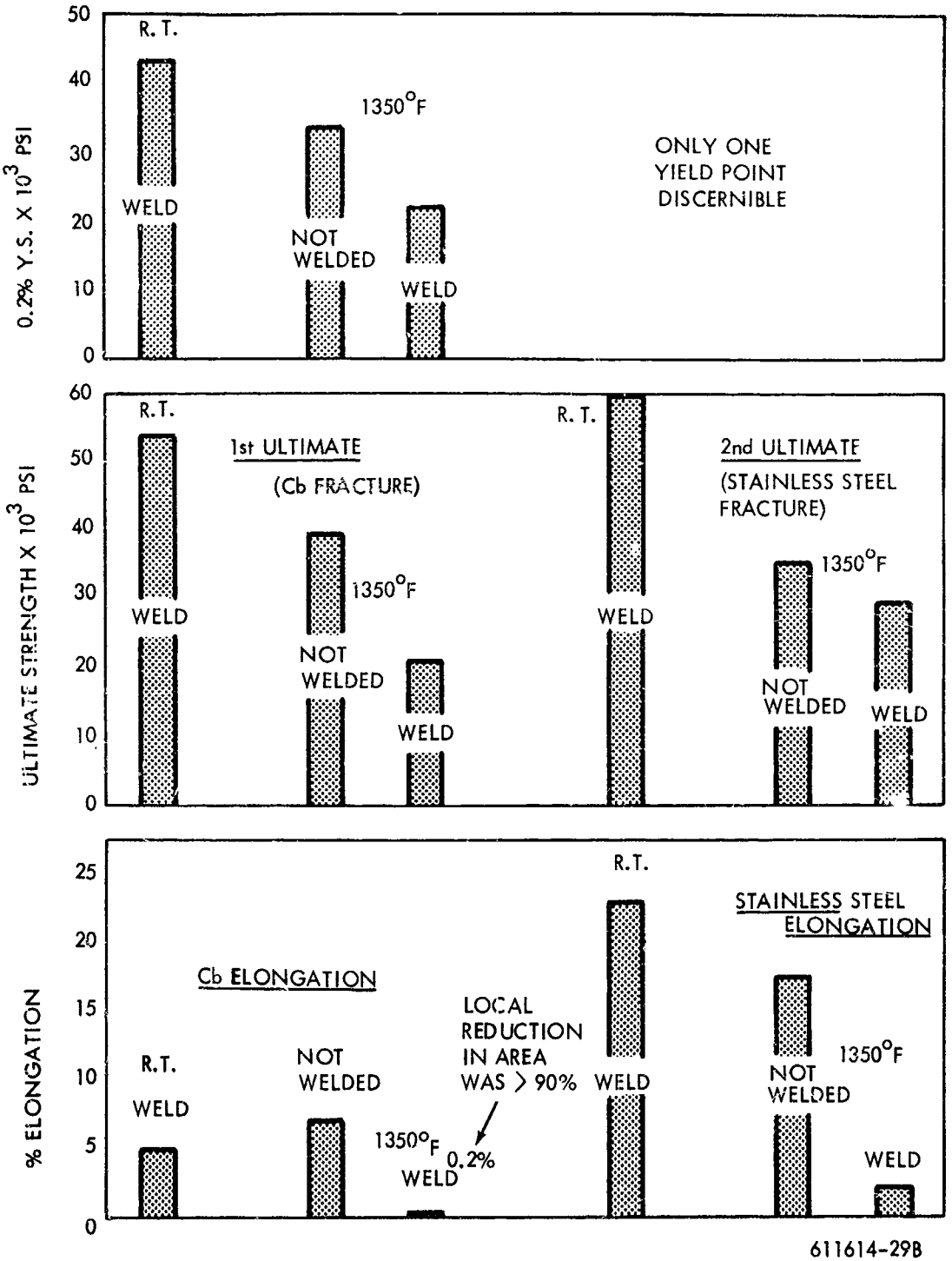

Figure 30. Tensile Test Results of Bimetal Tubing

TABLE 7

TENSILE TEST DATA FOR BIMETAL TUBING

Tube No.	Test Temp.	Y.S. PSI	U.T.S. PSI 316 S.S.+ Cb	U.T.S. PSI 316 S.S.	Elongation Cb %	Elongation 316 S.S.	Specimen Type
1	R.T.	43,670	54,440	59,300	5	23	Weld
14	1350°F	21,900	21,900	29,300	0.2	4	Weld
80-113	1350°F	34,200	39,700	35,900	7.3	16.7	Unwelded

* Reduction in area was >90 percent.

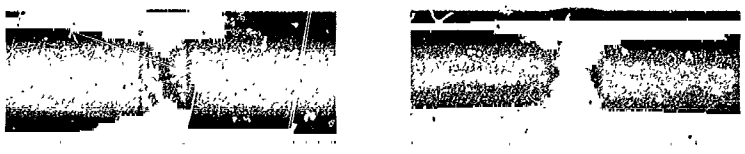

TUBE NO. 12

0° 90°

EXCESS PENETRATION IN LONGITUDINAL WELD

TUBE NO. 8

0° 90°

DEFECT IN COLUMBIUM LINER

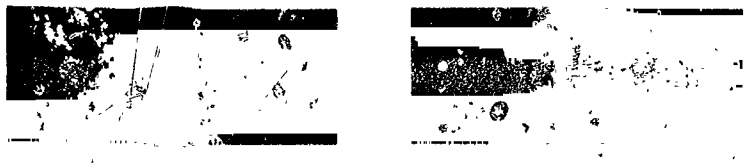

TUBE NO. 4

93% PENETRATION IN GIRTH WELD

0° 90°

TUBE NO. 5

60% PENETRATION IN GIRTH WELD

0° 90°

POSITIVE PRINTS, THIN AREAS APPEAR LIGHT

611614-34B

Figure 31. Radiograph of Butt Welds

The radiographs of tube No's 4, 5 and 8 were made at a slight angle to the X-ray beam to prevent the top and bottom weld views from overlapping. Improved definition could be obtained by shooting through only one wall at a time with film on the tube interior. In summary, radiographic techniques provide a means of measuring the weld penetration of both the longitudinal and transverse welds and also provide an inspection technique for tubing defects such as variations in bimetal layer thickness.

Summary

In review, two butt joint designs were developed; an electron beam and a gas tungsten arc welded version. Because of field welding considerations, the gas tungsten arc welded butt joint was more extensively evaluated. It demonstrated both adequate mechanical properties and a practical fabrication capability.

D. TEE JOINT DEVELOPMENT

Description and Fabrication

If bimetal tubing systems are to be used, a design solution for tee joints will be needed and will be applicable as well to crosses and other multiple joint assemblies. Instrumentation feed-throughs such as thermocouples and pressure transducers will also be required and these will usually take the form of tee joints on straight runs of pipe. The basic design of the tee joint is shown in Figure 32. The fabrication sequence includes the removal of stainless steel cladding, typically by machining, from both sections of the tee joint. In the Type A, two piece tee section, the clad is removed from the entire circumference of the large diameter tubing. An alternative single piece tee joint is shown, Type B, in which a saddle shaped section of cladding is removed. The first step in the normal fabrication sequence is to join the inner columbium liner. In Type A this is accomplished by manual, gas tungsten arc welding using 0.090 inch columbium filler wire in a helium atmosphere. In Type B, the electron beam welded version a cam guided fixture is used to trace the saddle shaped weld interface. The final fabrication sequence is to replace the stainless steel cladding. In Type A, this is accomplished using a relatively heavy, two piece stainless steel section that may be either electron beam or tungsten arc welded. Circumferential lap joints and longitudinal butt joints are required. In Type B, a light gage stainless steel saddle, (which would have been slipped on the small branch of the tee joint prior to the first columbium weld) is pressed into place and electron beam lap welded to the bimetal tubing outer clad. One full and two partial circumferential lap welds and two longitudinal lap welds are required. Figure 33 shows the columbium welding sequence used for Type A including the machined and fixtured joint in the top view and the welded joint in the bottom view. The weld is made by lightly tacking the columbium, removing the weld fixture, and clamping the entire joint in a heavy copper fixture to prevent overheating from the filler wire welding operation.

Figure 34 shows the stainless steel clad replaced, the top view being a tungsten arc welded specimen, and the bottom, the electron beam welded reference design. Closer control

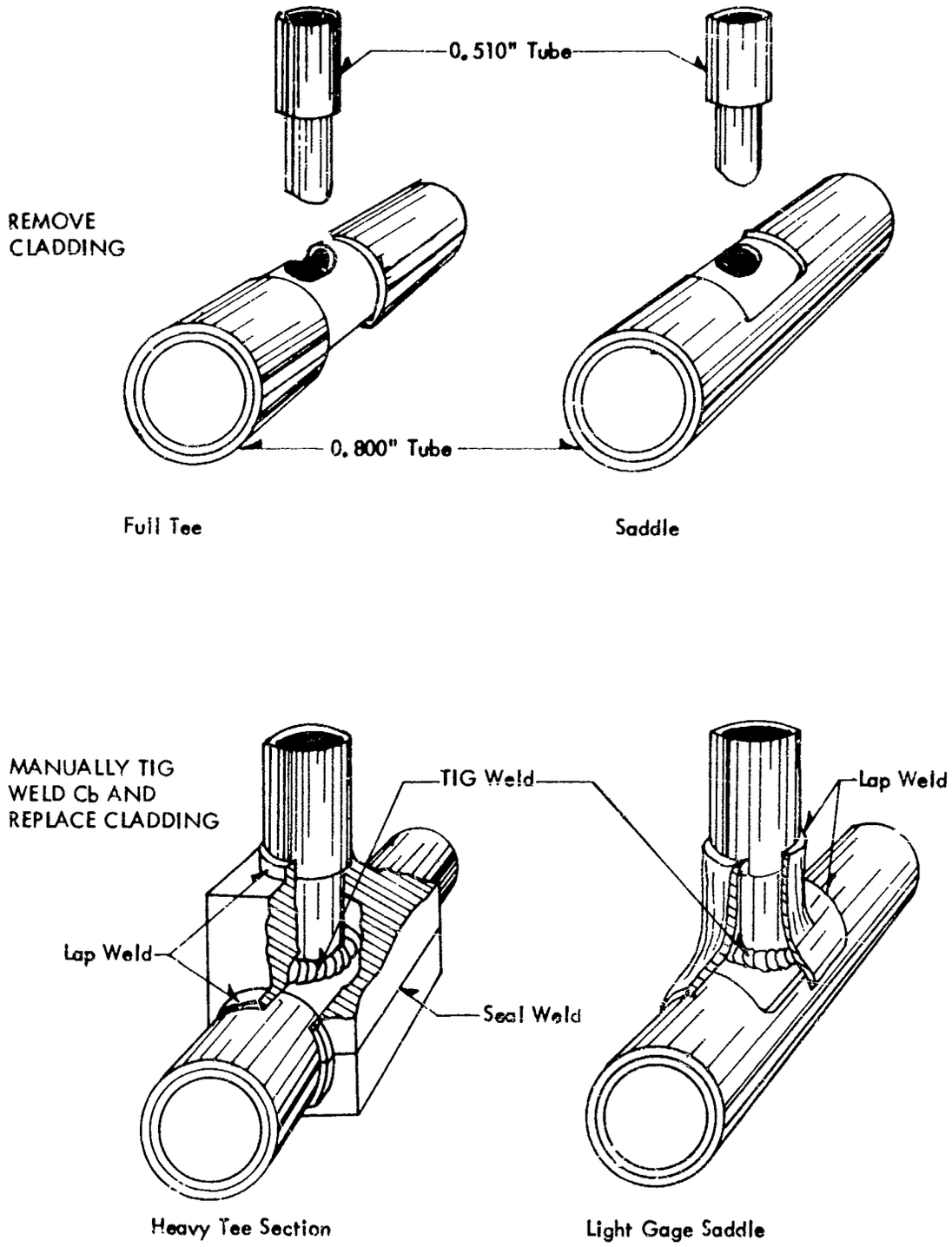

Figure 32. Tee Joint Fabrication Sequence

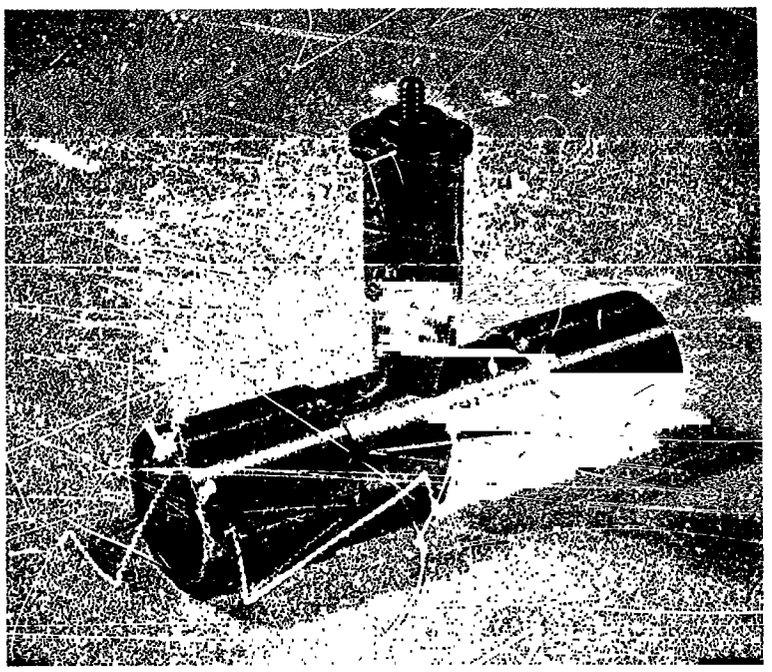

Fixtured for Manual Gas Tungsten Arc Weld

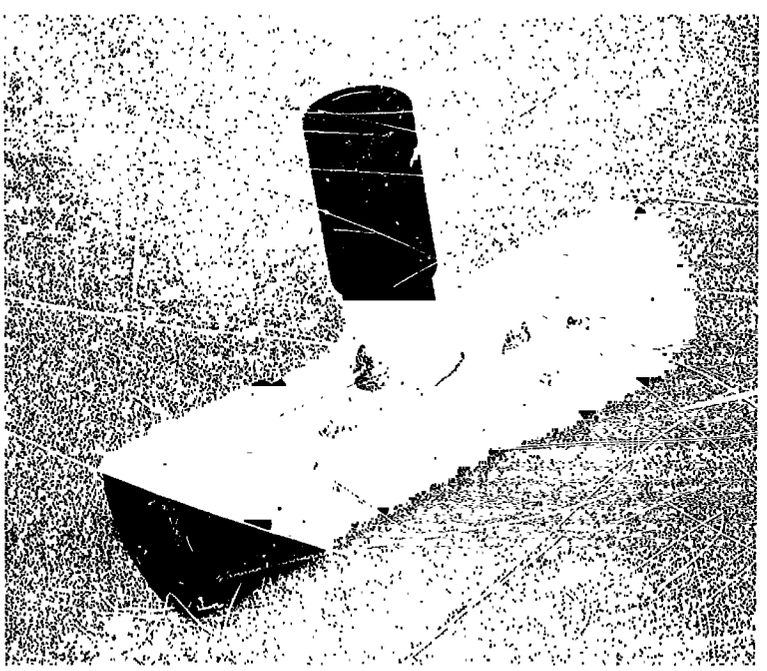

Welded Using Columbium Filler Wire

Figure 33. Columbium Weld Sequence for Type A Tee Joint

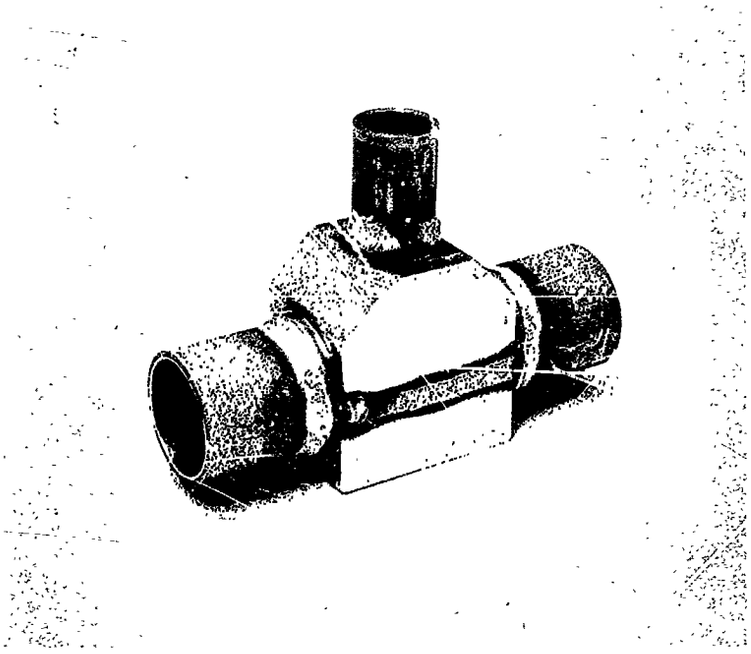

Gas Tungsten Arc Weld

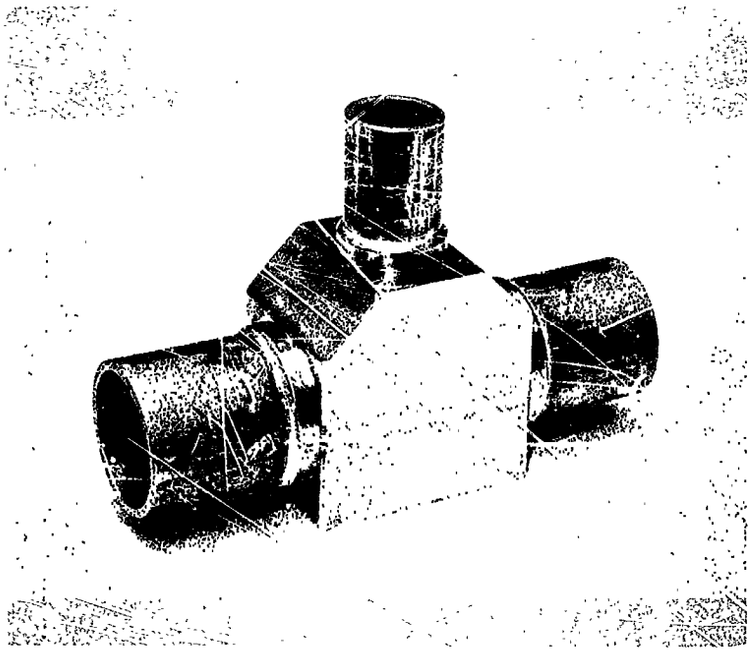

Electron Beam Weld

Figure 34. Completed Weld Joint for Type A Tee Joint

over weld penetration, particularly the lap welds, is available with electron beam welding. The weld sequence, using either gas tungsten arc or electron beam welding, includes tack welding the longitudinal joints, welding longitudinally, and finally welding circumferentially. The assembly sequence is shown graphically in the assembly view in Figure 35. Figure 36 shows two sectional views of a Type A design tee joint using manual gas tungsten arc and filler wire for the columbium saddle weld and electron beam welding for the stainless steel clad replacement. Several stainless steel reinforcement sections are observable and are required to support the interior columbium liner since the tubing will be internally pressurized in service. These are two piece sections and are handfitted prior to final assembly. Some undercutting, cold shuts and porosity are visible in the columbium weld (shown in Figure 36.) When these joints were helium leak tested after welding, no leaks were found. The excellent penetration control obtainable with the electron beam weld is apparent, both in the butt joint and lap joints.

Figure 37 shows the fabrication sequence for an alternative light gage saddle section joint, Type B, made entirely by electron beam welding, A cam guided fixture was made to provide automatic tracking around the columbium saddle joint and the same fixture was used for the weld fabrication of the external stainless steel light gage saddle. The saddle welding is completed using circumferential and longitudinal lap welds. The completed joint is obviously very attractive from a weight and size standpoint and would have been selected as the reference process, but for the following consideration. The heavy gage stainless steel section can be used to cover an all machined, non-welded, refractory metal tee joint liner, a design feature presently used in refractory metal systems and shown in Figure 38. This generally increases the joint reliability by eliminating one welding operation. The completely machined joints cannot be enclosed by a single piece light gage saddle.

In review, two acceptable processes were developed; a combination electron beam and tungsten arc process using a heavy steel clad replacement section and an electron beam process, using a cam guided electron beam saddle weld and a light gage clad replacement section. Because the heavy gage section was adaptable to non-welded refractory metal liners, this process was chosen as the reference design.

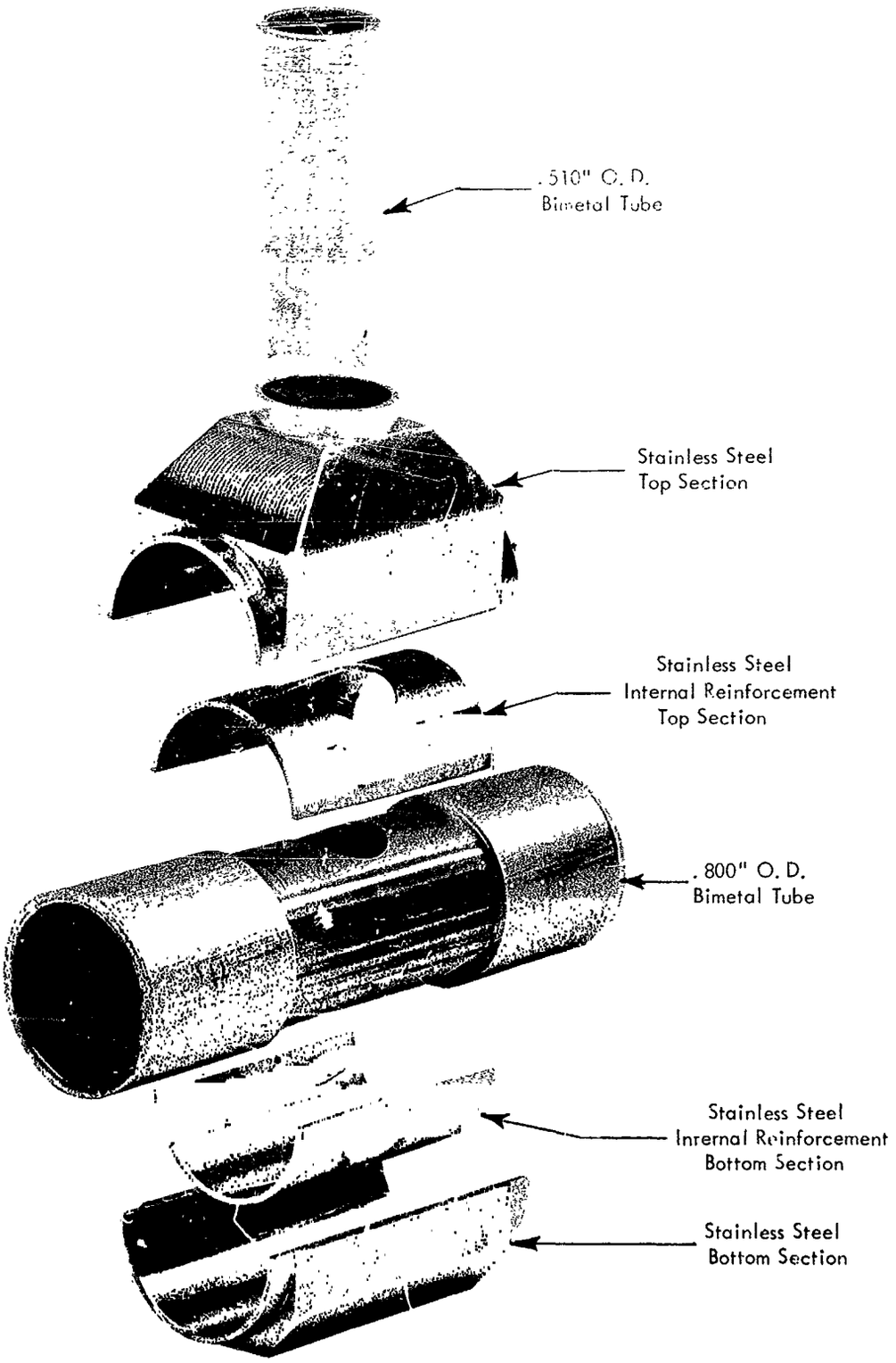

Figure 35. Reference Design Tee Joint - Assembly View

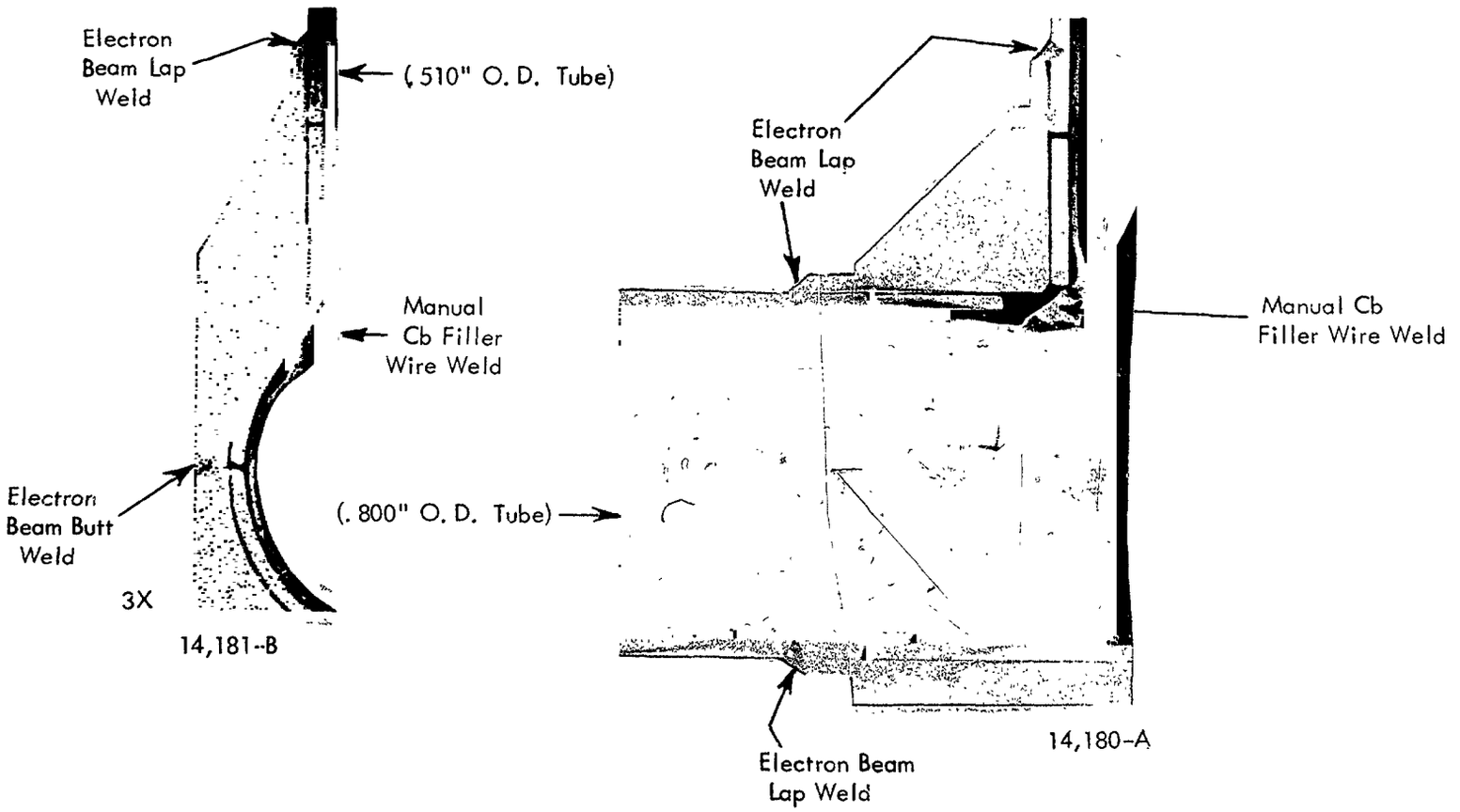

Figure 36. Reference Design Tee Joint - Section View

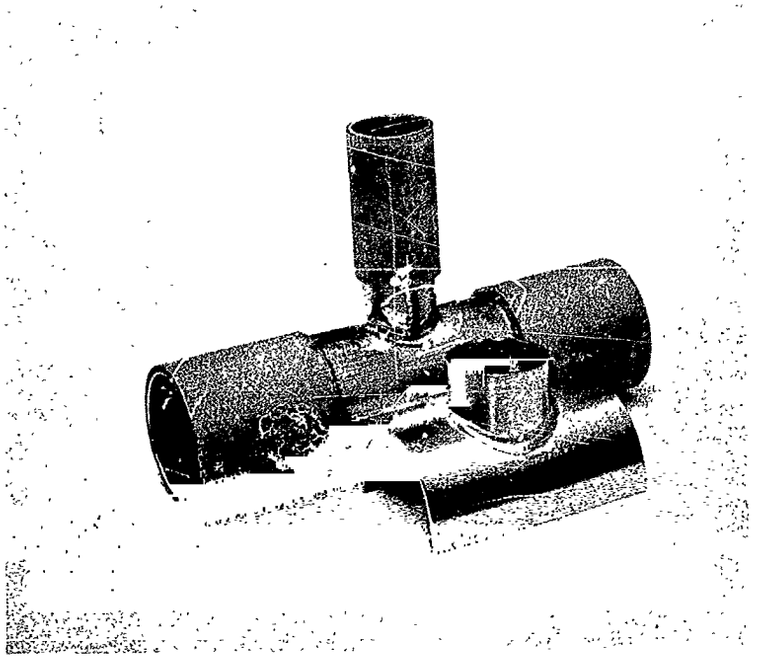

Partially Assembled Tee Joint

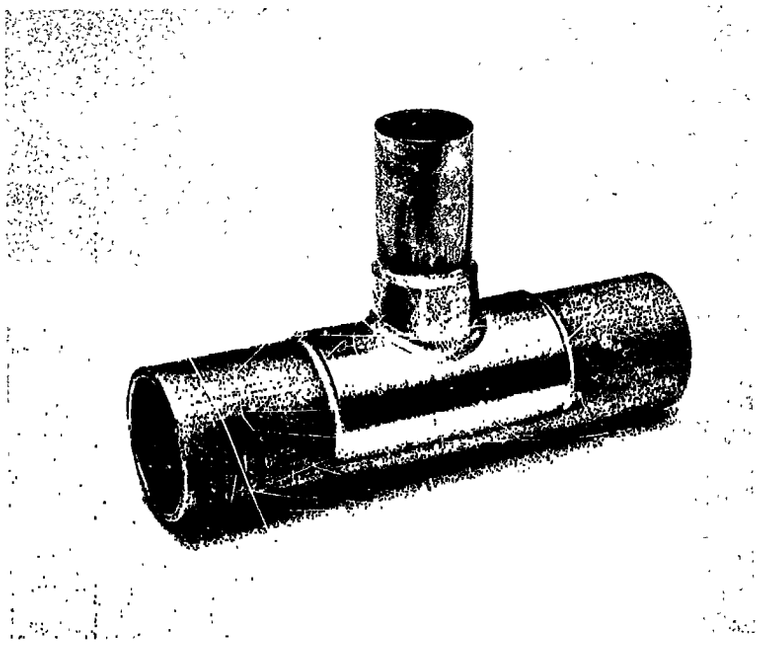

Completed Tee Joint

Figure 37. Weld Sequence for Type B Tee Joint

A. COLUMBIUM TEE MACHINED FROM SOLID STOCK

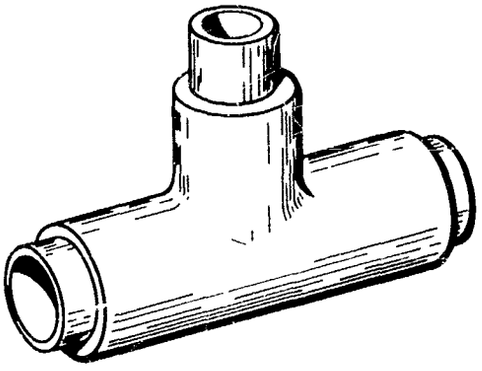

B. STAINLESS STEEL JACKET WELDED OVER COLUMBIUM SECTION

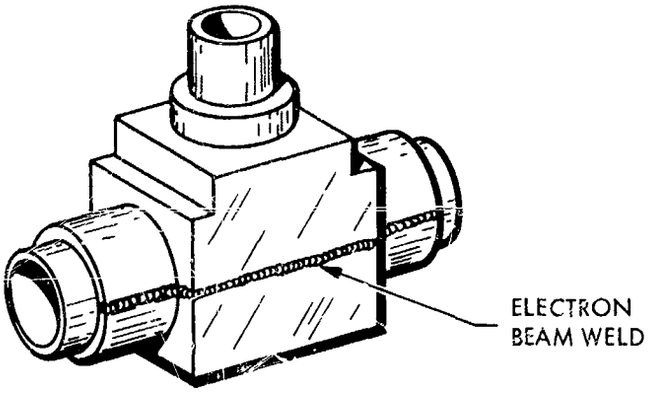

C. TEE JOINT INSTALLED IN TUBING SYSTEM

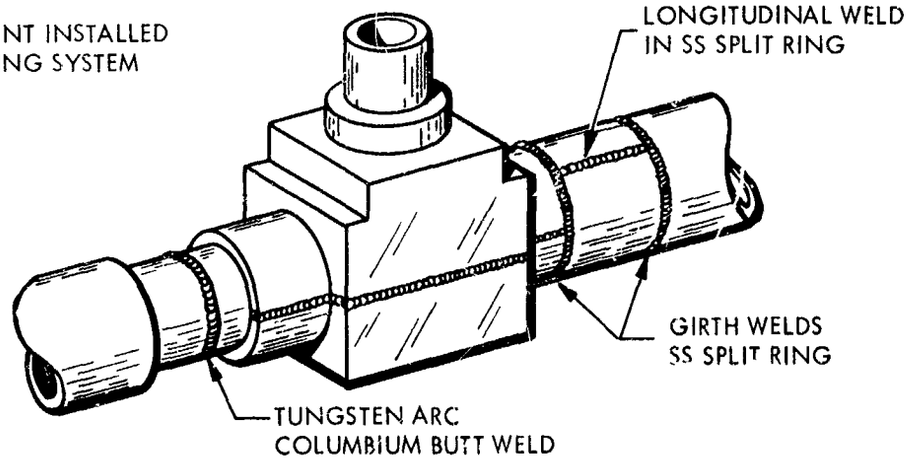

611614-14B

Figure 38. Alternate Design - Non Welded Refractory Metal Liner

Thirteen tee joint assemblies were machined and started into the fabrication sequence and in-process evaluation outlined below:

1) Manual gas tungsten arc weld of the columbium saddle joint using filler wire
2) Visual inspection
3) Dye penetrant inspection
4) Helium leak test
5) Radiograph
6) Electron beam weld stainless steel exterior
7) Visual inspection
8) Dye penetrant inspection
9) Radiograph

As previously mentioned, in-process inspection operations were used to more efficiently evaluate the weld joints. This is required since the final weld prevents effective examination of the interior weld. The process flow chart shown in Table 8 can be used as an approximation of the process capability. Ten acceptable specimens were completed out of the thirteen started into the process. Two out of the three were scrapped during the manual columbium welding process and one was damaged during final assembly of the stainless steel cover. The overall yield is not compromising to this design since the intention is to fabricate this weld configuration beforehand and install completed and inspected tee joints. The welding parameters used for the tee joint are listed in Table 9.

Sectioning Data - Weld Penetration Control

Three completed tee joints were sectioned into four quadrants each, and the sections were measured for weld penetration control. The data are presented in Table 10 and in Figure 39. As is indicated in Figure 39, the larger diameter lap welds appear to be in better control, in terms of weld penetration, than the smaller diameter lap welds.

TABLE 8

PROCESS SEQUENCE OF REFERENCE TEE JOINT DESIGN

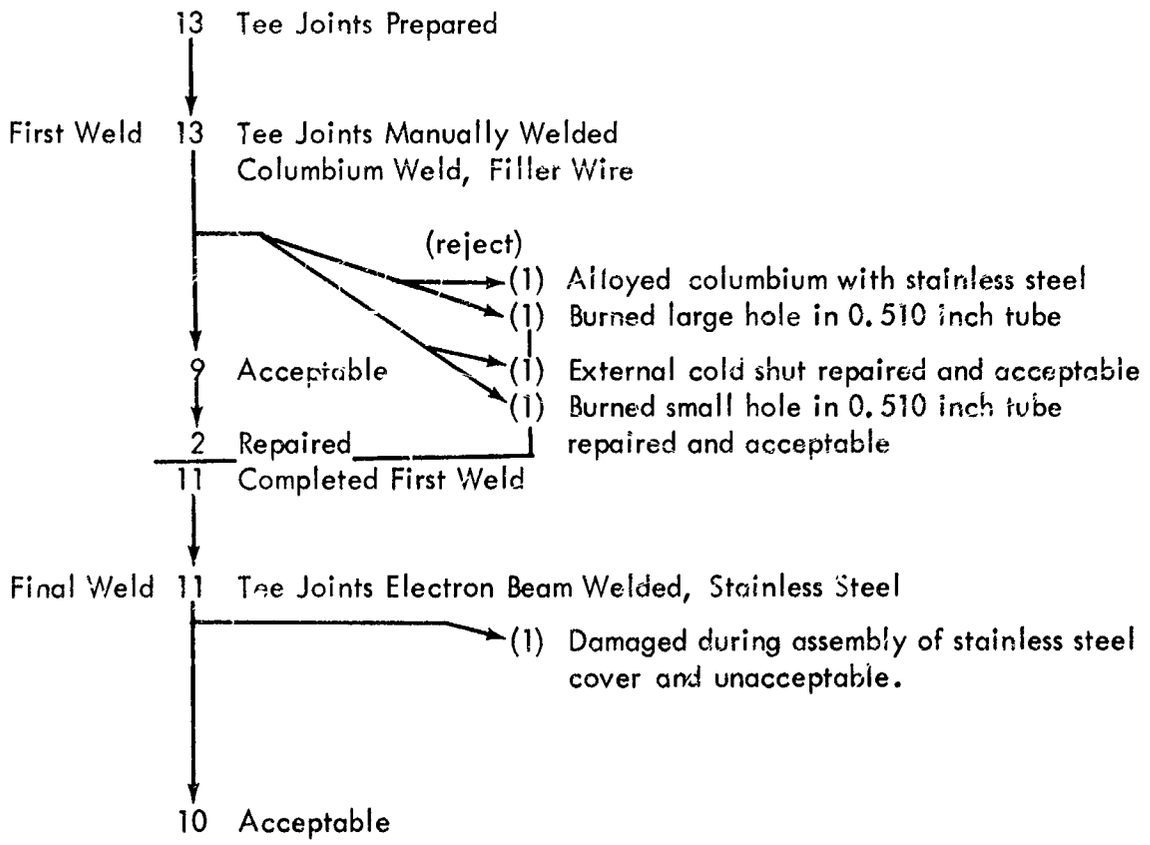

Process Yield 10/13 = 77 Percent

TABLE 9

TEE JOINT WELDING PARAMETERS

Initial Columbium Weld	Final Stainless Steel Weld
Gas Tungsten Arc - Helium Atmosphere Weld Chamber	Electron Beam Welding 10^{-5} torr Vacuum
Columbium Weld Gas Tungsten Arc	Stainless Steel Weld Electron Beam
DCSP Manual Welding Using 0.090" Columbium Filler Wire Approximately 50 amps.	100 KV 2.5 MA 25 ipm .018" transverse deflection

TABLE 10

TEE JOINT WELD PENETRATION SUMMARY

.510" Dia. Lap Weld			.800" Dia. Lap Weld			Longitudinal Weld		
Section	Min. Shear Mils	% Penetration	Section	Min. Shear Mils	% Penetration	Section	Width Mils	% Penetration
2A	22	91	2A-Top	17	86			
2B	20	85	2A-Bot.	20	68	2B	40	50
2C	15	86	2D-Top	28	73	2C	38	50
2D	20	77	2D-Bot.	25	73			
3A	25	91	3A-Top	25	64			
3B	28	80	3A-Bot.	20	41	3B	57	42
3C	20	82	3D-Top	30	81	3C	43	45
3D	28	78	3D-Bot.	17	67			
4A	23	59	4A-Top	17	50			
4B	25	50	4A-Bot.	22	70	4B	47	53
4C	22	64	4D-Top	17	65	4C	38	43
4D	25	65	4D-Bot.	23	65			
Ave. % Pen. = 76			Ave. % Pen. = 67			Ave. % Pen. = 47		
$\sigma = \pm 12.7\%$			$\sigma = \pm 10.5\%$			$\sigma = \pm 4.1\%$		
Ave. Minimum Shear, Mils = 23			Ave. Minimum Shear, Mils = 22					
$\sigma = \pm 3.6$ Mils			$\sigma = \pm 4.4$ Mils					

Astronuclear Laboratory

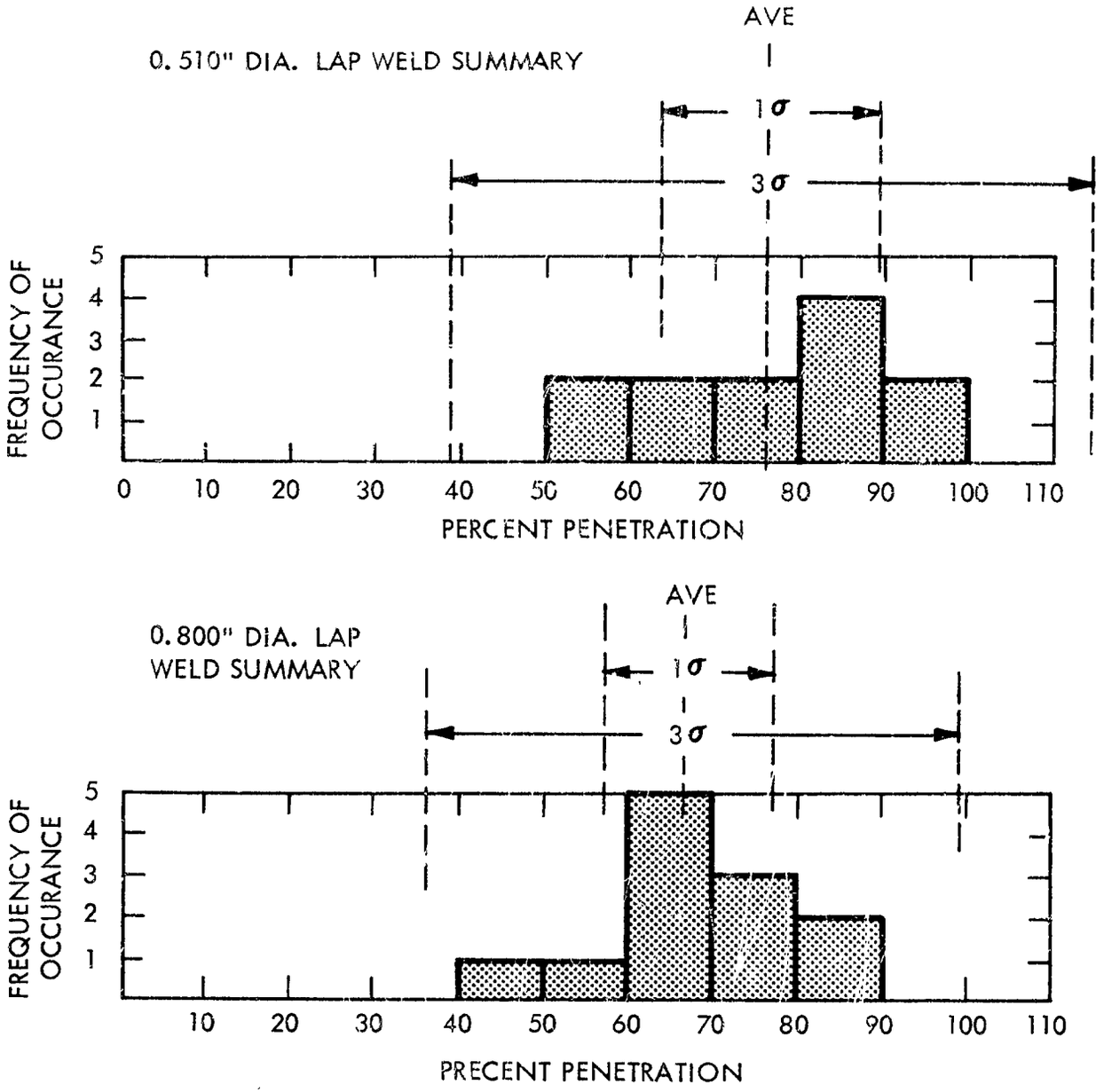

611614-28B

Figure 39. Statistical Distribution of Tee Joint Weld Penetration Data

Astronuclear Laboratory

The data indicate, that with the present process control, over 99 percent of the welds would have 30 percent to 100 percent penetration as compared to a target of 50 percent penetration. Excess penetration with the electron beam lap weld would produce alloying between the stainless steel and columbium. In terms of minimum shear area however, (see the bottom of Table 10) all of the lap welds averaged about 22 mils as compared to a target of about 35 mils (equal to the stainless steel clad thickness). The electron beam longitudinal butt weld showed excellent penetration control as gaged against a target of 50 percent penetration, Table 10. The manual filler wire technique used to join the columbium liner indicated problems of incompletely fused roots in the 90 degree angle of the saddle joint, Figure 36. Although no through-leaks were discovered, the presence of internal, partially closed voids is undersirable.

Thermal Cycling and Mechanical Property Testing

Similar to the butt joint, the basic evaluation for the tee joint was the thermal cycling test. Two of the 10 completed specimens were thermal cycled and compared to non-thermal cycled specimens for both structural strength and bimetal bond quality.

Thermal Cycle. Two tee joint specimens were thermal cycled 20 times from 1350° F to 600°F, similarly to the temperature curve for the butt joint shown in Figure 3. Due to the larger mass of the tee joint however, the cooling cycle required 36 seconds instead of 18 seconds. Control thermocouples were placed at the bimetal interface by the means of holes drilled in the tubing exterior. High purity helium gas was used to cool the induction heated specimens.

Crush Test. The destructive test used for the tee joint is shown in Figure 4. The specimens were crushed in a tensile test machine and the maximum loads developed were measured. Figure 40 shows the results of the crush test on the thermally cycled and as-welded tee joint. In the thermally cycled specimen, the small diameter lap weld supported a 6600 lb load and the entire specimen was considerably deformed. The as-welded specimen failed at a lower load by shear in the small diameter weld. The sheared weld is observable in the metallographic section in Figure 40. The section view of the thermally cycled specimen shows the considerable deformation tolerated by the electron beam butt weld and columbium weld.

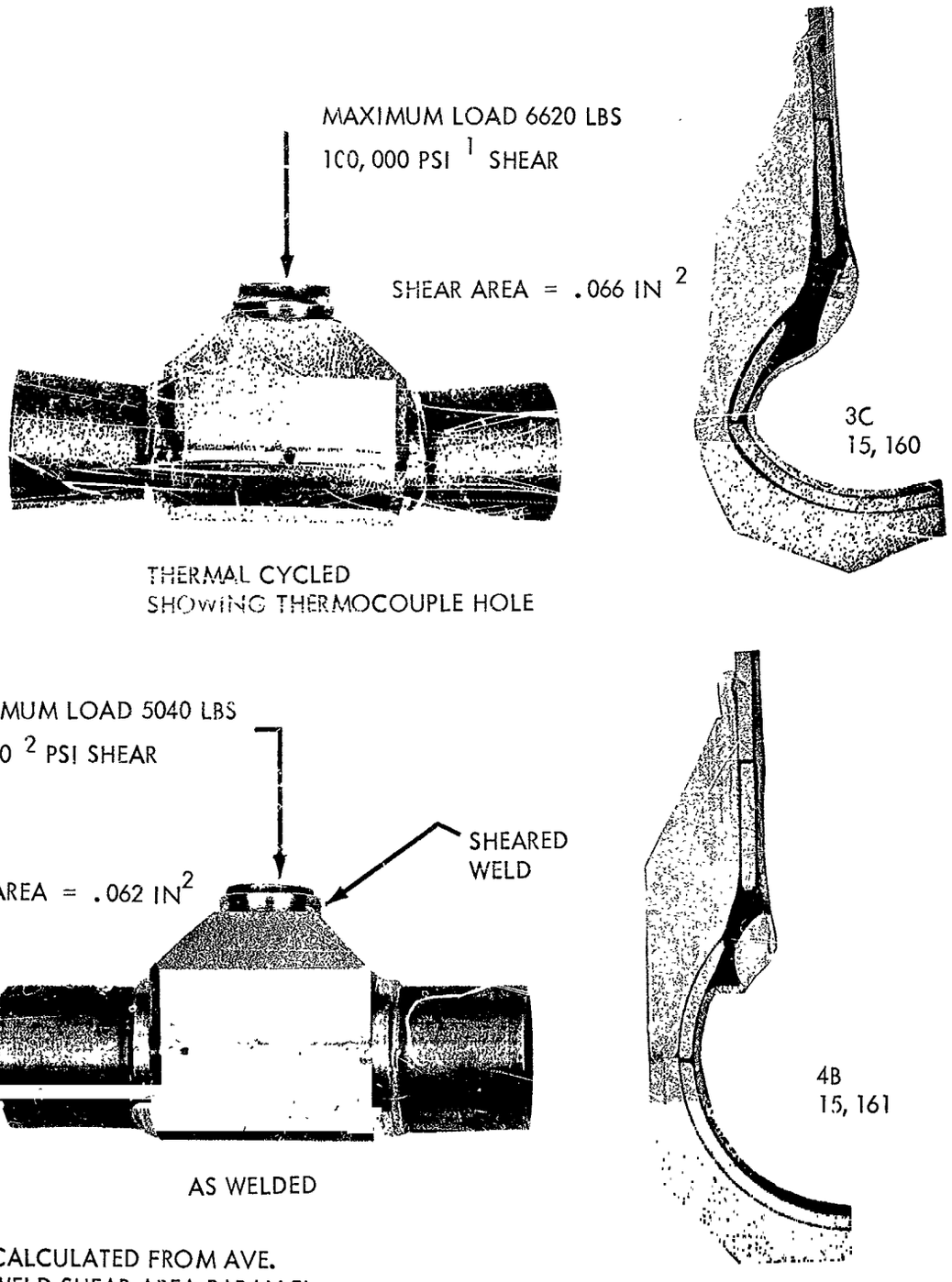

Figure 40. Crush Test of Tee Joint

Radiographic Inspection

Radiographic inspection techniques can be used to evaluate weld quality, both for the relatively thick manual filler wire welded columbium joint and for the final electron beam welds. Figure 41 shows an example of porosity in a manual filler weld.

Summary

Although the loads imposed by the crush test may not reproduce design loads, the test does show that the weld joint can accommodate considerable misalignment strain without failure. The small shear area produced by the electron beam lap weld provides sufficient structural strength. Thermal cycling does not significantly affect the structural strength of the weld joint.

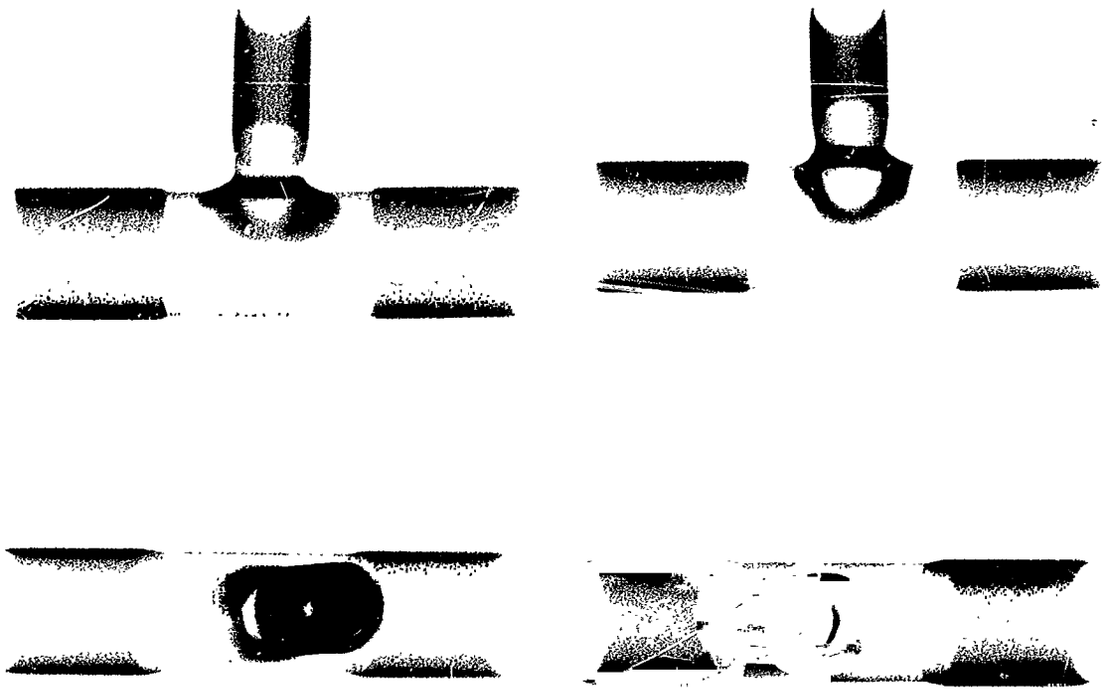

TEE JOINT NO. 3 TEE JOINT NO. 4

WELD POROSITY

POSITIVE PRINTS OF RADIOGRAPHS
THIN AREAS APPEAR LIGHT

Figure 41. Radiograph of Welded Tee Joints

E. TUBE-TO-HEADER JOINT DEVELOPMENT

Heat exchangers, both in the chemical industry and in liquid metal power systems, normally require tube-to-header configurations. Bimetal heat exchanger header assemblies have been constructed for the chemical industry by brazing and through-welding. Brazing has been employed when corrosion conditions are compatible with the braze alloys and through-welding, which causes alloy mixing, has been used on bimetal combinations of compatible alloys such as carbon steel and stainless steel. The particular demands of high temperature liquid metal heat transfer systems, however, impose strict requirements on braze systems and preclude any bimetal alloying during welding.

Two possible solutions, based on prior art, to produce tube-to-header joints for high temperature liquid metal service are shown in Figure 42. The header plate consists of a relatively thick plate of ferrous alloy covered with a layer of refractory metal sheet. Figure 42a shows the method of welding and back brazing with the columbium joint being welded and the stainless steel joint brazed. The simultaneous brazing of a multitube header assembly is difficult and fully satisfactory methods of assuring joint quality are not available. Further, acceptable brazing alloys, which must be compatible with liquid metals, generally require brazing cycle temperatures that exceed the interface temperature limitations for most stainless steel-refractory metal combinations. A completely welded joint is clearly most desirable. A possible all-welded joint design is shown in Figure 42b. Though applicable to single tube welding, it cannot be adapted to the typical multi-tube header assembly shown in Figure 42c because of welding inaccessibility.

Description and Fabrication

An all-welded bimetal tube-to-header joint was designed to meet the stringent requirements of high temperature liquid metal service. Figure 43 shows the unique feature of this joint design, the complete accessibility of both welds from the header side of the assembly.

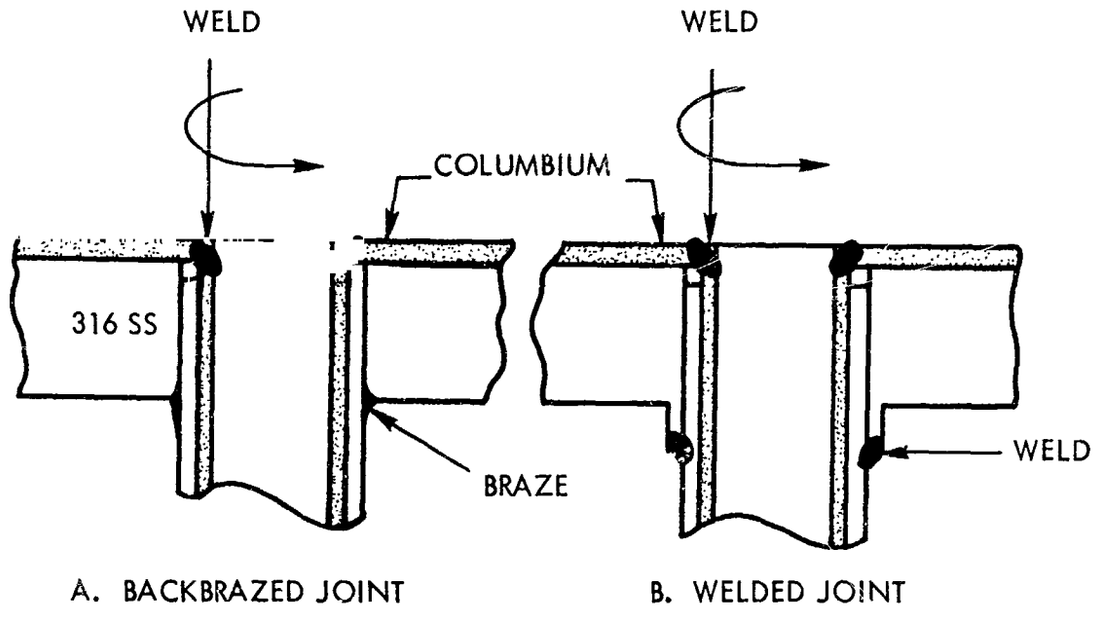

A. BACKBRAZED JOINT

B. WELDED JOINT

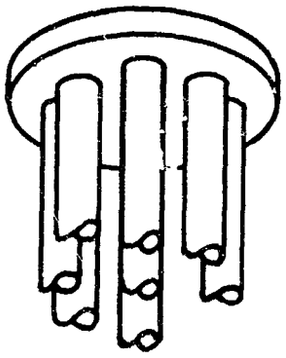

C. TYPICAL HEADER ARRAY

Figure 42. Possible Joining Technique for Bimetal Tube to Header Assemblies

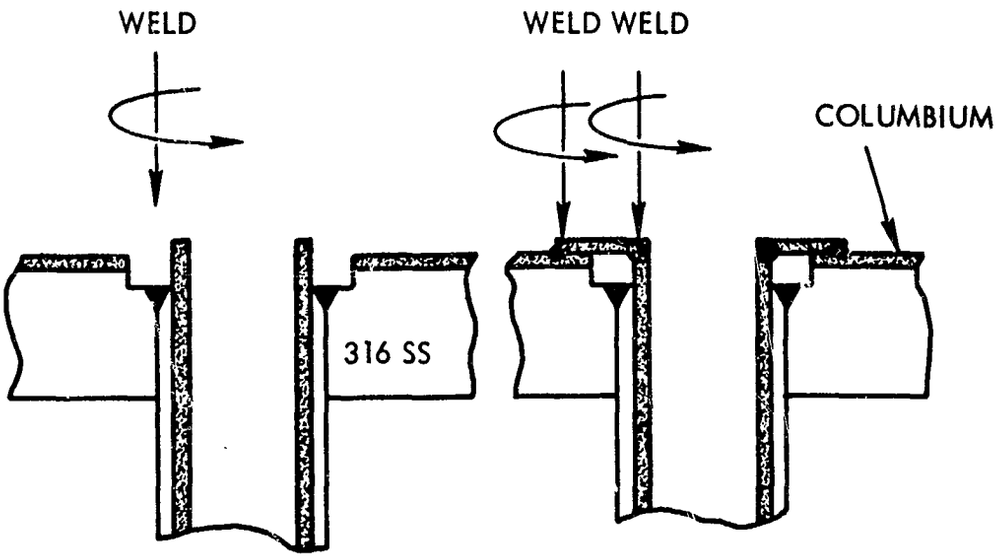

A. STAINLESS STEEL WELD

B. COLUMBIUM WELD

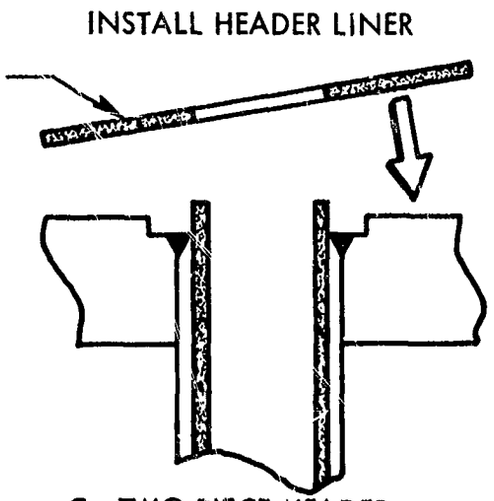

C. TWO PIECE HEADER

611614-13B

Figure 43. Preliminary Design of Tube-to-Header Joint

Figure 43a shows the first weld made in the assembly sequence, a stainless steel butt weld which does not require stringent (maximum as well as the minimum limit) penetration control. Electron beam welding is the joining process used since it permits welding in the annular crevice between the tubing and the header plate. Prior to welding, the area adjacent to the tube is machined to remove the columbium cladding and to slightly undercut the stainless steel. Figure 43b shows a section of columbium replaced and welded to complete the joint. A variation in the basic design is shown in Figure 43c where the entire columbium liner is placed on the header plate after the stainless steel weld is made. Thus, only one additional weld, an easily controlled columbium butt weld, is required to complete the bimetal header assembly. This approach is practical for header plates, which are not heat transfer surfaces, and the high thermal conductivity of metallurgically bonded material is not required.

Figure 44 shows the selected optimum design for the tube-to-header joint. The welding and assembly steps are shown in sequence. Electron beam welding is used since it provides precise control of the weld location and dimensions. A mechanical insert is used to reinforce the columbium tubing. Part or all of the insert may be made of columbium to avoid contamination of the columbium weld. A significant advantage of this joint design is that seal welds are made at both surfaces of the header plate so that the annular crevice between the tube and header is sealed, preventing both crevice and stringer corrosion. This is very important since header plates may contain stringers as shown in Figure 44, bottom, and corrosion occurs rapidly in the stringer direction. Several designs of the columbium weld were evaluated as shown in Figure 45. Type 1 required appreciably more power for adequate penetration and Type 3 warped considerably following welding. Type 2 was selected as the columbium weld reference design. An assembly view of the reference tube-to-header joint design is shown in Figure 46. Although a two piece header plate is shown, the

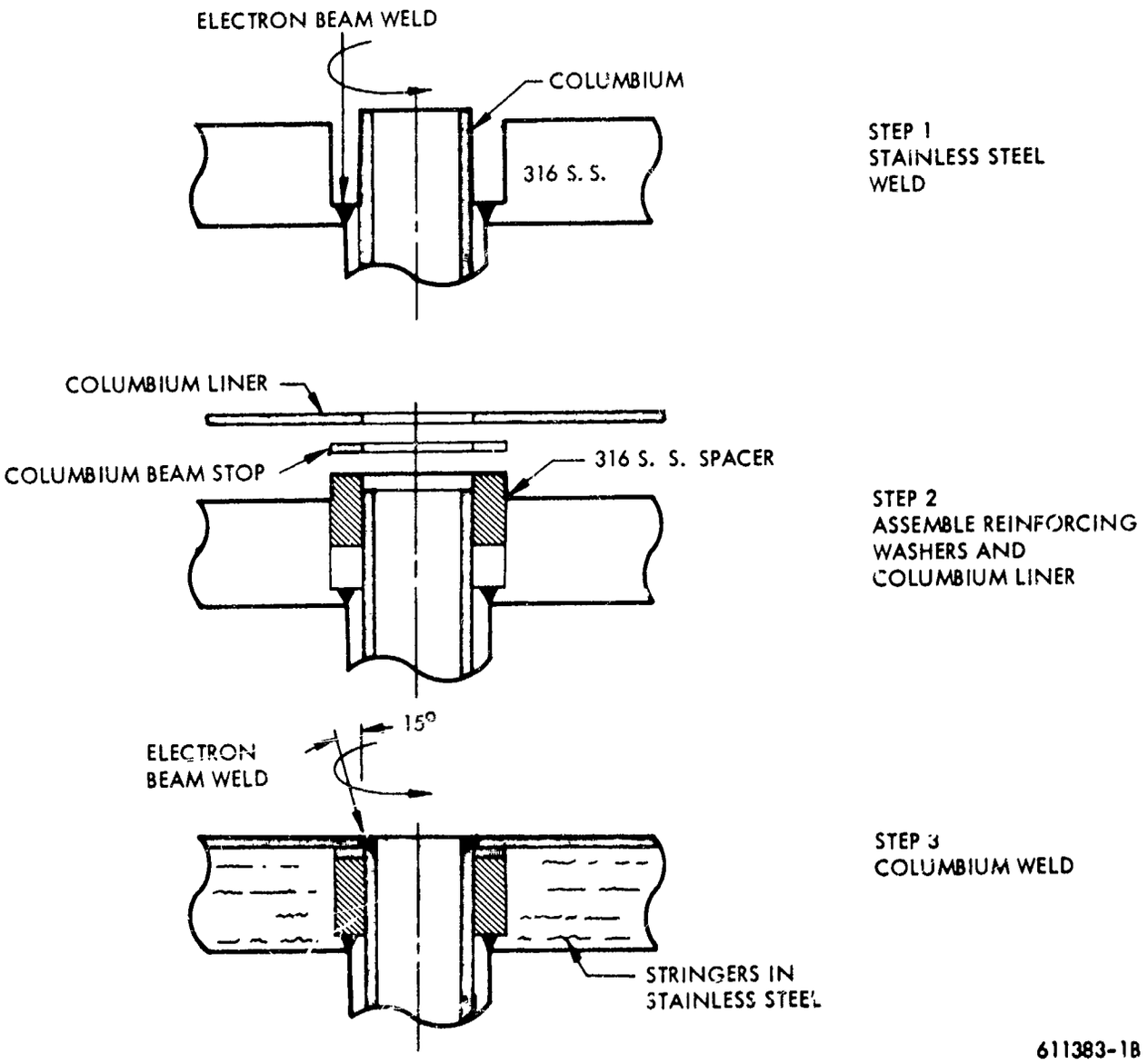

Figure 44. Optimum Tube-To-Header Joint Design

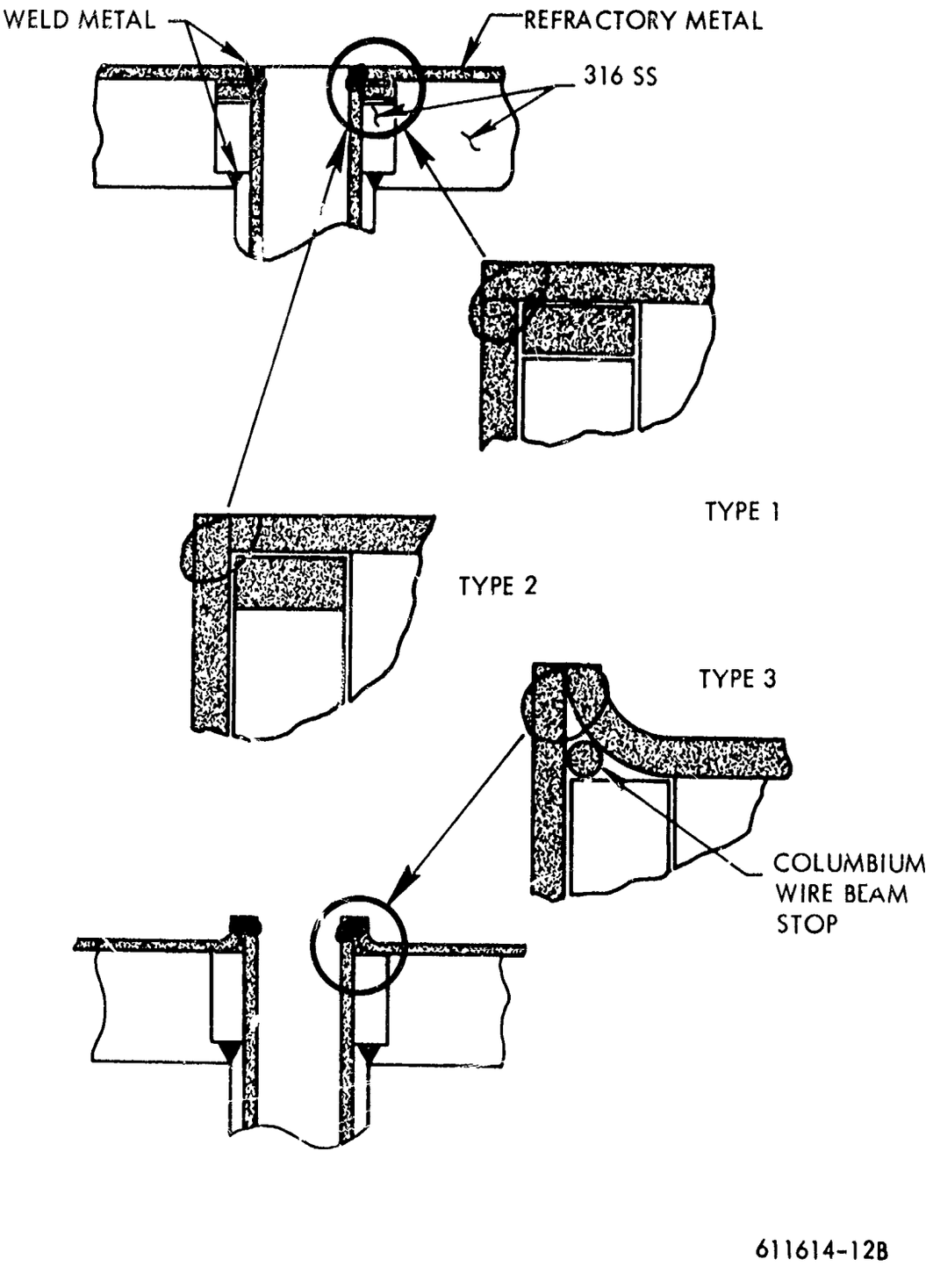

Figure 45. Design Variations of Columbium Weld

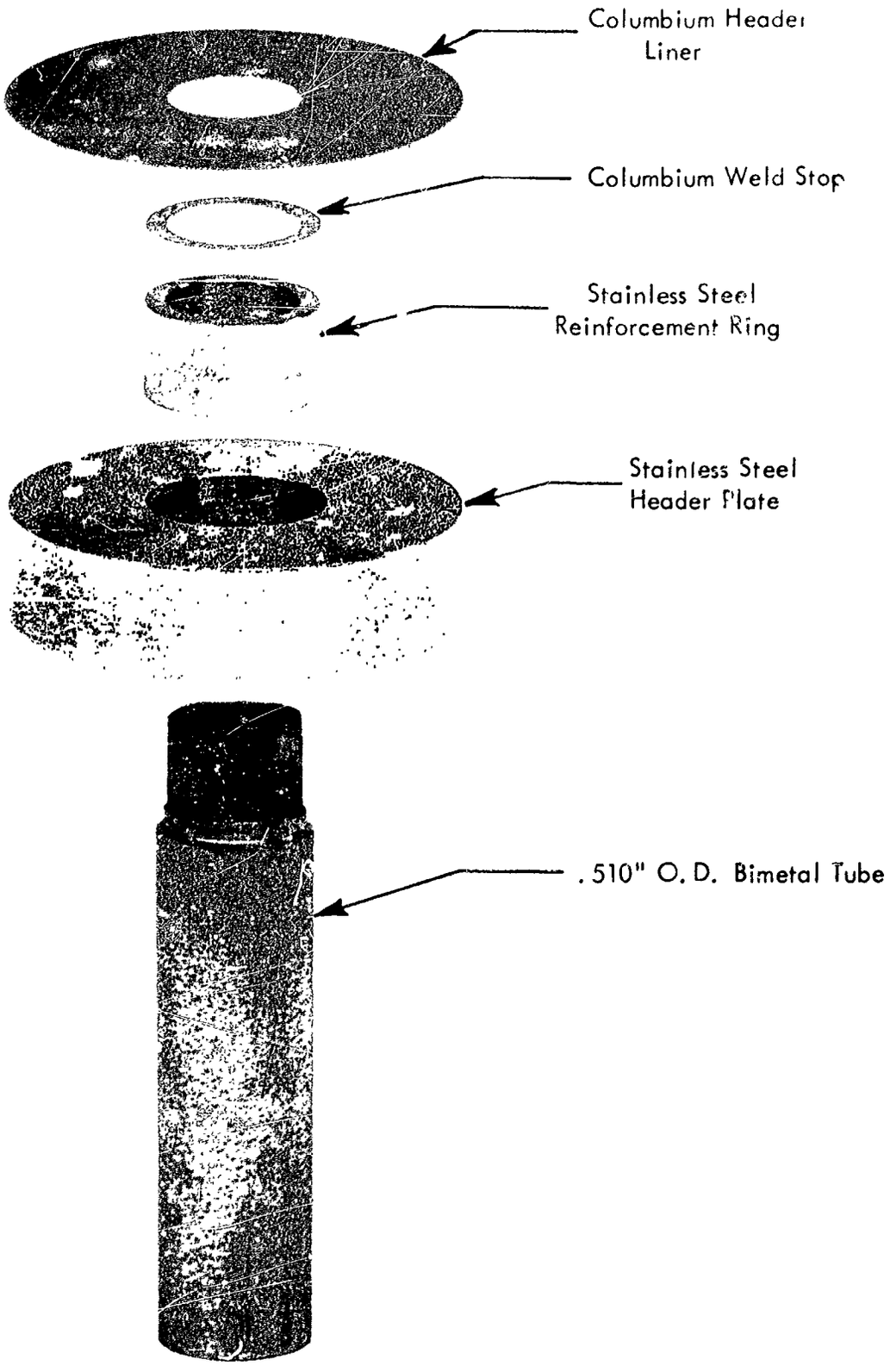

Figure 46. Reference Design Tube-To-Header Joint - Assembly View

process is applicable to a bonded header plate as shown in Figure 43. Figure 47 is a section view of a typical weld. Optimum welding parameters were readily established for the weld joint and are shown in Table 11. The welding equipment is fully described in the equipment section of this report.

In review, an electron beam welding process providing crevice sealing at both sides of the header plate was chosen as the reference process for the tube-to-header joint and was used to fabricate the 10 required specimens for the evaluation phase of the program.

Fifteen tee joint assemblies were machined and welded, (initial stainless steel weld) and 13 acceptable welds were made giving a process yield of some 85 percent, as shown in Table 12. Since the welds in a multi-tube header assembly will not generally be repairable, a welding process bordering on a 100 percent yield is required. Since two defective welds were due to a learning process, a 100 percent yield could be expected in future welds. One defect occurred during the optimization of the weld power setting and the other was due to a mistake in alignment, the weld bead being aligned on the bimetal interface instead of on the weld joint. Of the 13 successful preliminary welds, only 10 were further processed to produce 10 acceptable completed welds, a 100 percent yield. The other samples were sectioned to determine weld penetration and were prepared as "known defects" for radiographic and ultrasonic inspection.

The angled weld at the columbium joint was successful, producing a 100 percent yield for the second phase of the welding process. The in-process inspection sequence used for the tube-to-header joint is shown below.

1) Electron beam weld - stainless steel at the crevice bottom
2) Visual inspection - bead top and underbead penetration
3) Dye penetrant inspection of underbead
4) Helium leak test

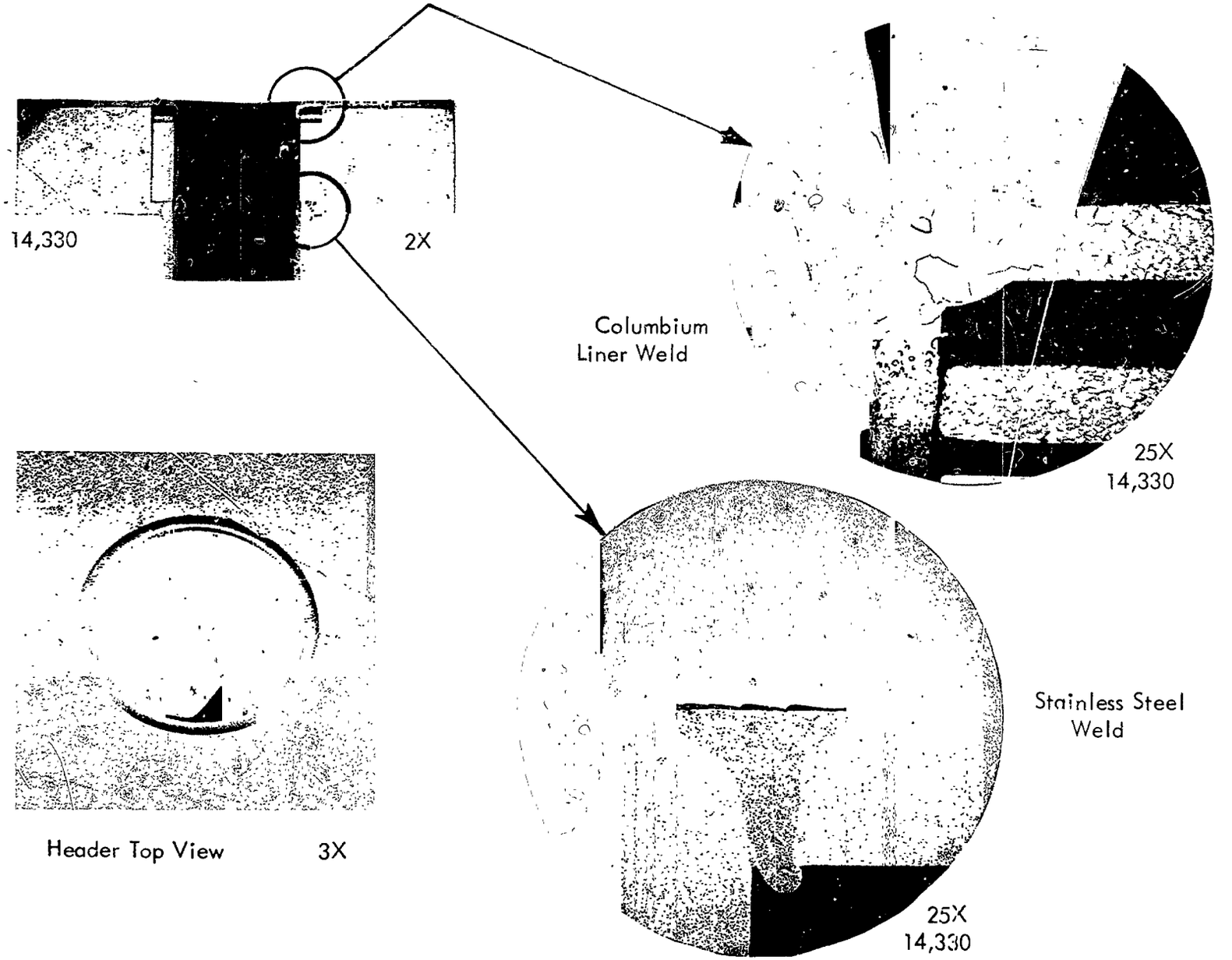

Figure 47. Reference Design Tube-To-Header Joint - Section View

Astronuclear Laboratory

TABLE 11

WELDING PARAMETERS FOR TUBE-TO-HEADER JOINT

	Stainless Steel Weld	Columbium Weld
KV	100	100
MA	3(1)	3
Speed	25 ipm	25 ipm
Deflection	0	0.018" transverse deflection

(1) Loose fit produced a narrow weld bead.

TABLE 12

PROCESS SEQUENCE OF REFERENCE TUBE-TO-HEADER JOINT DESIGN

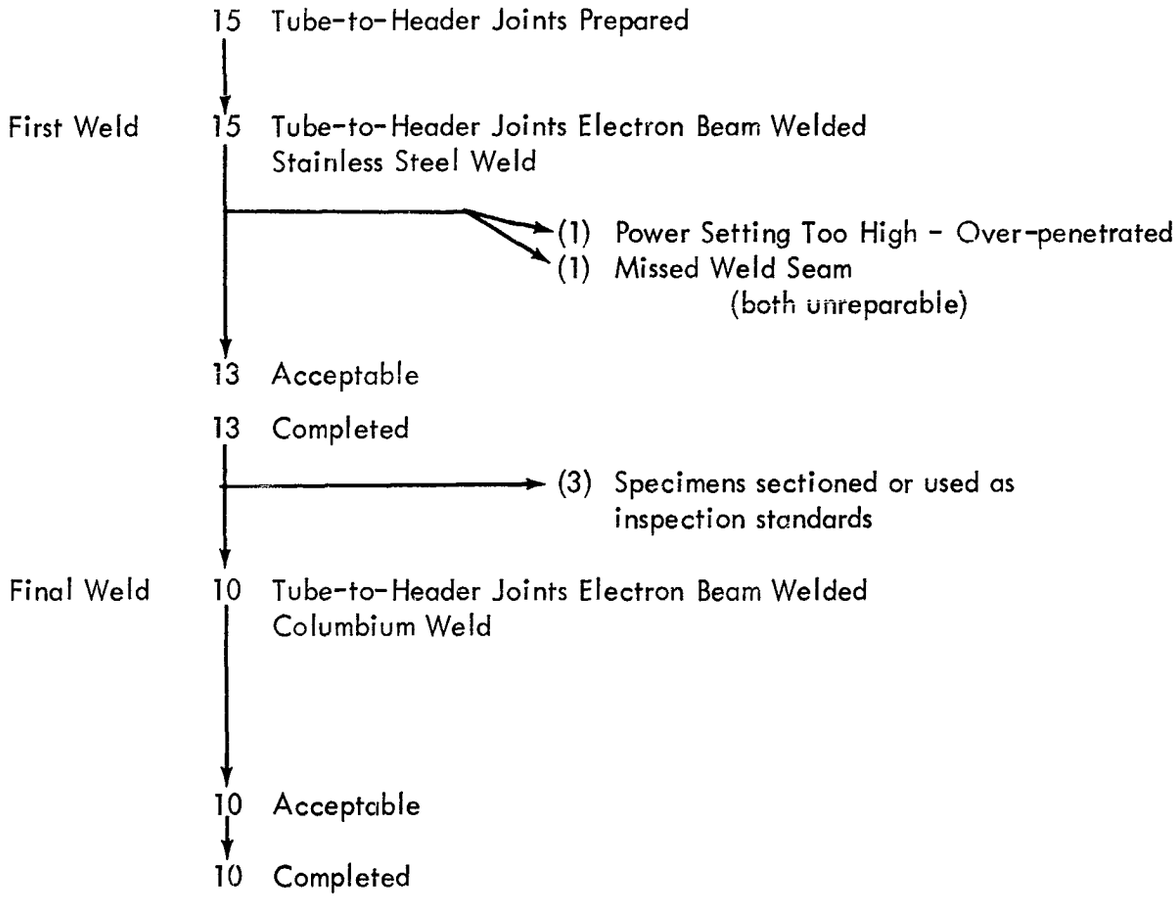

Process Yield 13/15 = 87 Percent

5) Electron beam weld columbium cover plate to tube

6) Visual inspection

7) Dye penetrant inspection

8) Ultrasonic inspection

After fabrication was completed, the evaluation program outlined in Figure 2 was followed.

Sectioning Data - Weld Penetration Control

Five tube-to-header specimens were sectioned into 4 quadrants each and the results are presented in Table 13. A typical quadrant section is also presented to show the measurement techniques used. Essentially 100 percent penetration was achieved with both the columbium and the stainless steel weld and the significant problem was the weld clearance, noted as C in Table 13. Some clearance must be maintained between the annular stainless steel weld and the columbium liner to prevent alloying. As shown in Figure 48, the statistical distribution of the measured clearance indicates poor control and the standard deviation indicates that alloying could be expected in about half of the welds made. If the tubes with a loose fit (approximately 1-2 mils diametral clearance between the bimetal tube OD and the stainless steel header plate) are segregated, an acceptable guarantee of weld clearance is apparent. The slight gap of the loose fit apparently confines the beam energy and prevents excessive weld widths.

Special Inspection Techniques

Ultrasonic Inspection of Columbium Weld. The columbium weld is difficult to inspect for complete penetration. The small weld size and shielding effects of adjacent parts make radiographic inspection difficult. The assembly seam lies perpendicular to the most usable radiographic direction. To alleviate this difficulty a shear wave ultrasonic inspection technique was devised. Figure 49 shows the shear wave beam layout and signals obtained from a calibrated defect. The defect was made by micro-drilling small holes in the interior surface of a weld to simulate lack of penetration. By adjusting the beam angle, an orientation was obtained at 34 degrees which produced signals proportional to the defect size.

TABLE 13

TUBE-TO-HEADER JOINT WELD PENETRATION SUMMARY

Tube	Section	Cb Weld % Penetration	316 S.S. % Penetration	Weld Clearance
5	A	87	100	0.0
	B	94	100	3.6
	C	81	100	0.0
	D	94	100	5.0
9	A	100	100	15.7
	B	100	100	14.3
	C	100	100	19.3
	D	100	100	17.9
11	A	100	100	14.3
	B	100	100	21.4
	C	100	100	17.1
	D	100	100	21.4
12	A	100	100	4.3
	B	94	100	10.7
	C	100	100	0.0
	D	100	100	12.9
14	A	100	100	17.9
	B	100	100	10.7
	C	100	100	7.1
	D	100	100	17.1

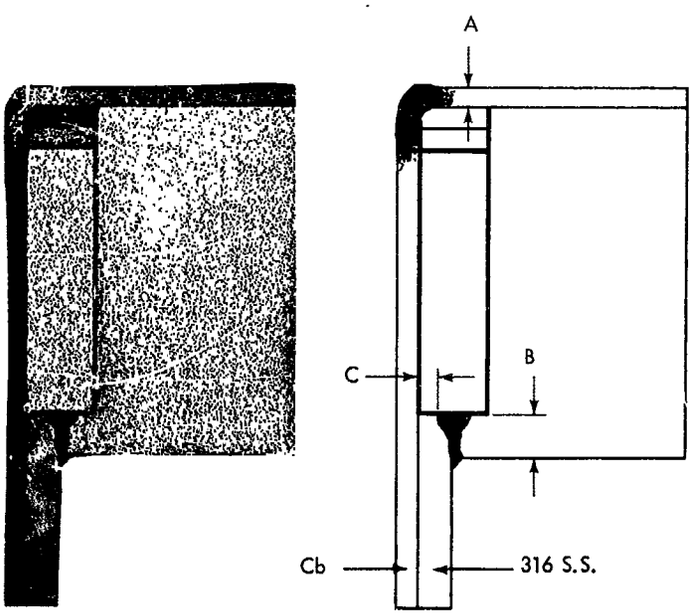

A = COLUMBIUM WELD PENETRATION

B = STAINLESS STEEL WELD PENETRATION

C = WELD CLEARANCE

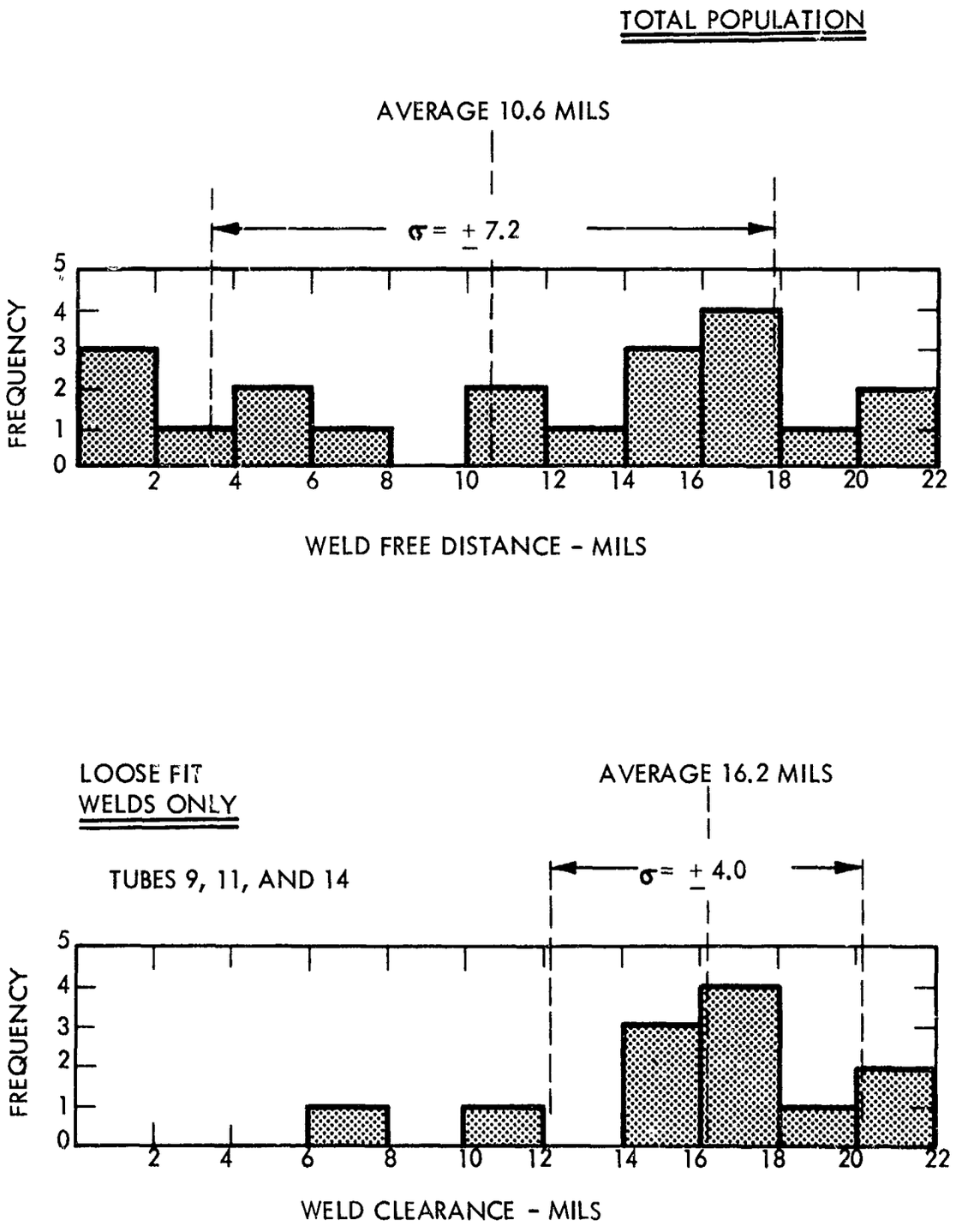

Figure 48. Statistical Distribution of Tube-To-Header Weld Penetration Data

Technique explored to detect lack of penetration or defects in columbium weld

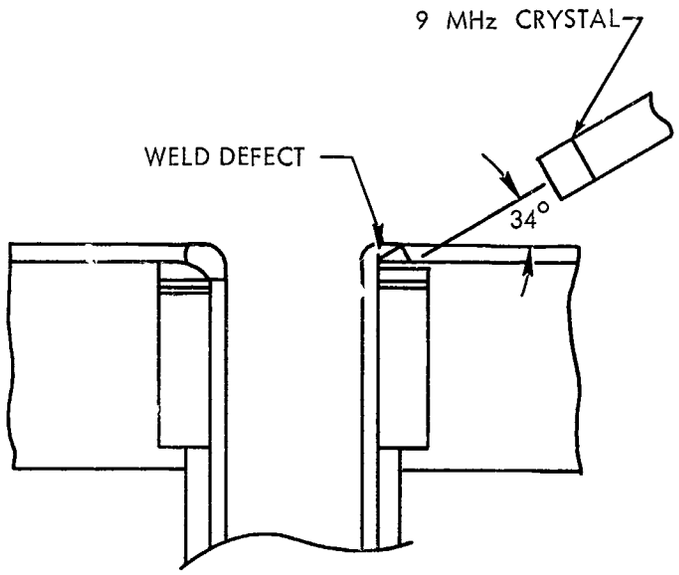

TUBE TO HEADER WELD

10 MHz OSCILLATOR
WATER IMMERSION

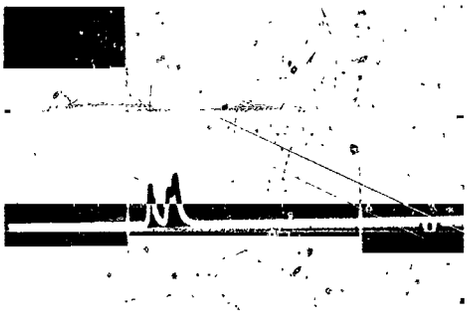

TWO
0.005" HOLES

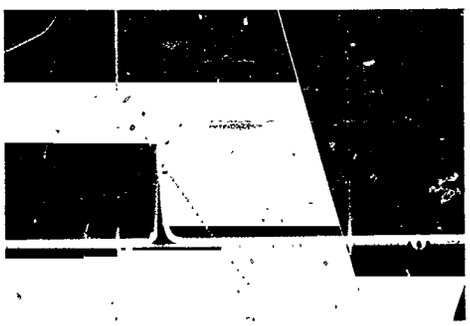

0.010" HOLE

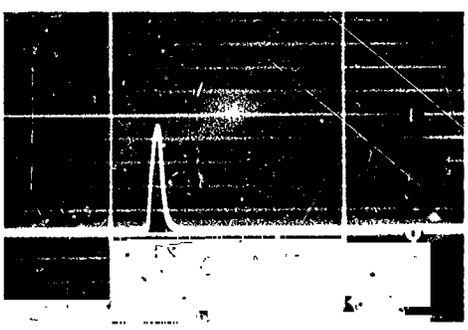

0.013" HOLE

611614-33B

Figure 49. Ultrasonic Inspection Technique for Tube-to-Header Weld

The inspection technique was put into practice by inspecting all 10 of the fabricated weld specimens. Defect indications were obtained on all of the specimens, the locations were noted, and 5 of the specimens were subsequently sectioned. No correlation was obtained between the defect indications and weld quality because all of the welds were fully penetrated. The lack of a positive defect probably led to the interpretation of surface flaws as defects and the technique remains to be fully evaluated.

Thermal Cycling and Mechanical Property Testing

Two specimens of the tube-to-header joint were thermal cycled 20 times from 1350°F to 600°F, similar to results shown in Figure 3 except that the greater mass of the tube-to-header joint required a longer cooling time. The first specimen tested required 48 seconds to cool from 1350°F to 600°F at the bimetal interface.

The second specimen was machined to remove about one half the weight of the stainless steel header plate and a cooling cycle of 36 seconds was achieved. High purity helium gas was used to cool the induction heated specimen and the process is described in detail in the equipment section.

Crush Test. As is shown in Figure 4, a tensile test was devised for the tube-to-header joint since this type of loading was expected in use. The results are shown in Figure 50. Both the thermally cycled and non-thermally cycled specimen supported a considerable load before fracturing, showing no significant difference in fracture behavior. The maximum load was equivalent to a homogeneous wall stress of over 60,000 psi. In both specimens, the columbium liner failed before the stainless steel, similar to the butt weld tensile specimens. Both the stainless steel and columbium fractures appear ductile with considerable local reduction in area.

Summary

An adequate tube-to-header joint was developed that promises superior corrosion resistance and mechanical strength.

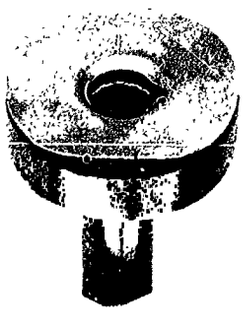

TOP VIEW

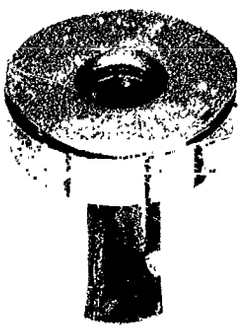

BOTTOM VIEW

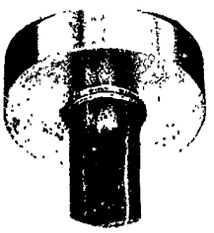

AS-WELDED

MAXIMUM TENSILE LOAD
4830 LB

61, 400 PSI UNIT WALL STRESS

THERMAL CYCLED

MAXIMUM TENSILE LOAD
4470 LB

56, 900 PSI UNIT WALL STRESS

0.05"/MIN HEAD SPEED

611614-21B

Figure 50. Destructive Test of Tube-To-Header Weld

F. WELD PREPARATION

During machining operations for the removal of the stainless steel clad on all joint designs, complete internal support was required to prevent collapse or distortion of the columbium liner from the tooling pressure. Generally, a castable alloy such as "Cerrolow-136" was used as support although expandable mandrels could be used. The geometry of most of the sections required lathe turning to remove the stainless steel. A change in color and machine finish was observable as the machining operation passed from the stainless steel to the columbium.

To completely remove the stainless steel from the columbium liner section, a combination of careful handwork and pickling was used. The last traces of stainless steel are difficult to remove because of slight smearing from the machining operation and because of an uneven bimetal interface. It is, of course, necessary to remove all traces of stainless steel to prevent alloying of the columbium, and iron, chromium, and nickel of the stainless steel. To remove and identify traces of stainless steel, a dual pickling operation was used. The initial pickling solution, 30 percent HNO_3, 30 percent HF, and water, is a strong general etch which removes both stainless steel and columbium. The final etch, aqua regia (8 percent HNO_3, 42 percent HCl, and water) was used to selectively attack the stainless steel. The etch also effectively identifies residual areas of stainless steel by producing a dull matte finish on the steel. Hand filing using a 10X microscope, followed by repickling, was used to clean up the identified areas.

The pickling solutions strongly attack the bimetal interface and a protective seal was used to prevent corrosion and acid entrapment at the bimetal interface. Duco Cement was applied with a hypodermic syringe and, after the pickling operation, was dissolved in acetone.

SECTION III

EQUIPMENT AND GENERAL EXPERIMENTAL PROCEDURE

A. ELECTRON BEAM WELDER

The electron beam welds on the tube-to-header and tee joints were made with a high voltage, vacuum chamber electron beam welder. The unit shown in Figure 51 is a Hamilton Standard WO-2, capable of operation at 150 KV and up to 3 KW power. The minimum electron beam spot size is 0.010 inch. The 6 inch oil-diffusion pumped unit may be operated as low as 10^{-6} torr and a chamber extension has been obtained to accommodate parts and tooling up to 10 feet in length. Automatic X, Y, and rotary motion is available. The precision welds in the annular crevice of the tube-to-header joints required the small beam size and beam coaxial optical system of this unit.

B. GAS TUNGSTEN ARC WELDING CHAMBER AND EQUIPMENT

Arc welding was accomplished in a 50 cubic foot, vacuum purged, inert atmosphere welding chamber. An interior view of the chamber is shown in Figure 52 with the manual torch installed for manual filler wire welding of the tee joint. Ultra-high purity helium was used for backfilling, providing a total active impurity level of about 1 ppm. During welding of the contamination sensitive columbium, both oxygen and moisture were continuously monitored. The development and evaluation of the atmosphere measurement and control techniques have been reported in detail by Stoner and Lessmann.[4] The welding chamber can accommodate a variety of automatic and manual welding torches and power supplies and for this program a Vickers 300 Ampere d-c unit was installed. This is an analog computer controlled unit, type 51E93-2, which permits complete weld programming including "hot starts" up or down starting slopes, and tail slopes. Synchronous timers provide accurate sequence control. Both automatic and manual control modes are possible with this unit.

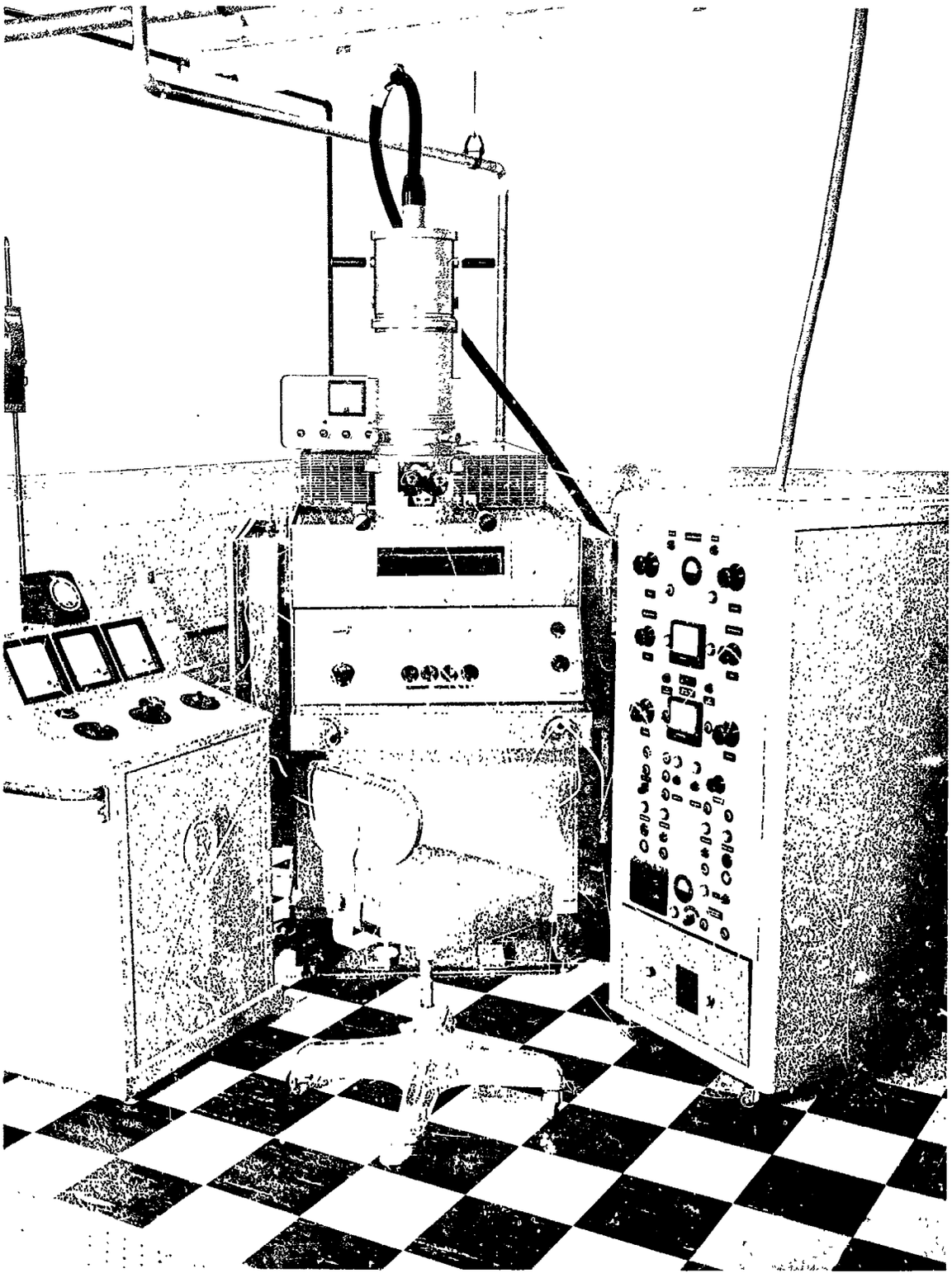

Figure 51. Electron Beam Welding Equipment

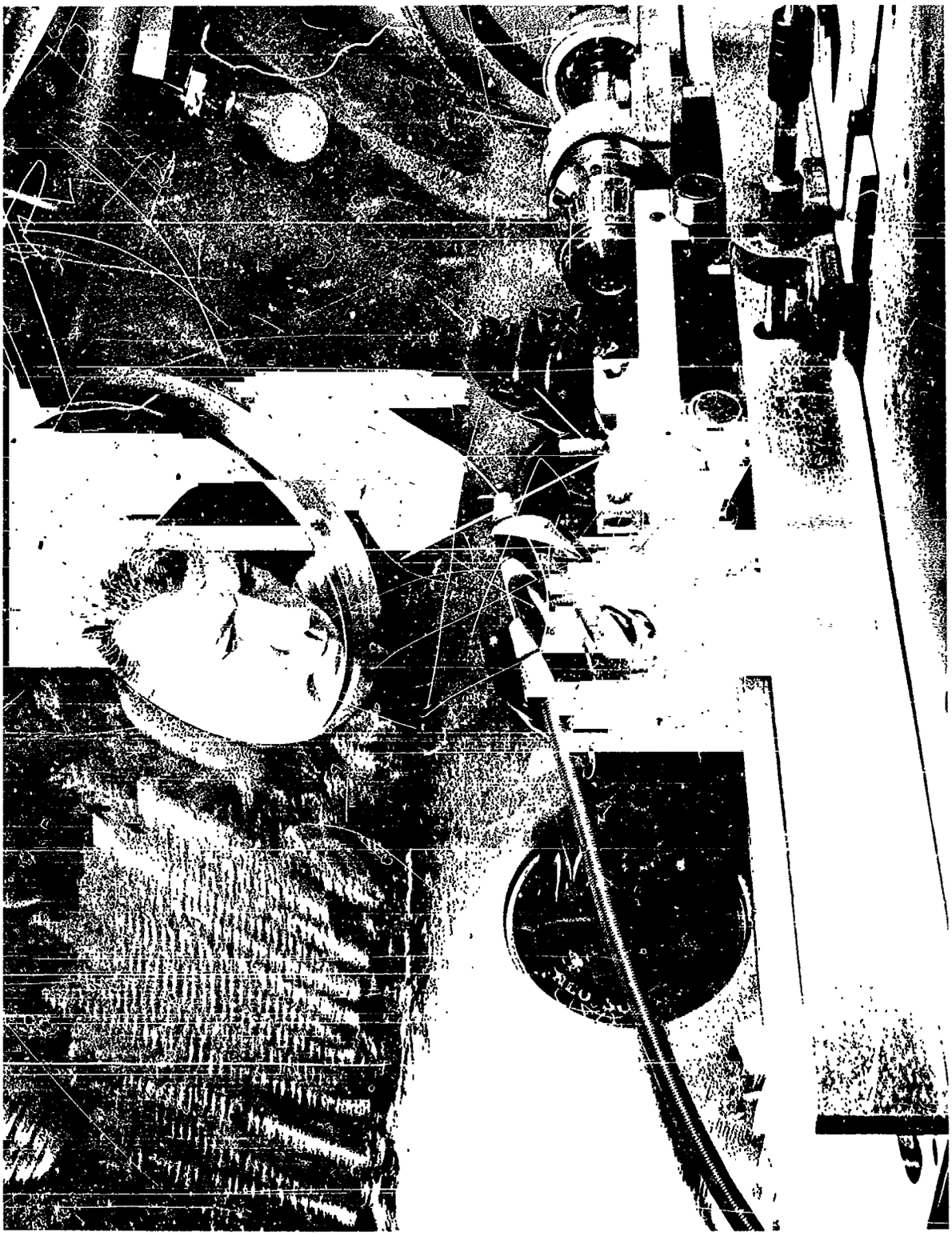

Figure 52. Interior View of Welding Chamber

C. PLASMA ARC WELDING APPARATUS

The plasma arc welding equipment is shown in Figure 53 and consists of a Westinghouse designed and fabricated control console and a modified Thermal Arc U-CT torch. Dual arc modes are provided with 20 KVA available for both the plasma and transferred arc. A gas controlled powder feed apparatus is used for filler metal additions. Argon gas was used for both the powder feed and plasma arc gas. For the low metal deposition rates and power inputs required for bimetal tubing cladding, a small sized, 3/16 inch diameter nozzle was designed, but considerable difficulty was experienced with nozzle erosion and arc stability. The majority of the work was done with a 1/4 inch nozzle and electrode, and the welding parameters are listed in Table 14.

D. THERMAL CYCLING APPARATUS

The basic test for weld joint durability was a rapid cooling thermal cycling test between 1350°F and 600°F. Heating was to be accomplished in 5 minutes and cooling in 30 seconds with a hold time at 1350°F of 10 minutes. Since refractory metals react with oxygen and nitrogen at temperatures over 600°F, helium gas cooling and vacuum induction heating were used to avoid contamination during the required 20 thermal cycles. Figure 54 is a schematic of the thermal cycling apparatus. Because of the substantial mass of the weld specimens, a high flow of helium gas was required to cool the specimens within 30 seconds and approximately $10ft^3$ of ultra high purity helium was used per cycle. The system was evacuated to 10^{-7} torr prior to the thermal cycle runs and to 10^{-6} torr during the heating cycle. Temperature was determined using Pt/Pt 13Rh thermocouples located at the bimetal interface. A typical temperature trace for the butt weld specimen is shown in Figure 3.

The system leak tightness was tested by sampling the helium exit gas using a Lockwood and McLorie oxygen gage and a C.E.C. Moisture Monitor. Typical readings following a thermal cycle run are shown in Figure 55. The gradually decreasing readings are due to the flushing of residual oxygen and moisture from the sampling lines and the analytical instruments. Thus the actual moisture and oxygen values are somewhat lower

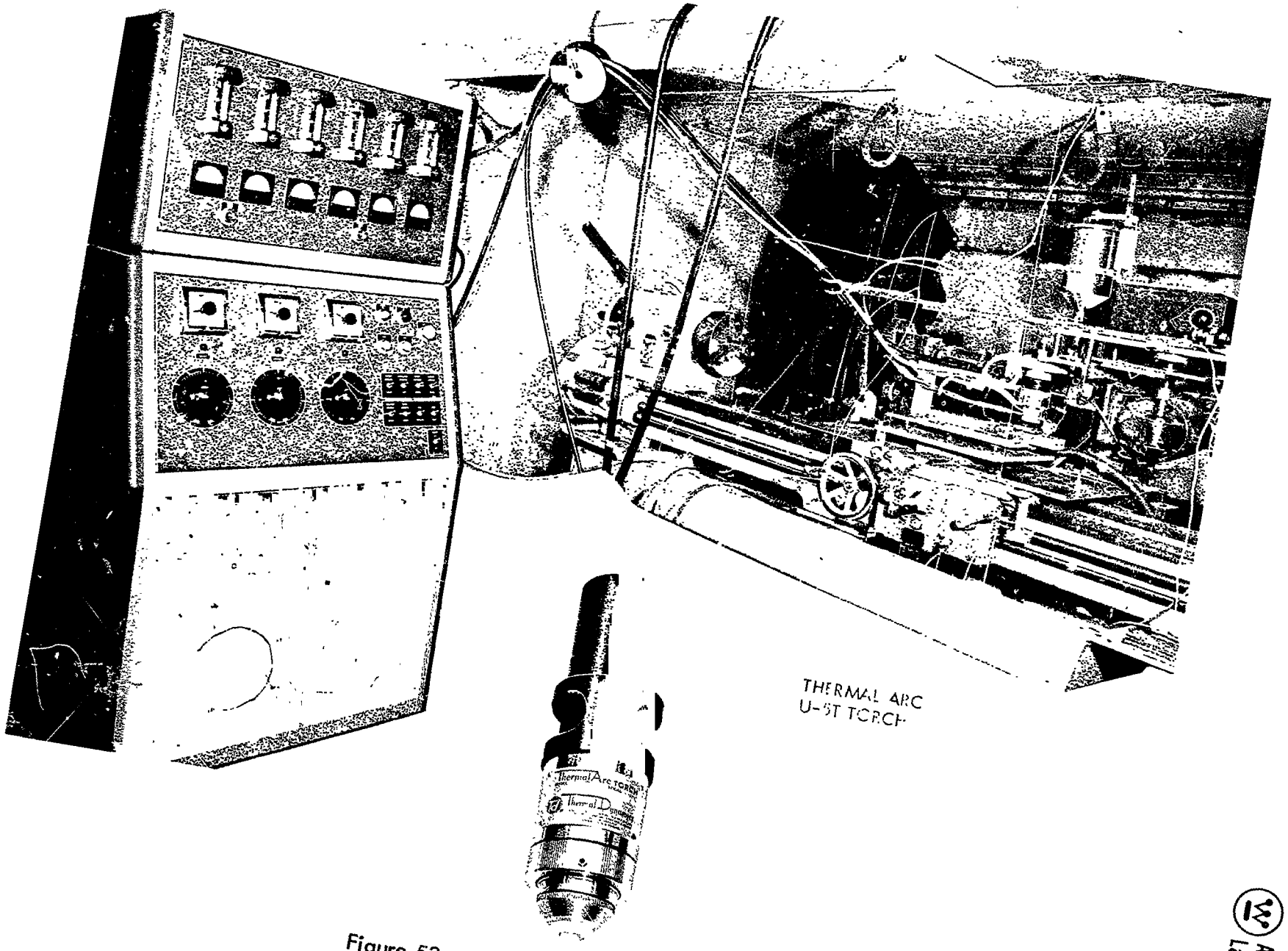

Figure 53. Plasma Arc Welding Equipment

TABLE 14

PLASMA ARC WELDING EQUIPMENT AND PARAMETERS

Equipment

Power Supply
Plasma Arc - Westinghouse WSR 20 KVA

Power Supply
Transferred Arc - Westinghouse DCR 20 KVA

Nozzle - 1/4" Westinghouse designed

Torch - Thermal Dynamics U-5T

Parameters

Plasma Arc - 50 amps DCSP

Transferred Arc - 35 amps AC

Speed - 14 ipm

Plasma Gas - 10-30 scfm Argon

Power Gas - 5 scfm Argon

Powder - Glidden 100 - 200 mesh 316 S.S.

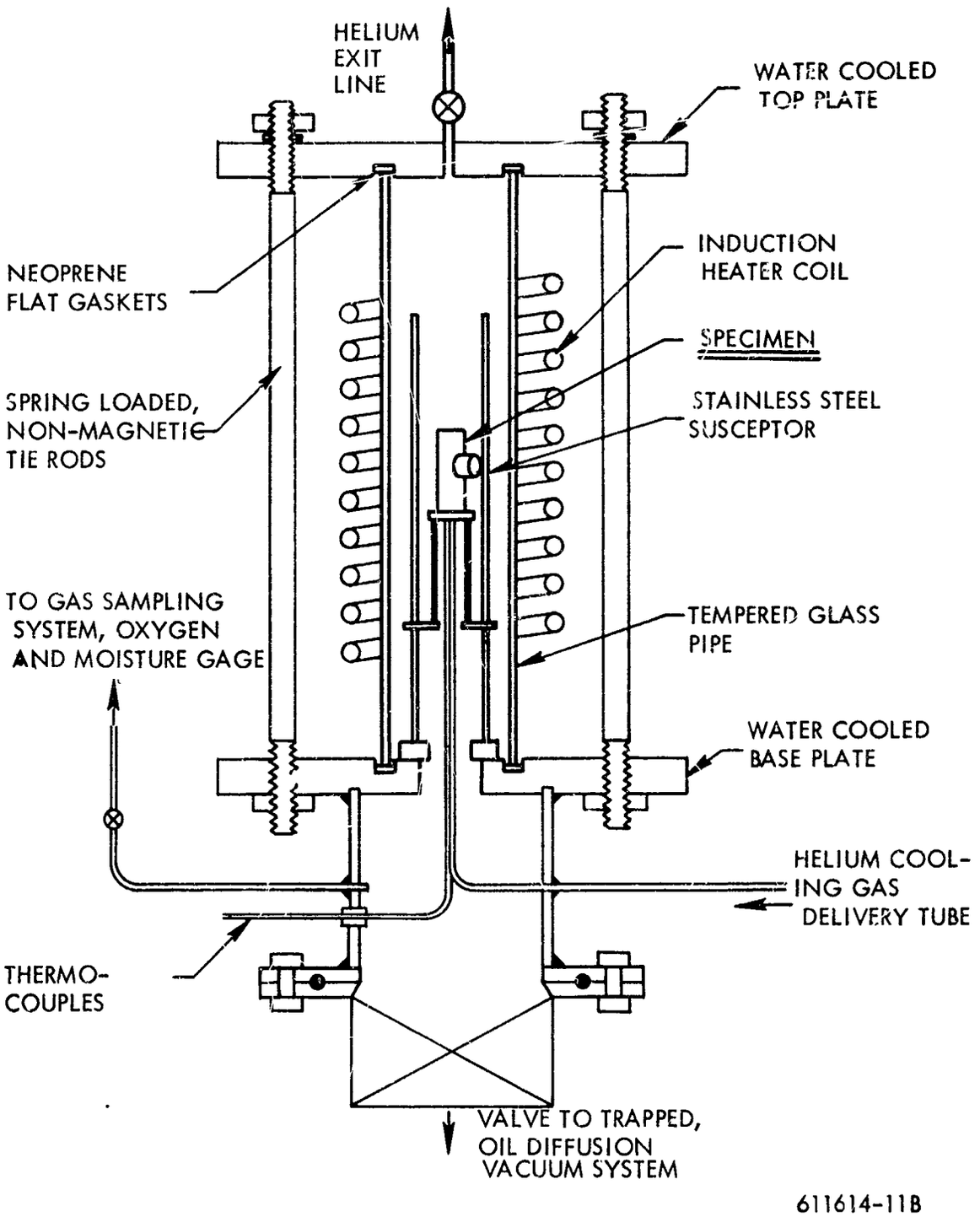

Figure 54. Schematic of Thermal Cycling Apparatus

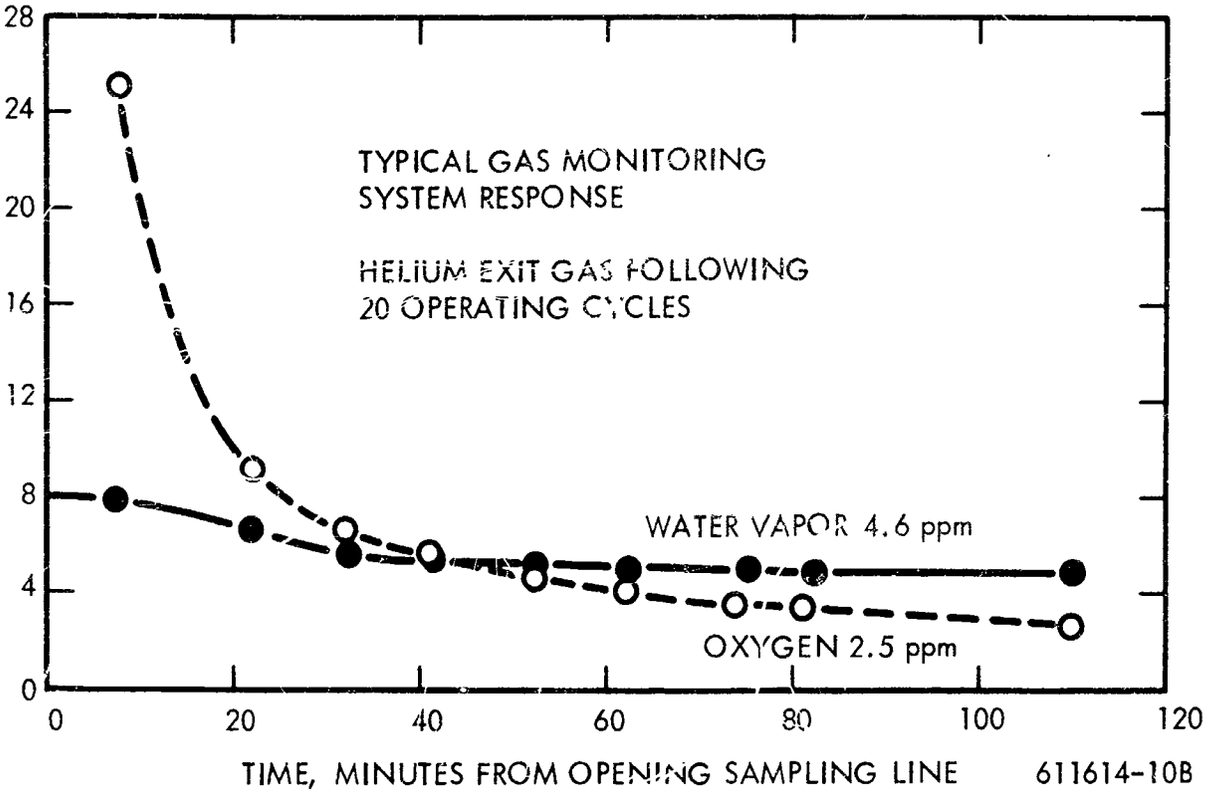

CHEMICALLY ANALYSED OXYGEN CONTENT
OF COLUMBIUM SECTION OF BIMETAL TUBING

AS RECEIVED	-	160 PPM
THERMAL CYCLED	-	190 PPM
1000 HR. PRESSURE TEST	-	220 PPM

Figure 55. Helium Gas Purity Control in Thermal Cycling Apparatus

than indicated and are quite acceptable. Also shown on Figure 55 are oxygen chemical analyses from both as-received and thermal cycled specimens. The results indicate a small oxygen pickup during the test. A photograph of thermal cycling apparatus is shown in Figure 56. Included in the view are the helium gas supply, monitoring gages, and thermal cycling traces.

E. PRESSURE TEST APPARATUS

One of the proof tests for the butt weld joint was an internal pressure test at the design operating temperature of 1350°F. Two specimens were tested; one at a low stress level of approximately twice the expected operating pressure (2 x 275 psi = 550 psi), and another at a higher stress level calculated to produce rupture within 500 hours. Although remote strain transducers to provide continuous strain measurements were not included, interrupted strain measurements were obtained from a preliminary specimen and the two regular specimens. High temperature, internal pressure testing equipment was designed similar to that used by F. Yagee at the Argonne National Laboratory.

High purity helium gas was used as the internal pressurizing medium and a vacuum of 10^{-6} torr was maintained on the heated tube exterior. Commercial gas bottles providing a maximum pressure of 2400 psi were adequate for the creep rupture tests required. An external ballast tank, a spare gas bottle, was used to minimize pressure changes as the specimen increased in diameter. The system pressure did vary as a function of room termperature, approximately $\pm$ 1% of the total pressure or $\pm$ 5 psi during the 550 psi, 1000 hour creep test. A recording "Heise" pressure gage was used which could be read to within $\pm$ 2 psi. The specimen temperature was also continuously recorded during the 1000 hour test and the single zone furnace was controlled by a proportional SCR power supply to within $\pm$ 5°F. A hot cathode ion gage was operated continuously and activated a "shut down" circuit through an adjustable pressure limit set at 1×10^{-5} torr. In case of tube rupture or system failure at any time during the 1000 hour test, the entire vacuum and furnace system is safely shut down without damage to the specimen or the system. A high pressure gas valve shown in Figure 57

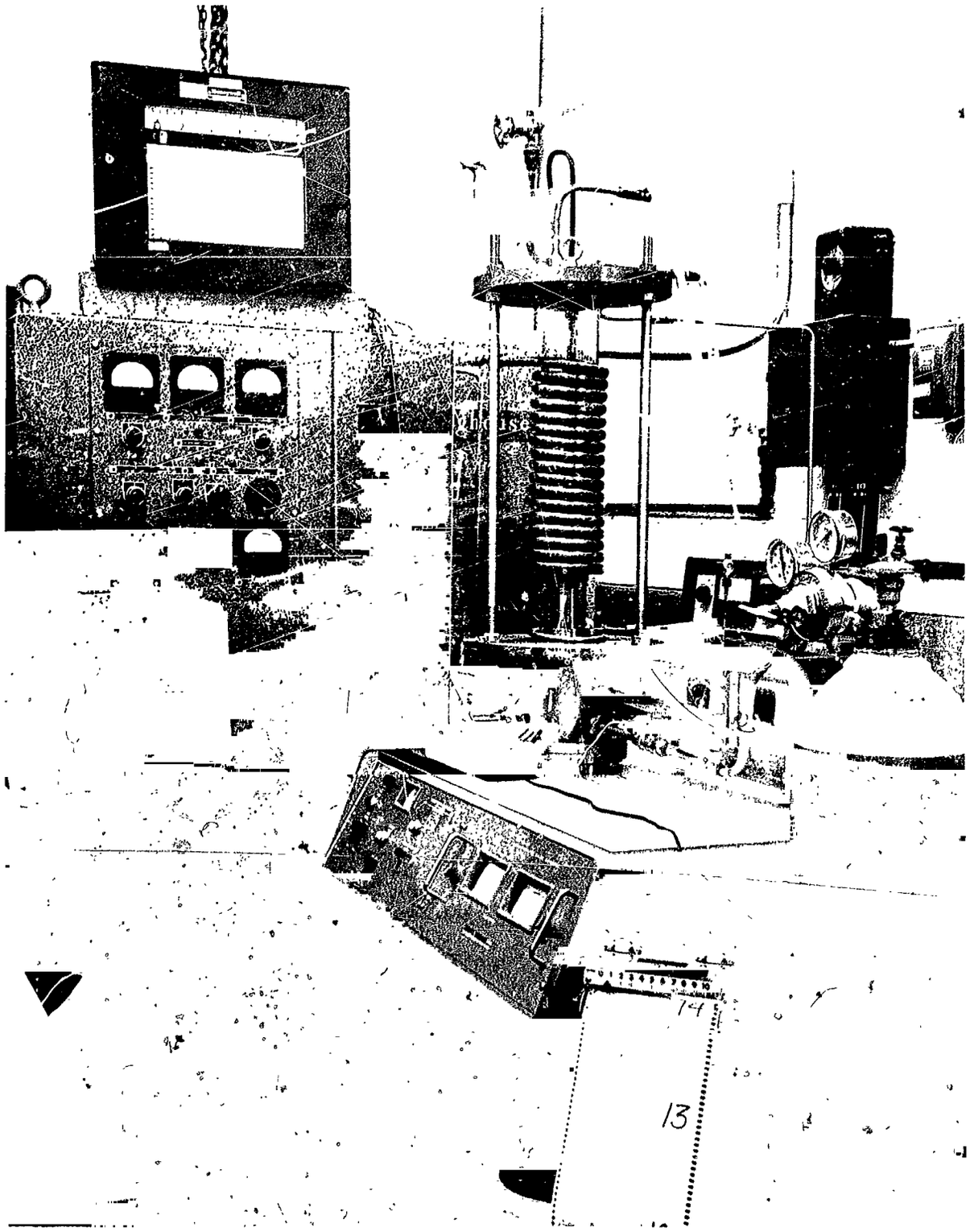

Figure 5(Thermal Cycling Apparatus

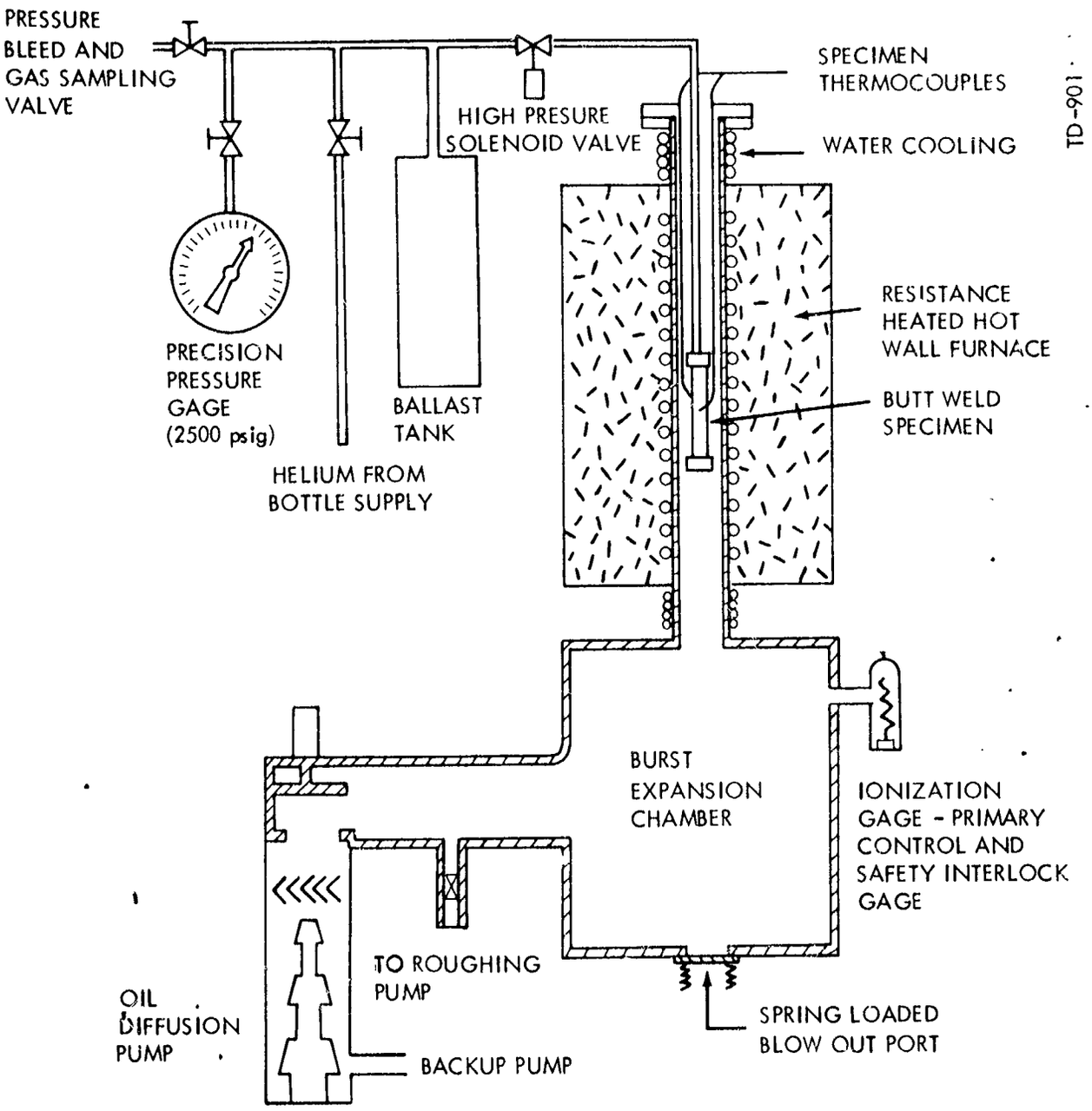

Figure 57. Schematic of Pressure Test Apparatus

was included in the safety circuit and rupture of the specimen would close this valve, thus preventing the large volume of gas in the ballast system from entering the furnace chamber. The ratio of furnace volume to specimen volume was 2000 to 1, producing a maximum resultant furnace pressure of 1 psia. The entire safety system was checked by purposely rupturing a tube. A spring loaded blow out port was also provided to release at 5 psi over atmospheric pressure in case all of the primary safety devices failed. The system operated quite satisfactorily during both the 1000 hour, low stress level test and during the 172 hour high stress level test which ended in a tube rupture and an automatic shutdown. A section of the columbium inner cladding was removed from the 1000 hour test specimen and analyzed for oxygen content. The results, shown on the bottom of Fig. 55, indicate a slight oxygen increase of 60 ppm, but no more than would be expected from a 1000 hour vacuum exposure at 1350°F. A photograph of the pressure test system is shown in Figure 58.

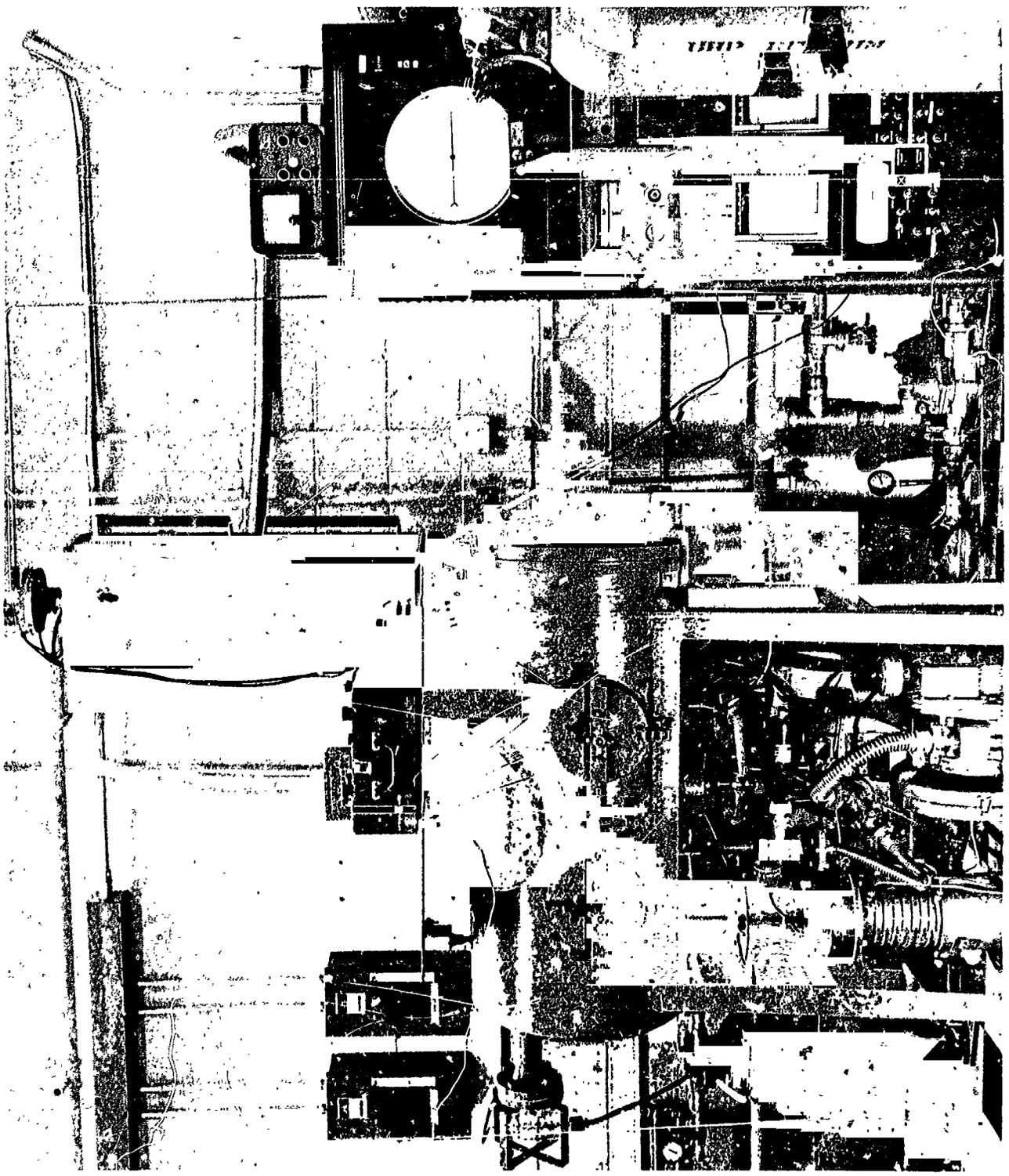

Figure 58. Pressure Test Apparatus

SECTION IV

SUMMARY

Practical fabrication techniques are available for the incorporation of bimetal tubing into complex engineering systems. The joining techniques developed are compatible with the severe environment (high temperature alkali metals and mercury) and are contemporary, state-of-the-art, joining processes. Field welding capability is maintained to permit the final assembly of large apparatus using portable, clamp-on gas tungsten arc welders and associated gas shielding apparatus.

A. TUBE BUTT WELDS

Essentially two successful processes were developed for the tube butt weld; an electron beam lap weld process and a gas tungsten arc process having field welding capability. Ten specimens were made using the tungsten arc process which demonstrated adequate strength and leak tightness. Hardness and electron microprobe studies indicate the stainless steel weld may be cast directly onto the refractory metal liner without appreciable alloying, and parent metal corrosion resistance could be expected at both surfaces of the weld joint. Creep rupture tests indicate the slightly reinforced weld area to be stronger than the unwelded tubing.

B. TEE JOINTS

Two basic fabrication procedures were developed for the tee joint, both involving the removal of an area of stainless steel cladding, welding the exposed columbium, and replacing the stainless steel cladding. An electron beam welding process, incorporating a cam guided electron beam, produced a light weight and small sized tee joint. A larger two piece tee joint was developed that was applicable to a wider range of designs, and for this reason it was chosen as the reference design and extensively evaluated. Either tee joint process could be applied to "cross" and other variations of the tee joint.

C. TUBE-TO-HEADER JOINT

A completely sealed, all welded joint was developed for heat exchangers and boilers that permits the necessary welding to be done from the accessible side of a header plate. Precision electron beam welding is employed to its greatest advantage, providing seal welds at both surfaces of a header plate. The resultant joint is immune to crevice and stringer corrosion and simplifies bimetal tube-to-header designs.

SECTION V

REFERENCES

1. "SNAP-8 Topical Materials Report for 1963", Volume II, "Component Materials Development", Contract NAS5-417, Report No. 2822, Aerojet-General Corp., Azusa, California, March 1964.

2. Harrison, R. W., "The Compatibility of Biaxially Stressed D-43 Alloy with Refluxing Potassium", Topical Report No. 2, NAS-3-6012, General Electric, Cincinnati, Ohio.

3. Soderberg, C. R., "Interpretation of Creep Tests on Tubes", ASME Transactions, Volume 63, 1941.

4. Stoner, D. R. and Lessman, G. G., "Measurement and Control of Weld Chamber Atmosphere", Welding Journal, August 1965.